L-Università ta' Malta

Trueness and Adaptation Comparison Between Chairside and Laboratory CAD-CAM Zirconia Crowns: An in-vitro study.

Laura Althea Cuschieri M.D.S. (Melit.)

Trueness and Adaptation Comparison Between Chairside and Laboratory CAD-CAM Zirconia Crowns: An in-vitro study.

by

Laura Althea Cuschieri

A dissertation presented to the Faculty of Dental Surgery in part fulfilment of the requirements for a Master of Digital Dentistry at the University of Malta

May 2024

UNIVERSITY OF MALTA

FACULTY OF DENTAL SURGERY

SUBMISSION OF DISSERTATION/THESIS FOR EXAMINATION

Student's ID/Code ______________________________

Student's Name & Surname

____

Course____

Title of Dissertation/Thesis____

____

____

I am hereby submitting my dissertation/thesis for examination by the Board of Examiners.

______________________ ______________

Signature of Student Date

Submission noted.

______________________ ________________________

Principal Supervisor Signature

(in Caps)

____

Date

Acknowledgements

In completing this master's dissertation, I am deeply indebted to several individuals whose guidance, support, and encouragement have been invaluable throughout this journey. Firstly, I extend my heartfelt gratitude to my main supervisor, Professor Arthur R. G. Cortes, whose constant guidance and insightful feedback have been instrumental in shaping this research. His expertise and dedication have been a constant source of inspiration, and I am truly grateful for his mentorship.

I would also like to express my sincere appreciation to my co-supervisor, Dr Emre Tezulas, whose wealth of knowledge and constructive inputs have significantly enriched the quality of this dissertation. His perspectives and guidance have broadened my understanding of the subject matter, and I am immensely thankful for his support.

I am deeply grateful to my fiancée, Dr Nicole Calleja, whose unwavering support, understanding, and encouragement have been my rock throughout this academic endeavour. Her patience, love, and belief in me have sustained me through these challenges, and I am profoundly thankful for her presence in my life.

Special thanks are also due to Dr Ana Paula Ayres Pinheiro de Lima for her invaluable guidance in navigating software tools and methodology, which greatly contributed to the completion of this research. Her expertise and support have been instrumental in overcoming various hurdles, and I sincerely appreciate her assistance.

Lastly, I extend my heartfelt gratitude to my parents, whose unconditional love, sacrifices, and encouragement have been the cornerstone of my journey. Their values and teachings have shaped me into the hardworking and persistent individual I am today.

This project would not have been possible without the company Zirkonzahn (Gais, Italy) for providing us with their devices and materials. Special thanks to Mr. Jürgen Feierabend for training me with the Zirkonzahn CAD-CAM system. I would also like to acknowledge Geomagic Control X (3D systems) for providing us with the license to use their software.

Abstract

Background: In the presence of tooth structure loss from either carious or non-carious (tooth wear) origin, dental restorative treatment is required to rehabilitate and restore the tooth's form and function. Restorative treatment can be direct using restorative material, or indirect using dental prostheses fabricated using additive or subtractive methods of manufacturing. These dental prostheses can be temporary or long-term depending on the case and material of choice. Over the years there has been an increase in demand for aesthetic restorations. With superior aesthetics, biocompatibility, and good mechanical properties, zirconia ceramic has become an increasingly popular restorative material for fixed dental prostheses. The fabrication (milling and sintering) of partially sintered monolithic zirconia in a single visit is time-consuming taking up to 12 hours with the conventional laboratory (lab) workflow. With recent advancements, the sintering process can be completed in as little as 15 minutes with high-speed sintering. Regardless of which system the clinician decides to choose, loss of retention and caries are the most common reasons for failure. Both are influenced by the adaptation of the restoration to the prepared surface, expressed as internal and marginal gap measurements.

Objectives: The purpose of this in-vitro study is to compare the adaptation and trueness of monolithic zirconia crowns milled using a laboratory workflow (Zirkonzahn, Zirkonzahn GmbH, Gais, Italy) with a chairside workflow (CEREC, Dentsply Sirona).

Materials and Methods: A maxillary right second premolar typodont tooth from a mounted prefabricated dental study model was prepared by the CEREC zirconia clinical guidelines with a chamfer finish line. The model's fully dentate arches with the prepared tooth and bite registration were scanned with an intraoral scanner (Primescan scanner; Dentsply Sirona). A fully anatomical zirconia crown was first designed using the CEREC chairside CAD software with one reference marker on the buccal and lingual aspects. The resulting crown design was exported and used as a reference to create a similar shape and mimic the position of the markers using the scanned arches from the initial scan. The other crown was designed using integrated CAD software (Modellier, Zirkonzahn) for the lab group. Monolithic zirconia crowns were fabricated for both the chairside group (Zirconia+; CEREC, Dentsply Sirona; n=15) and the lab group (Prettau 2; Zirkonzahn GmbH, Gais, Italy; n=15) with the system's integrated milling and sintering devices (Primemill and SpeedFire, and Zirkonzahn M1 and Zirkonofen Turbo respectively). The internal and marginal gap of each crown was assessed using the triple scan method, scanning the prepared tooth (MS) on a scanning aid, the crown (CS), and the seated scan (SS) after cementation with light-body silicone following timed constant finger pressure. Measurements were taken using 3D software (Zeiss Inspect Optical 3D 2023) on the virtual buccolingual and mesiodistal cross-sectional images. Trueness (3D-deviations between digital wax-up and manufactured crown) of all crowns was evaluated by mesh superimposition of standard tessellation language (STL) files using another software (Geomagic Control X, 3D systems). The root mean squared of the positive and negative deviations of the scanned crown along with a colour map demonstrating these variations were obtained. Statistical analysis was achieved using the Independent Sample *t*-test for the marginal and internal gap, and the Mann-Whitney U-test for trueness considering that $p < 0.05$ is significant.

Results: Normal distribution was rejected for trueness analysis ($p<0.05$ with Shapiro-Wilk test) whilst normality was accepted for internal and marginal gap analysis ($p>0.05$ with Shapiro-Wilk test). The Independent Samples *t*-test revealed a significant difference in the overall internal and marginal fit between the chairside 81 ± 48.1 µm, 100.7 ± 43.6 µm and lab group 60.9 ± 32.0 µm, 67.8 ± 59.0 µm ($p<0.001$). No significant difference was found in the axial internal gap ($p=0.043$). According to the Mann-Whitney U-test the internal trueness of crowns manufactured with the lab workflow was significantly higher (lower deviation) than that of the chairside group with an RMS of 24.2 ± 6.09 µm and 30 ± 7.89 µm respectively ($p=0.041$).

Conclusion: Within the limitations of this *in-vitro* study, the findings observed herein suggest that both CAD-CAM systems fabricate monolithic zirconia crowns with clinically acceptable cement space and marginal fit. However, the laboratory workflow using the Zirkonzahn software and its respective milling and sintering devices exhibited higher trueness and better marginal and internal fit than the chairside workflow using the CEREC system by Dentsply Sirona.

Table Of Contents

List of Figures

Chapter 4

Chapter 5

List of Tables

List of Abbreviations

OHRQoL	Oral Health-Related Quality of Life
Y-TZP	yttria-stabilised tetragonal zirconia polycrystalline
MPa	Megapascal
3D	Three-dimensional
FDP	Fixed dental prosthesis
CAD	Computer-aided design
CAM	Computer-aided manufacturing
STL	Standard Tessellation Language
CNC	Computer Numerical Control
μm	Micrometres
DV	Direct view method
SRT	Silicone replica technique
TST	Triple-scan technique
Micro-CT	Micro-computed tomography
2D	Two-dimensional
mm	Millimetres
CS	Crown scan
SS	Seated scan
MS	Master scan
RMS	Root mean square
SPSS	Statistical Package for the Social Sciences
CI	Confidence Interval
SD	Standard Deviation
Lab	Laboratory

Chapter 1: Introduction

Several aetiological factors can alter the shape and strength of a tooth's anatomical form. The most common causative factors of tooth surface loss can be of carious and non-carious (tooth wear) origin (Bettie et al. 2017). Despite the multifaceted multicausality concept, every clinician's approach should start with diagnosis and treatment planning (Dawson, 2006). With improvements in restorative and preventive dentistry in the last decade, lower rates of complete edentulism were noted (Al-Rafee, 2020). Tooth surface loss negatively impacts aesthetics and the patients' Oral Health-Related Quality of Life (OHRQoL). In cases where tooth reconstruction is required an extra-coronal prosthesis, also referred to as a crown, can be fabricated (Dolan et al., 2001).

Therefore, crowns may be used to protect and reinforce the remaining tooth tissue in cases where the tooth is compromised due to tooth decay or tooth wear (Azouzi et al., 2018). In such cases, a crown can be fabricated as a temporary or definitive prosthesis reproducing the morphology and shade of the pre-existing dentition. The most commonly used materials are ceramics and resins. Resins can be milled but also 3D printed giving the possibility of inexpensive and reliable interim or long-term temporary restorations (Komine et al., 2020).

Among the main options for definitive restorations are ceramic materials such as zirconium dioxide (ZrO_2). The light-scattering nature of ceramics gives rise to a more aesthetic result (Stawarczyk et al., 2017a). The material of choice should not only be aesthetic and biocompatible but also have good mechanical properties indicated in both anterior and posterior regions as well as for fixed dental prostheses (FDP). Due to the inherent weakness of ceramic restorations, case selection used to be paramount. However, this limitation was overcome with the introduction of yttria-stabilised tetragonal zirconia polycrystalline (Y-TZP) based restorations. With superior aesthetics, biocompatibility, and good mechanical properties, zirconia ceramic has become an increasingly popular restorative material for FDPs (Wang et al., 2019a). Over time, the translucency of zirconia has significantly improved. This has led to the use of monolithic zirconia restorations manufactured from a single ceramic material, eliminating the risks of chippings of restorations that used to require veneered porcelain to improve aesthetics (Ilie & Stawarczyk, 2015). In addition, the use of monolithic material involves a simplified fabrication process and reduced manufacturing costs. The term "monolithic" is a Greek word that describes a single ("mono") stone ("lithos") indicating that the material has a consistent appearance.

The fabrication of monolithic zirconia restorations can be done using analogue or digital impression techniques. The quality of the fabricated crowns is usually influenced by the accuracy of the impression, the type of restorative material, operator experience, the milling system and a few other factors (Manisha et al., 2023). The analogue impression technique consists of a conventional impression with a silicone material of varying viscosities (dependent on the case) which will be used to create a stone cast. From there, the dental technician can fabricate a dental crown based on the minimum thickness of the material of choice, the patient's occlusion, and adjacent teeth through a wax-up and eventually ceramic design. Similar steps are carried out in the digital workflow. However, every step is executed on a CAD software of choice based on the CAM system available. The digital manufacturing process for fixed dental prostheses (FDP) can be divided into either the laboratory systems or the chairside workflow. The latter allows clinicians to design and manufacture the restoration in a single-visit appointment in their dental practice (Sannino et al., 2014).

Zirconia powder (ZrO_2) is usually pressed in blanks of varying shapes (blocks or discs). Zirconia can be milled in either the soft chalk-like state (white stage or green stage) or in an already partially or full-sintered state. The green stage zirconia has already undergone pre-sintering with the material minimally hardened but still soft enough to allow ease for milling (Aktas et al., 2013). This zirconia needs to be sintered to achieve adequate clinically acceptable hardness. Zirconia has three crystallographic phases: monoclinic, tetragonal, and cubic phase. The monoclinic phase is stable at room temperature up to 1170^{o}C, whilst the tetragonal phase is stable between 1170^{o}C up to 2370^{o}C. The milling process is carried out when the zirconia is in the softer monoclinic phase and then sintered in a furnace to change to the tetragonal phase. This transition leads to a volumetric decrease (Stawarczyk et al., 2017a). Partially-sintered zirconia blocks are more cost-effective as they require less robust milling systems however this is followed by a 15%-30% sintering shrinkage, which is usually compensated by the CAD software (Liu et al., 2019; Rezende et al., 2017; Suttor et al., 2001). Therefore, FDP accuracy is dependent on the accuracy of the device/machine and the degree of sintering shrinkage (Moldovan et al., 2011b; Rezende et al., 2017).

All dental ceramics need to undergo sintering to reach their final stable state with clinically acceptable mechanical properties. Sintering is a process in which atoms in the material fuse together to become one piece through high temperatures without melting. This gives rise to a decrease in volume (sintering shrinkage) due to an increase in contact areas and overlapping of grains. It is not feasible to create sintered ceramics from pure zirconia due to the sudden increase in volume during the cooling process when the cubic phase crystallises out of the pure molten mass undergoing the transformation to the tetragonal phase and eventually monoclinic phase at room temperature. The increase in volume (approximately 4%) leads to high tension and inevitably causes the ceramic structure to develop undesired cracks. This is described as martensitic transformation. With the addition of stabilising oxides to the zirconia crystal lattice this transformation during the cooling phase is prevented. This enables the structure to be fixed in the cubic state at room temperature. The zirconia is usually stabilised with yttrium oxide (Y-TZP). Yttrium oxide content has increased in the new generation of zirconia. This led to the formation of metastable tetragonal and cubic phases simultaneously also known as fully stabilised zirconia (third generation). As opposed to the first and second generations of partially stabilised zirconia, the third generation does not undergo phase transformation under induced stresses. This mixed cubic/tetragonal structure allows variations in light scatter due to variations in crystal volumes. Light scatters less strongly at the grain boundaries and with the cubic crystals being more isotropic than the tetragonal ones the material is more translucent. This gives rise to an increase in monolithic zirconia use due to it feasibility, ease of manufacturing, and improved mechanical and aesthetic properties (Stawarczyk et al., 2017a; Stawarczyk et al., 2017b).

Fabrication (milling and sintering) of partially sintered monolithic zirconia in a single visit has previously been described as challenging and time-consuming, taking up to 12 hours (Jansen et al., 2019). With the advent of chairside systems (Kaizer et al., 2017), the sintering process can be completed in as little as 15 minutes with high-speed sintering (e.g. CEREC SpeedFire by Dentsply Sirona). On the other hand, chairside systems usually require specific integrated CAD software and do not usually allow for designing and fabricating long-span bridges or full-arch appliances such as frameworks and surgical guides. Regardless of which system the clinician decides to choose, loss of retention and caries are the most common reasons for failure both influenced by restoration-preparation adaptation also referred to as internal fit (Dahl, Bjørn Einar et al., 2017a; Sailer et al., 2015). Very little is known about the accuracy and marginal discrepancy of the final prostheses milled from the CEREC Primemill and sintered with the SpeedFire sintering machine compared to other sintering machines with longer sintering times. Studies have compared other chairside workflows with the 5-axis milling machines (Camargo et al., 2022; Hamza & Sherif, 2017), however to our knowledge, very little is known about the trueness and adaptation of milled monolithic zirconia crowns fabricated by the latest Chairside Dentsply Sirona CEREC workflow which includes the Primescan intra-oral scanner, the Primemill milling machine and the furnace CEREC SpeedFire (Sirona Dental Systems, Benheim, Germany) with a high end lab-based integrated system (Zirkonzahn M1 and Zirkonzahn Zirkonofen Trubo, GmbH, Gais, Italy).

Chapter 2: Literature Review

2.1 History of Zirconia Restorations

In the presence of tooth decay, fractures and/or tooth wear, the remaining tooth structure requires restorative treatment to strengthen and restore the original morphology of the tooth (Azouzi et al., 2018). Restorative treatment can be direct, using dental composite material constructed in situ, or indirect, using chairside or lab workflow to produce prostheses that can be cemented onto the prepared tooth structure. The prosthesis should mimic the pre-existing dentition's anatomy and shade. Full-coverage crowns are usually the treatment of choice in cases where tooth reconstruction is indicated (Dolan et al., 2001). Ceramic and resin-based restorations are usually the materials of choice. Resins can be milled or 3D printed as low-cost interim or long-term temporary restorations (Komine et al., 2020).

There has been an increase in demand for aesthetic restorations over the years. Due to superior aesthetics, biocompatibility, and good mechanical properties, zirconia has become a material of choice for many clinical situations. During the early applications of zirconia restorations, the material was used mainly as a high-strength aesthetic core followed by a feldspathic porcelain veneer. Layering or veneering was used to improve aesthetics. However, this may lead to chipping of the restorations (especially at the interface) and coping fractures (Ilie & Stawarczyk, 2015; Solá-Ruiz et al., 2022). To overcome this limitation, a monolithic design has been used which eliminated the veneering steps and allowed sufficient zirconia thickness (Pontevedra et al., 2022). This drastically changed the overall workflow, simplifying the manufacturing process, reducing the costs, and duration of fabrication whilst reducing mechanical complications (Alqutaibi et al., 2022). This enables the use of a fully digital workflow with minimal buccal surface veneering to improve prosthesis aesthetics in cases where shade and shape customisations are necessary. In such cases, a physical cast is necessary which can either be a stone case (in the case of a conventional workflow) or a 3D printed model (digital workflow).

As compared to other types of ceramic materials, zirconia (ZnO_2) provides enhanced flexural strength, with average values of 1200-1500 MPa (Zhang & Lawn, 2018a). Monolithic zirconia was found to outperform all-ceramic restorations regarding mechanical properties and chipping potential. It can also be used in minimally prepared teeth resulting in a more conservative preparation (Monaco et al., 2019). There are several zirconia grades on the market mainly based on the yttria content with different translucencies. Some manufacturers do not specify the specific composition of their product but based on their main properties such as translucency, flexural strength, sintering temperatures, and manufacturer's indications, one can only assume. The composition ranges from the 3 mol% yttria-stabilised tetragonal zirconia polycrystalline (3Y-TZP) which is the strongest and most opaque type, a more translucent and slightly weaker 4 mol% yttria (4Y-PSZ) to the mechanically weakest but most translucent types 5 and 6 mol% yttria (5Y/6Y-PSZ) (Zhang & Lawn, 2018b). A systematic review found that zirconia FDPs had an 89.43% survival rate with chipping of veneered ceramic in 16.97% of cases (Pjetursson et al., 2015). Furthermore, zirconia FDP frameworks had a 100% 5-year survival rate, greater than resin-bonded metal-ceramic prostheses (Thoma et al., 2017).

2.2 Zirconia Crown Fabrication

Zirconia blocks fabricated for CAD-CAM allow the manufacturing of restorations with uniform quality and allow standardisation as well as reduction in costs and time (Davidowitz & Kotick, 2011). Zirconia processing can take place using hard machining of already sintered blocks or soft machining of partially sintered blocks. Hard machining is considered to be a difficult and expensive route because it involves milling of zirconia at its highest strength and hardness. This usually leads to longer milling times as well as wear of the tools (Stawarczyk et al., 2017a). Zirconia milling in the soft pre-sintered porous state, also known as the "green state", requires sintering post-milling to achieve the final hardness and strength. Each manufacturer has different sintering parameters depending on the product selected. The additional sintering procedure and post-processing protocol takes 6 to 8 hours requiring a furnace to reach 1500ºC (Stawarczyk et al., 2017a). This would not be possible to execute in a single visit. With the development of novel induction furnaces, chairside zirconia milling speed and sintering (high-speed) have been reduced to 60-120 minutes and 10 minutes respectively (Sulaiman, T. A. et al., 2015).

A previous study found no significant difference in the marginal gap and fracture load after ageing in monolithic zirconia produced by high-speed sintering (using SpeedFire by Dentsply Sirona) and conventional sintering (Nakamura et al., 2020). Similar results were obtained in another study regarding the fracture load values, however, better marginal and occlusal fit was observed with the SpeedFire speed sintering protocol when compared to conventional sintering using the inFire HTC speed (Dentsply Sirona) (Kauling et al., 2020a). In a systematic review by Al-Haj et al. (2022), it was concluded that mechanical results as well as precision were similar or in some cases higher when using speed or high-speed sintering protocols for all 3 types of zirconia (3Y-TZP, 4Y-PSZ, and 5 Y-PSZ). Translucency was found to reduce when using the speed sintering methods with 3 Y-TZP (Al-Haj Husain et al., 2022).

In contrast to hard milling where the milling is carried out at a 1:1 ratio, due to the 25%-30% sintering shrinkage, the crown is milled at a larger size to compensate for the shrinkage (Liu et al., 2019; Rezende et al., 2017; Suttor et al., 2001). The CAD software designs the prosthesis in a way that compensates for the predicted shrinkage to achieve the desired dimensions (Edwards Rezende et al., 2017). Therefore, zirconia FDP adaptation is dependent on device accuracy and 3D control of sintering shrinkage (Moldovan et al., 2011a). These variables, along with several clinical ones, may lead to a certain degree of misfit. The assessment of post-sintering dimensional change has been investigated in several studies utilising marginal and internal fit measurements of the final prosthesis (Ahmed et al., 2020). Subtractive manufacturing has other limitations which include waste of material when cutting from a block/disk, the quality of milling burs, and the accuracy is dictated by the bur's diameter which may result in over-milled areas (Bosch et al., 2014; Wang et al., 2019a).

Post-processing treatments such as sintering, polishing, grinding, and glazing influence the surface microstructure and roughness of the prosthesis (Zucuni et al., 2019). It has also been stated that polishing after grinding, for example after sprue removal after milling, can either improve or degrade the mechanical properties. However, manufacturers usually recommend polishing after grinding and studies have shown it is the most appropriate surface treatment after any modification (Zucuni et al., 2018).

Due to the increased accuracy of intra-oral scanners and 3D printing, several clinical studies have confirmed the reliability of single zirconia crowns using a fully digital workflow (Abualsaud & Alalawi, 2022; Camargo et al., 2022; Çin et al., 2023; Hamza & Sherif, 2016; Sanchez-Lara et al., 2023; Tabesh et al., 2021). Crown fit was either comparable (Liang et al., 2018) or superior (Tabesh et al., 2021) to zirconia crown fabrication using conventional impressions.

2.3 DIGITAL WORKFLOW

When using a digital workflow for FPD fabrication the prepared tooth is scanned using an intra-oral scanner or if a hybrid method is used the impression is scanned using a desktop scanner. The restoration is then designed using CAD software and the prosthesis is milled using the milling machine of choice (Kim et al., 2022). The main advantages of using CAD-CAM technology are: 1) reduction in labour; 2) cost-effectiveness; and 3) quality control (Cortes, 2022). The use of a prefabricated ceramic block ensures almost no internal defects as the quality has been confirmed by the manufacturer as opposed to conventional powder build-up which usually contains internal porosities (Davidowitz & Kotick, 2011; Miyazaki, 2007).

There are two different types of dental software: either an open ecosystem or an integrated one. The open system, such as the Zirkonzahn software, allows the user to integrate and import different files/scans from other machines and manufacturers. An integrated system, such as the CEREC system (Dentsply Sirona), requires the entire digital workflow to be performed from data acquisition such as scanning (Primescan) to designing in the software (CEREC software) and manufacturing using the hardware (CEREC Primemill and SpeedFire) of the same company. There is limited compatibility between other systems (Kim et al., 2022).

Most CAD software programs exhibit the following sequence to design a single crown:

1. Importation of preparation scan, antagonist, and bite registration usually in STL format.
2. Model orientation leaves all margins of the preparation visible.
3. Margin line detection of the preparation and outlining.
4. Insertion axis orientation adjustments.
5. Adjustment of cement gap thickness and minimum thickness.
6. Crown shape design either from the in-software library, mirroring the contralateral tooth or depending on which system is being used an additional scan or mesh can be ustilised.
7. Adjustment of the crown using modelling tools which allow 3D positioning and fine-tuning of the shape of the restoration using the "±Add/Remove" and "Smooth" options.
8. Occlusal adjustments based on the antagonist arch.
9. The final crown can then be directly sent for milling or exported as a standard tessellation (STL) file.

An STL file describes the surface geometry of a scanned or designed 3D object. It does not represent the colour or texture of the object, however in most cases that type of information is not necessary as the zirconia blanks/blocks are industrially dyed resulting in a predetermined shade. Zirconia is also manufactured as a non-dyed block which has a hard-white monochromatic colour. This will later require manual colouring oxides after the milling and sintering process to resemble the desired tooth shade (Stawarczyk et al., 2017a).

2.4 CAD-CAM SYSTEMS

The removal of material from a prefabricated block to the desired shape is known as subtractive manufacturing. Milling removes material using a rotating tool either by its rotation or by rotating the material block. These movements and the path of cutting are processed and planned out by CAD software using a technology known as computer numerical control (CNC) (Vasques et al., 2022). These machines function with a spindle rotating the cutting tool positioned either horizontally or vertically. These parts will move in three linear axes (X, Y, Z) with or without further rotational movements in those planes (A, B, C). Therefore, there are six possible axes of movement however the majority of milling machines operate with four or five axes. These would include the three linear axes with additional rotational axes (Cortes, 2022). In dentistry, the 5-axes milling machines yield the highest milling accuracy. These are usually machines used in milling centres and laboratories (Hamza & Sherif, 2017). Chairside milling devices are usually 4-axes and are faster and more simplified for a single-visit workflow (Bosch et al., 2014; Hamza & Sherif, 2017; Moldovan et al., 2011b; Zeltner et al., 2017).

All CAD-CAM systems rely on three components: image acquisition (scan/impression), CAD software, and the manufacturing system (additive or subtractive). All three are different based on whether the workflow is lab-based or chairside. For ease of use, chairside systems tend to have an integrated system in which acquisition is carried out by the company’s scanner (e.g. Primescan by Dentsply Sirona), which is integrated with the CAD software and also synced with the in-house milling and sintering machine. There are open systems that offer a simplified version of the in-lab software such as ChairsideCAD from Exocad that are intended to be more user-friendly for dentists (Kim et al., 2022). Since the software is open source, the design can be exported and sent to third-party software and devices that are also part of an open system.

Other software can be part of an integrated system but is also open to other devices such as the Modellier software from Zirkonzahn.

Hamza & Sherif (2017) carried out a study comparing 5 different CAM devices about the manufacturing capabilities of monolithic zirconia restorations. In this study, a statistically significant marginal discrepancy was noted in restorations fabricated from Incoris TZI using a 4-axis milling device, CEREC MXCL (Dentsply Sirona). This study obtained similar results with all the 5-axis milling motion devices, producing accurate restorations. As expected, milling machines with 5-axis milling capabilities were found to take more time to mill a restoration. They all showed clinically acceptable marginal fit with the 5-axis and dry milling producing better marginal accuracy. In another study, the 4-axis MCXL and MCXL-EF (with extra-fine burs) were found to be more practical for chairside use and the additional time required for the use of extra-fine burs outweighed the disadvantage of adjustments to the prosthesis (Kirsch et al., 2017). Kirsch et al. (2017) found that 3- or 4-axis milling machines produce a trueness of 61 ±22μm for the intaglio surface and 55 ±18μm for the occlusal surfaces. Five-axis milling machines were found to have a higher trueness value of 41 ±15μm for the intaglio surface and an equal trueness of 55 ±18μm for the occlusal surface. The extra-fine mode in the 4-axis machine produced good results comparable to those of the 5-axis. Trueness is a means of quantifying how close the measured value is to the true value.

2.5 Preparation Designs

Different tooth preparations may influence the crown adaptation of the zirconia crown. In 2014, it was found that anatomical occlusal designs (30^o) demonstrated better marginal and internal adaptation when compared to semi-anatomical (15-30^o) and non-anatomical (0^o) (Habib et al., 2014). Superior marginal and internal adaptation were observed in occlusal surfaces that had anatomical contours with no correlation noted in mean gap values amongst the three groups. In the literature, abutments varied from manual preparation of typodont maxillary molars (Hasanzade et al., 2020b) or premolars (Ji et al., 2015; Miura et al., 2022; Refaie et al., 2023) or using one acrylic resin maxillary first molar as a master die (Hasanzade et al., 2020b) to extracted maxillary molars (Camargo et al., 2022) or premolars (Habib et al., 2014; Refaie et al., 2023) that were either sound or minimally restored in areas that did not influence the margin line. Others used fabricated custom stainless-steel dies with a U-shaped groove (Hamza &

Sherif, 2016) or brass master dies (Sasany & Yilmaz, 2023). A prospective clinical study used premolars or molars that required single complete-coverage crowns (Sanchez-Lara et al., 2023). There is no predefined standard for conducting clinical research on the marginal accuracy of restorations, even though these studies offer a more controlled structure (Tabesh et al., 2022).

2.6 Marginal Assessment

The restorative clinical success of indirect dental restorations is determined by the marginal and internal fit of the prosthesis. Having good marginal adaptation can give rise to reduced gingival irritation and cement dissolution as gaps result in marginal leakage (microleakage), periodontal disease, and secondary caries with eventual crown failure (Felton et al., 1991; Paul et al., 2020; Refaie et al., 2023). Large internal gaps may influence the retention and resistance form of the restoration with a reduction in fracture toughness of the material (Pedroche et al., 2016; Wettstein et al., 2008).

Several areas have been used to measure the marginal fit such as marginal gap, vertical marginal discrepancy, horizontal discrepancy, and absolute marginal discrepancy with the internal aspect divided into the cervical, axial and occlusal areas/points. The internal gap and marginal gap are the distances perpendicular to the internal (intaglio) surface of the restoration to the axial wall of the preparation or margin (Holmes et al., 1989). The vertical marginal gap was defined as the measurement between the crown margin and the preparation finish line. Due to cement solubility, some studies chose to assess the vertical marginal discrepancy to determine the marginal gap (Refaie et al., 2023).

To assess prostheses designs, marginal fit, finishing, and cement thickness one must address which area is being measured. Holmes and collaborators (1989) used a set of definitions to avoid misunderstanding and properly term the area being assessed and measured in the study as shown in Figure 2.1. In a recent study, Sanchez-Lara and collaborators (2023) used the mean vertical and horizontal marginal gap, along with the internal gap to evaluate marginal and internal fit. The number of measurements vary between studies starting with a minimum of three different locations for each crown (marginal, axial and occlusal). In this study, all three measurements were performed at 4 locations for each crown and for each milling system a spacer thickness of 50 µm was used. Digital spacer thicknesses vary between studies from 30 µm (Ji et al., 2015), 50 µm (Hamza & Sherif, 2016; Pilo et al., 2018), 60 µm (Hasanzade et al., 2020b; Rues et al., 2023), 70 µm (Refaie et al., 2023) up to 80 µm (Camargo et al., 2022) with some not specifying the exact value. Svanborg (2020) highlighted the importance of disclosing this information in his systematic review, especially since the parameters and settings may influence the study's results. In his review, 25 of the excluded 60 studies did not include the spacer thickness. Svanborg (2020) explained that the accuracy of the device should be influenced by how close the final fit and measurements are to the spacer setting of the software not just the clinical acceptability or the measurements as compared to the other device/material. Dahl and collaborators (2017) disclosed the internal cement space setting (70 µm) however this setting did not influence the final readings or was not discussed in the interpretation of the results and conclusion. According to the CEREC Zirconia clinical guidelines, the recommended spacer thickness by Dentsply Sirona was 80 µm (Dentsply Sirona, *Clinical guidelines for CEREC Zirconia*).

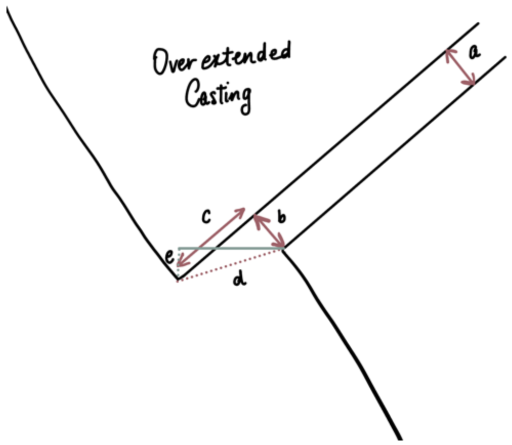

Figure 2.1 *The labelled areas are defined as follows: a. Internal gap, b. Marginal Gap, c. Overextended margin, d. The absolute marginal discrepancy, e. Vertical marginal discrepancy (the distance between the crown margin to the edge of the finish line preparation). Figure by author.*

Table 2.1 *Overview of acceptable internal space proposed by authors in the literature (by author).*

Internal Space	Studies
20 to 40 µm	(Fransson et al., 1985)
25 to 40 µm	(Boening et al., 2000; Øilo & Evje, 1986)
50 µm	(Beuer et al., 2009)
50 to 100 µm	(Martins et al., 2012)
60 to 83 µm	(Christensen, 1966; Reich et al., 2005; Sulaiman, F. et al., 1997)
120 µm	(McLean, 1971a)

As shown in Table 2.1, there is lack of consensus in the literature regarding the clinically acceptable maximum marginal gap. Most authors chose to accept 120 µm as a threshold, as suggested by Mc Lean and von Franhoufer (1971) (Boitelle et al., 2018; Camargo et al., 2022; Contrepois, Mathieu et al., 2013; Hasanzade et al., 2020b). Most studies were carried out *in-vitro* due to the limitation of marginal adaptation analysis and the need to assess ultimate fit after cementation. One prospective clinical study (Sanchez-Lara et al., 2023) assessed the fit of the crowns using digital superimposition after the dies and the intaglio surfaces were scanned using a tabletop scanner and the seated crowns were then scanned using IOS to develop the alignment scan. These scans were then imported onto DentalCAD (exoCAD; Exocad DentalCAD, Darmstadt, Germany) and superimposed manually using reference points and the best-fit algorithm. The vertical and horizontal discrepancy including the internal gaps were then measured using a reverse engineering software program (Geomagic; 3D Systems, Morrisville, NC, USA). It was concluded that CAD-CAM posterior crowns exhibited a greater vertical margin discrepancy (120 µm) than those fabricated using the conventional technique (100 µm).

In the literature, various methodologies for fit accuracy and marginal adaptation evaluation of FDP were used (Camargo et al., 2022; Contrepois, Mathieu, D.D.S. et al., 2013; El-Ashkar et al., 2023; Park, Jin-Young et al., 2017; Son et al., 2019). Marginal adaptation can be measured with subjective and qualitative methods (Mously et al., 2014) using an explorer or visual examination. Evaluation of the intaglio surface can also be carried out with low-viscosity polyvinyl siloxane material (Fit Checker; GC Corp), however, visual analysis can be subjective and dependent on the researcher's experience (Mitchell et al., 2001). For quantitative analysis, there are two different approaches:

(1) Destructive protocols include the cementation of the restoration on to dies which are then embedded into epoxy resin. The samples are then sectioned buccolingually and/or mesiodistally along the long axis to assess and measure the cement layer (marginal and internal gaps) directly under a microscope (Ji et al., 2015; Sachs et al., 2014),

(2) Non-destructive protocols include:

    a. Direct view (DV) which involves the cementation of the crown and assessed under magnification to evaluate the external marginal gap (crown-abutment interface)

b. Silicone replica technique (SRT) which involves making images of the discrepancy volume from silicone sections by using light-body silicone to simulate the cement layer followed by heavy-body impression material which is then sectioned to be examined under a microscope (Revilla-León et al., 2020; Ryu et al., 2020). Due to its non-destructive nature, the SRT can be used for in-vivo and in-vitro studies.
c. Triple-scan method (TSM) (Boitelle et al., 2018; Boitellea et al., 2016; Dahl, Bjørn Einar et al., 2017a; Holst et al., 2011; Park, Ji-Man et al., 2017) which was later confirmed to be a suitable method for 3D assessment of zirconia crowns (Li et al., 2021),
d. Electron microscopy (Camargo et al., 2022; Habib et al., 2014),
e. Micro-computed tomography (micro-CT) using a cone-beam x-ray source to allow 2D and 3D analysis of seated or cemented restorations (Camargo et al., 2022; Pimenta et al., 2015).

In 2019, a validation study was carried out for the SRT, and it was concluded that this technique was found to overestimate gaps by 2% to 11% (Segerström et al., 2019). It's a frequently used approach, and despite the good results, like the destructive cross-section technique, it offers a limited number of points similar to other 2D analysis techniques. Other disadvantages include a risk of light-body material rupturing during the restoration removal process, incorrect seating of the restoration, and inaccuracies of replica sectioning. It was also considered to be time-consuming, and difficult to standardise. Twelve studies were found to use this technique, with one of these studies using a digitalised version of the RT (Dahl, Bjørn E. et al., 2018) according to a systematic literature review (Ahmed et al., 2020). The quality of marginal fit assessment along with internal fit evaluations is correlated to the number of points of measurement.

The *in-vitro* cross-section method (CSM) is a method adopted by several studies (Habib et al., 2014; Ji et al., 2015; Nawafleh et al, 2013). It directly assesses fit by sectioning the specimens along the same plane (mesiodistal or buccolingual) after cementation of the milled crown with the cement of choice, conventional glass-ionomer cement or resin cement (e.g. Rely X Unicem, 3M, St. Paul, Minnesota) respectively and measuring the cement gap using an electron or light microscope. The measurements of internal and marginal fit of the prosthesis are measured from the actual cemented prosthesis, which reflects the clinical scenario. However, due to the destructive nature of this method, there is a loss of information with two-dimensional (2D) limitations (Kirsch et al., 2017; Kuhn et al., 2014). Several articles have expressed the other limitations and errors that arise from these methods of gap size estimation, which include the importance of a consistent identical cross-sectioning angle, limited number of measurement points confined within the cross-sectioned area, assessment limited to the vertical direction and within the cross-sectioned plane; buccolingual or mesiobuccal (Camargo et al., 2022; Holst et al., 2011; Moldovan et al., 2011a; Revilla-León et al., 2020).

Refaie and collaborators (2023) used a stereomicroscope with a digital camera to assess the vertical marginal gap before using the SRT to evaluate internal fit. A similar method was used using a rotating measuring chuck and a digital microscope measuring standardised predetermined positions (Ahmed et al., 2019). Seating problems tend to be masked along with other differences such as premature contacts and chippings (Mahmood et al., 2019).

To overcome challenges with replicating the exact points of silicone sectioning or virtual plane positioning, Hasanzade and collaborators (2020) created an aluminium hex-shape index which assisted in virtual alignment and sectioning. Other studies used a spatial reference system (Boitelle et al., 2018) or a guide template that fit over the master model (Son et al., 2019).

Some authors have concluded that basing clinical acceptability on mean marginal gap size does not provide adequate information on the overall fit and the relationship between the FDP and the tooth prep (Camargo et al., 2022). This is overcome using micro-CT (Rungruanganunt et al., 2010) or the triple-scan protocol (Holst et al., 2011) both of which address all the above problems and allow full 3D evaluation of fit using a non-destructive quantitative approach. One main disadvantage of the triple-scan protocol is the risk of miscalculations and inaccuracies that may occur with scanned data, especially with few matching points. It is more practical and affordable when compared to the use of micro-CT (Son et al., 2019). It overcomes other challenges that the latter must face which include the risk of exposure to radiation and metal artefacts.

2.7 TRIPLE SCAN PROTOCOL

The triple scan method of crown evaluation is a more recent method of marginal and internal gap assessment. This method consists of three different scans: the preparation, the fabricated crown (most importantly the intaglio surface) and the crown seated on the master die, allowing virtual alignment and evaluation of fit. The scans can be made with an intra-oral, industrial or desktop scanner. Assessment of single units was found to be effective using this approach, as described by Holst and colleagues (2011). Due to the nature of this technique, this protocol can also be used for implant-retained prostheses not just limited to tooth-borne restorations. A virtual registration of a digitalised restoration and its master die/abutment will avoid any errors or obstacles associated with the cement space and cementation process. It also allows repeatability of the prosthesis' virtual alignment due to its non-destructive nature.

In an attempt to prove this protocol's repeatability, the 2011 study obtained near-perfect association ($r = 1$) in terms of Pearson's correlation coefficient amongst all three attempts (measurements I, II, III). No significant differences regarding the mean distances measured were noted ($p = 0.170$) (Holst et al., 2011).

When the measurements of fit are performed on the original abutment, one eliminates the use of other materials and processes which may be difficult to replicate precisely. Extrinsic factors which may give rise to errors include the morphology of the preparation and prosthesis, and the quality of the surfaces even though these errors are dependent on the noncontact scanner's quality and are not specific to this protocol (Cortes et al., 2022; Holst et al., 2011). This technique can be used in a clinical situation but is limited to distinct landmarks (e.g. teeth) that may assist the registration process for the superimposition of the scans (Loetzerich et al., 2023). Several studies have reported it to be a reliable and reproducible method of crown fit assessment (Boitelle et al., 2018; Li et al., 2021; Li et al., 2023).

2.8 TRUENESS (3D DEVIATION)

To assess the accuracy of milling devices one must assess the trueness and/or precision of the produced crowns. Trueness refers to the closeness between the measured values (e.g. milled crown) to the true value (e.g. CAD crown). This can be influenced by one of the three main steps of CAD-CAM systems: scanning, designing, and manufacturing.

Intraoral scanners have been regarded as the most accurate method for CAD-CAM crowns and short-span FPD compared to conventional impressions (Morsy et al., 2021). Digital impressions eliminate distortion errors of impression materials, improve comfort and acquisition, and reduce long-term costs (Memari et al., 2019). The mean IOS trueness was found to be between 19 and 26 µm (Mejía et al., 2017). In 2022, a systematic review assessed 9 studies which compared 3D data from IOS meshes (a set of triangles that make up the 3D file) with the reference scans obtained from either industrial optical scanners or desktop scanners (Cortes et al., 2022). It was concluded that the Trios 3 (3Shape) exhibited the highest trueness in all the comparisons with Omnicam (Dentsply-Sirona) (Ashraf et al., 2020; Kernen et al., 2022; Resende et al., 2021). However, Primescan (Dentsply-Sirona) the latest addition to the Dentsply-Sirona line-up, was found to have superior trueness to Omnicam (Kontis et al., 2021; Kontis et al., 2022) and exceeded the Trios 3 in best trueness values in a separate study (Kim et al., 2022).

To quantify the quality of the milling process, the entire milled surface needs to be compared to the CAD data (the designed prosthesis). After the manufactured crown is scanned, the software aligns the CAD file (reference file) with the milled crown using the best-fit algorithm using 3D correspondence between two points in the meshes. This allows the superimposition of both files, enabling the software to determine the distance between the objects via positive (+) and negative (-) deviations. Three-dimensional superimposition allows complete visualisation of the entire crown surface including the intaglio surface with multiple points compared to other methods which tend to have only selected measurements. This is usually represented with a colour-difference map. Previous studies have investigated the trueness and precision of milling devices using this method (Al Hamad et al., 2021a; Bosch et al., 2014; Cho et al., 2019; Kirsch et al., 2017). In the literature, most commonly the MCXL (Sirona Dental Systems) and inLab MC X5 (Sirona Dental Systems), authors used mesh deviations to determine the accuracy of the milling devices (Abualsaud & Alalawi, 2022; Kirsch et al., 2017). Kirsch and collaborators (2017) concluded that the MCXL with extra-fine burs (EF) showed significantly higher overall trueness than the other groups (34.4 ± 7.5 µm inner surface and 25.7 ± 9.4 µm occlusal surface), with the inner surfaces exhibiting the highest trueness. The MCXL-EF and the X5 had the longest milling time of approximately 35 minutes.

2.9 Statement of the Problem

By appreciating the importance of a well-adapted crown and the risk factors that may lead to its failure, the importance of an accurate and precise milling machine is crucial. However, with this fast-developing field of dentistry, it has become increasingly difficult to determine whether to proceed with a lab-fabricated workflow that is more time-consuming and at times more expensive as opposed to a faster, relatively cheaper, and more convenient workflow done chairside. Very little is known about the trueness and marginal discrepancy of a monolithic zirconia crown fabricated by the latest high-end chairside systems, compared to the integrated laboratory ones.

2.10 Aims and Objectives

The purpose of this *in-vitro* study is to compare the trueness and adaptation of 15 monolithic zirconia crowns milled using a chairside workflow (CEREC Dentsply Sirona) with a laboratory workflow (Zirkonzahn).

2.11 Null Hypothesis

The null hypotheses of the study are that:

1) The marginal and internal fit of monolithic zirconia restorations would not be affected by the type of digital workflow.
2) The trueness of monolithic zirconia restorations would not be affected by the type of digital workflow.

Chapter 3: Materials and Methods

This in-vitro study was approved by the Faculty Research Ethical Committee (FREC) of the Faculty of Dental Surgery, University of Malta, under the protocol number: DSG-2023-00025 (Appendix A).

3.1 Tooth Preparation, Scanning and Crown Manufacturing

A fully dentate maxillary typodont (basic study model, KAVO) was used to prepare a maxillary right second premolar tooth to receive a full coverage zirconia crown.

Using a silicone index as a preparation guide, the tooth was prepared with Intensiv Universal Prep Set Prof. Christoph Hämmerle, Clinic for Fixed and Removable Prosthodontics, University of Zurich bur kit, creating a chamfer finish line using the 305L bur. The configuration and dimensions of the prepared tooth are found in Table 3.1.

Table 3.1 *Maxillary right second premolar typodont tooth preparation dimensions.*

Preparation Features (In accordance with CEREC Zirconia clinical guidelines)	
Finish line	Supragingival chamfer with smooth continuous finish line
Convergence	Max of 10 degrees
Height	Min of 4 mm
Minimum thickness	Margin: 0.5 mm Axial: 0.8mm Occlusal: 1mm
Type of preparation	Anatomical

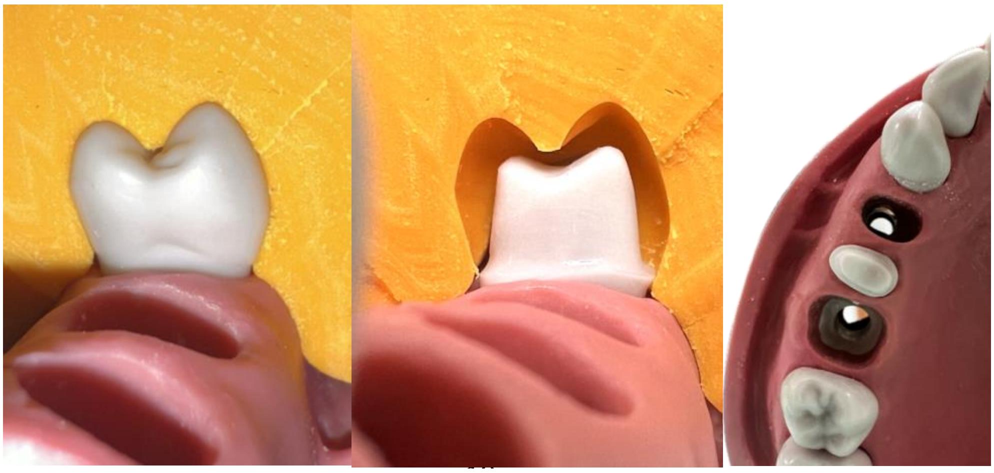

Figure 3.1 *Typodont upper first premolar preparation. Left: Silicone index of unprepared tooth. Middle: Silicone index with prepared tooth using the recommended dimensions. Right: Occlusal view of preparation with adjacent teeth removed for better visualisation during preparation.*

Sample size selection calculation using Noether's formula resulted in a minimum of n = 15 milled crowns for each group (Lab and Chairside) (Noether 1987). The prepared Kavo tooth (master die) was scanned using the Primescan Scanner (Dentsply Sirona). The upper arch and lower arch scans were exported after bite registration as STL files to the Lab software.

For the chairside group, the scans were used to design a monolithic zirconia crown using CAD software (CEREC chairside software). The restoration was designed using the recommended parameters as shown in Table 3.2. The final crown file was exported to be used as a guide for the lab workflow enabling the design of a similarly shaped crown to that of the chairside group.

Table 3.2 *Manufacturer's recommendations for zirconia crown fabrication using CEREC Zirconia Chairside Workflow.*

Restoration Parameters (In accordance with the CEREC Zirconia Clinical Guidelines)	
Spacer	60 µm*
Occlusal Milling Offset	0 µm
Proximal Contacts Strength	0 µm
Occlusal Contacts Strength	-25 µm
Dynamic Contacts Strength	-50 µm
Minimal Thickness (Radial)	800 µm
Minimal Thickness (Occlusal)	1,000 µm
Marginal Thickness	30 µm (milling fine)

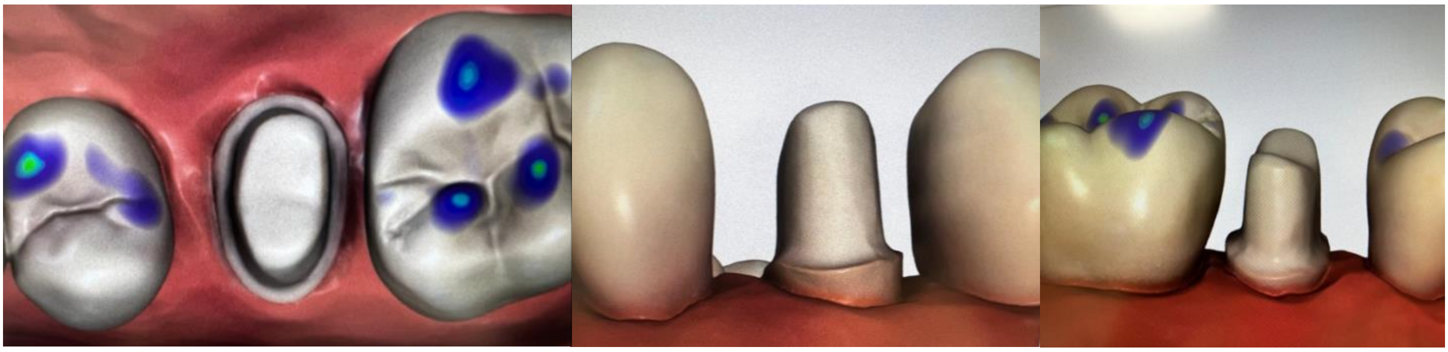

Figure 3.2 *Screenshots from the Sirona design software after scanning with CEREC Primescan.*

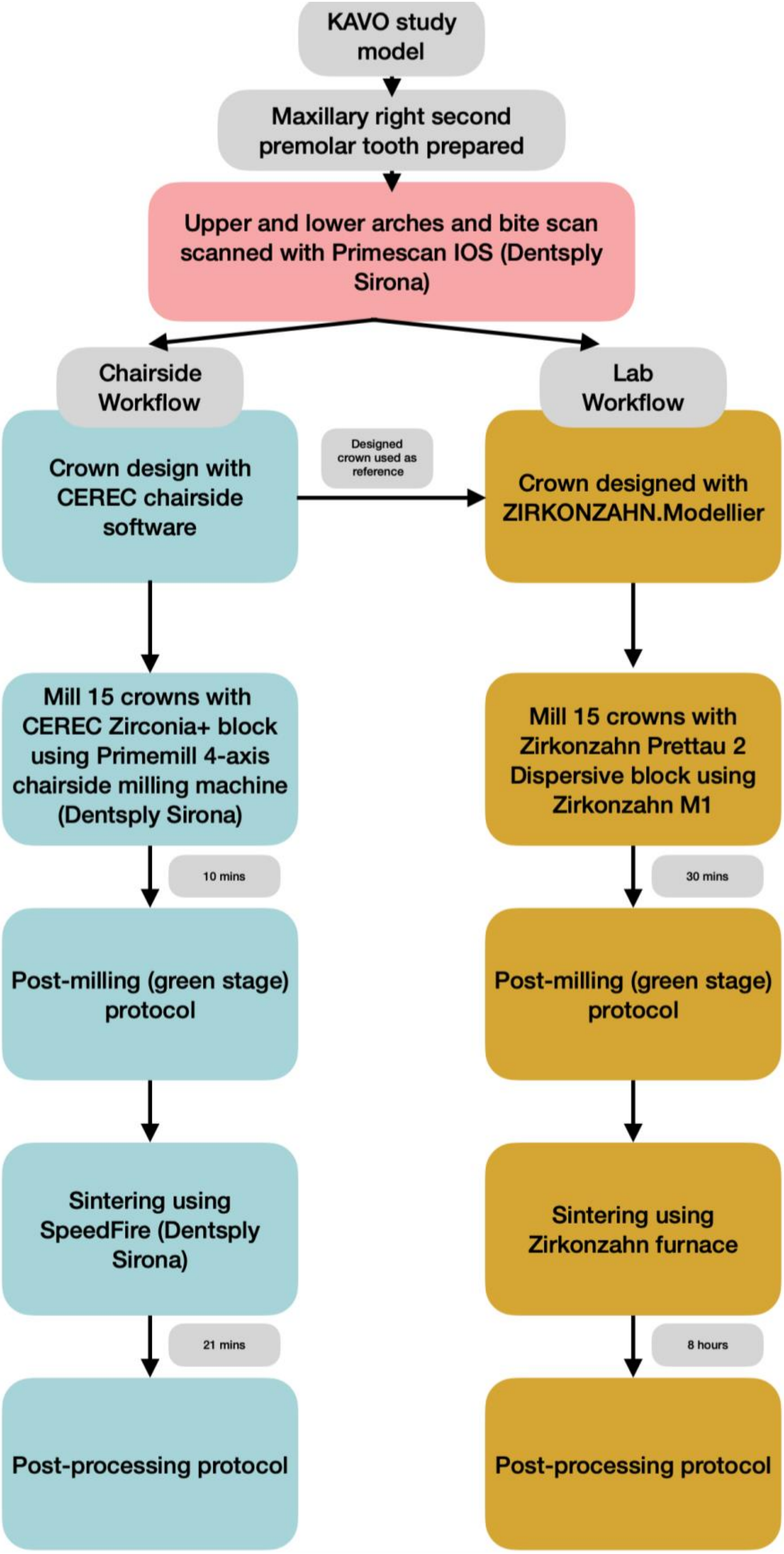

Figure 3.3 *After the upper and lower model scans, including the bite-registration scan, the STL files were sent to the workflow's respective software. CAD/CAM workflow for Chairside group (left) and Lab group (right).*

3.2 CHAIRSIDE CAD-CAM WORKFLOW

1. Upper and lower arch scan followed by buccal bite registration scan using Primescan intra-oral scanner.
2. Tooth 15 was selected (on the CEREC SW 5.0; Sirona Dental Systems, Bensheim, Germany) for an anatomical crown followed by the selection of the material of choice, Zirconia+, and the devices of choice, CEREC Primemill and CEREC SpeedFire.
3. Model axis tool used to align arches according to the curve of Spee.
4. The crown margin was marked manually to define the preparation-finish line.
5. The milling axis/insertion axis was adjusted.
6. Adjustment of restoration parameters according to Table 3.2.
7. A biogeneric variation software tool was used to create the 'master' CAD model.
8. Assess the positioning of the crown, buccal and palatal positioning using the shape tool and form tool (add, smooth, and remove) (Figure 3.4).
9. One reference marker, in the form of a circular dome, was added on the buccal and lingual aspect of the restoration using the "add" tool, followed by the "smooth" tool.
10. Mild fine-tuning of occlusal and interproximal contact using the adjust contacts tool to the pre-determined parameters.
11. The CEREC Primemill 604550 was switched on and connected to the design software.
12. The extra fine milling setting was selected with the CEREC Primemill.
13. The add block button was selected and the QR code on the new Zirconia+ mono A2 milling block was scanned by the device.
14. All burs were above the recommended percentage use.
15. The milling time was approximately 10 minutes.
16. The restoration was separated from the attachment and polished before pre-sintering using the Jota Green Stage Finishing bur box (Figure 3.5):
    a. The C31RL.HPL.010 bur was used to detach the attachment.
    b. The ZIR9972M.HP.100 bur was used to smoothen the residual connector area and surface smoothening.
    c. The 9840.HP.140 bur was then used for the final polishing stage before sintering.
17. The crown was then airdried and any residual powder was removed using a microbrush.

18. The crown was then placed and positioned on the firing chamber according to the orientation requested by the SpeedFire display.
19. The sintering duration was around 21 minutes.
20. The restoration was then removed from the oven using tweezers and placed on the SpeedFire's fan area until cooling down to be able to touch.
21. No glazing or other post-processing steps were carried out.
22. The designed crown was exported as an STL file via inLab CAD software (inLab Software; Sirona Dental Systems, Bensheim, Germany).

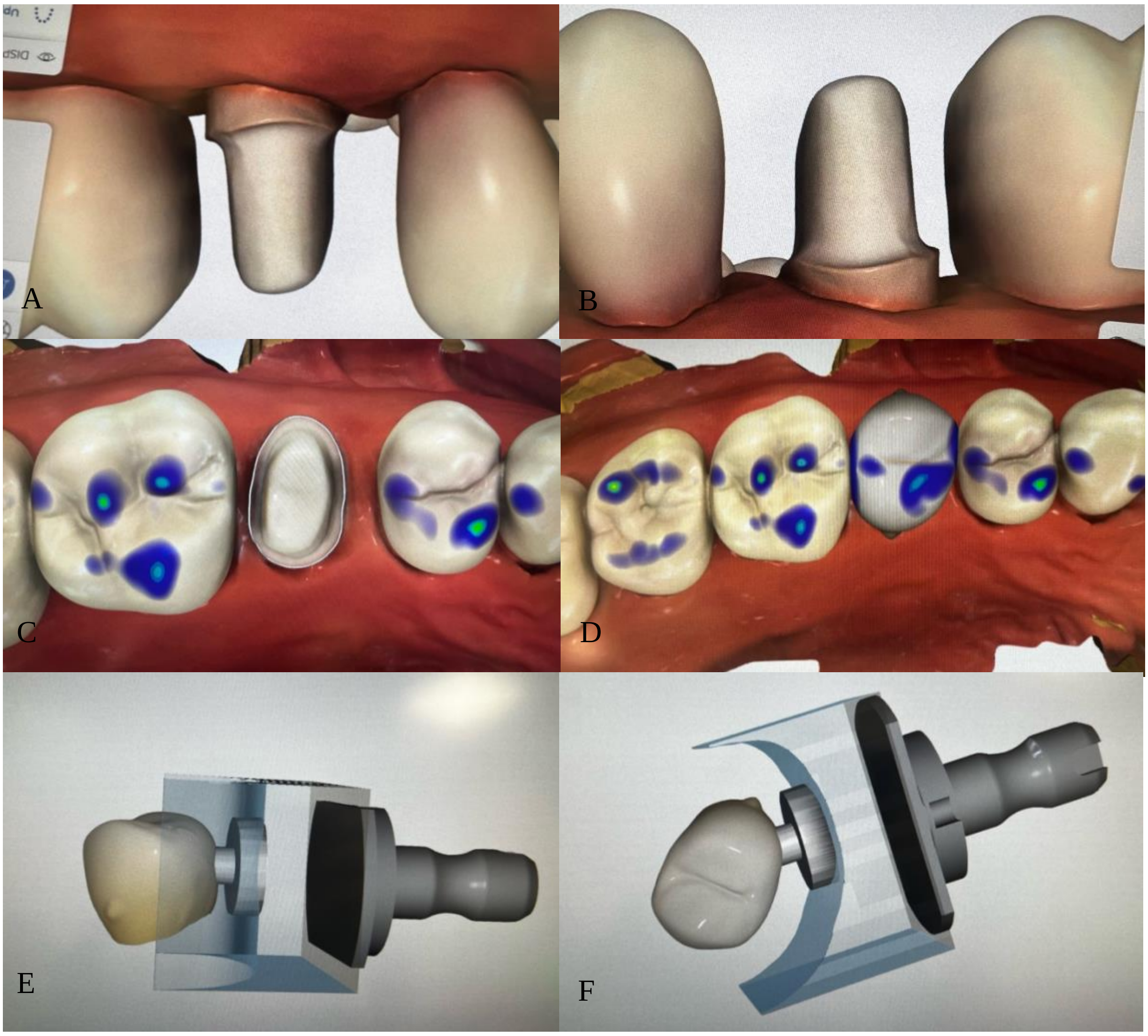

Figure 3.4 *Screenshots of the chairside crown fabrication workflow using the CEREC software. (A) Occlusal view of the scanned preparation and adjacent teeth. (B) Buccal view of the supragingival preparation of the upper right second premolar. (C) Manual margin identification and outlining. (D) Biogeneric tooth selected with additional buttons one on the lingual and another on the buccal aspect. (E and F) Positioning of the final crown in relation to the spur location.*

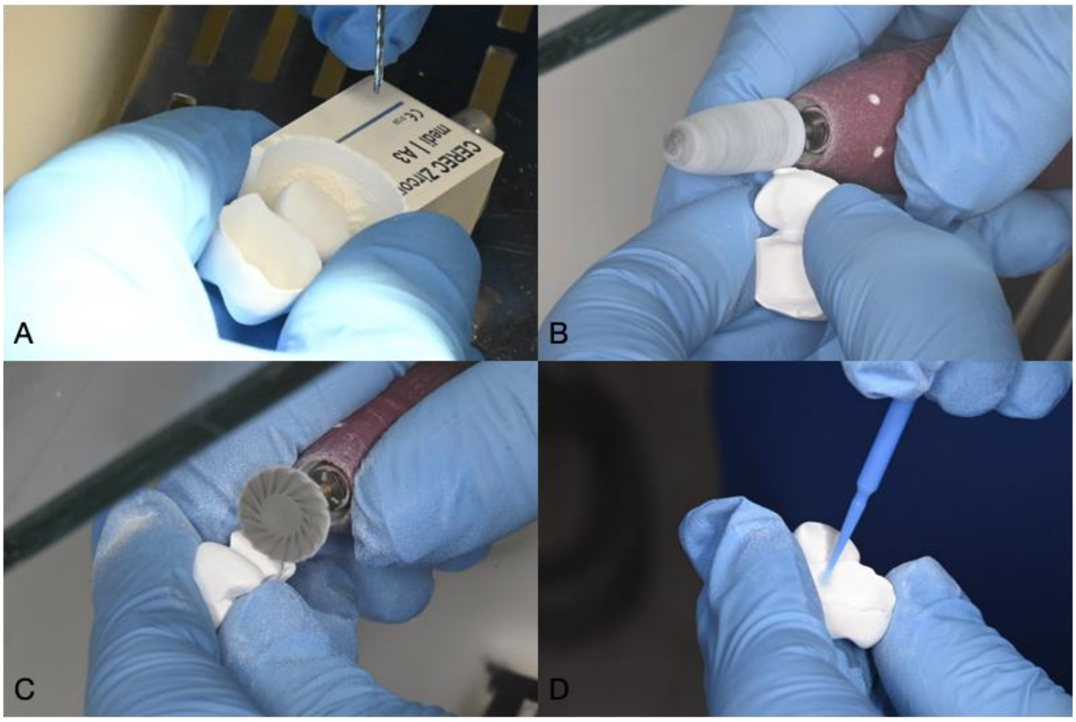

Figure 3.5 *Pre-sintering polishing protocol. The photos were taken during another case of a mesial cantilever bridge. The steps, machine and burs used were identical to those used for this thesis. Photos were taken by the author. (A) The C31RL.HPL.010 bur was used to detach the attachment at 10,000 rpm. (B) The ZIR9972M.HP.100 bur was used to smoothen the residual connector area and surface smoothening at 6,000 rpm. (C) The 9840.HP.140 bur was then used for the final polishing stage before sintering at 7-12,000rpm. (D) The crown was then airdried using a 3-in-1 syringe and any residual powder was removed using a microbrush.*

3.3 Lab CAD-CAM Workflow

1. A new project was selected on the ZIRKONZAHN.Archiv Software and tooth 15 was selected, followed by Anatomic Crown and the adjacent and antagonist teeth were selected.
2. After the project was saved the Modellier Software was then selected to proceed to crown fabrication Figure 3.6.
3. The exported STL files of the scanned upper and lower arches using the Primescan were imported in the ZIRKONZAHN.Modellier software.
4. The path of insertion was selected followed by a manual margin selection.
5. The recommended gap parameters for zirconia milling remained unchanged:
    a. Cement gap start 0.50mm
    b. Cement gap 0.035mm
    c. Block out angle 0^0

    d. Additional occlusal distance 0.010mm
    e. Border parameters:
        i. Horizontal 0.15mm
        ii. Vertical 0.00mm
        iii. Angled 0.30mm
        iv. Angle 65^0
    f. Milling diameter 1.05mm

6. The copy/mirror tooth option was used to import the new crown to the margin.
7. The chairside STL file of the designed crown was added to the project using the right-click "add mesh" option.
8. The chairside mesh was superimposed on the lab crown and modifications were carried out to best match the anatomy of the other system including the reference markers.
9. Modifications to the crown were carried out using the "Free forming" mode and the "±Add/Remove" and "Smooth" options.
10. The "Adjacents" button was selected for the Adaptation Option to adjust interproximal contacts.
11. The chairside mesh was then deleted and the "Finalize" option was selected.
12. The final crown was then sent to the ZIRKONZAHN.Nesting software in the nesting queue.
13. The Zirkonzahn Prettau 2 Dispersive block was registered on the system and the queued crown was then added to the block.
14. A minimum of three supports were added to each crown and placed on the equatorial region (Figure 3.6).
15. The high-quality milling strategy was selected, and the parallel CNC path calculation was carried out.
16. Milling of one unit takes approximately 30 minutes.
17. After milling, similar pre-sintering steps were carried out to the chairside workflow (step 16).
18. The crowns were then seated on a sintering tray with fine grain sintering granules and placed in the sintering chamber of the Zirkonofen Turbo sintering machine (Zirkonzahn) (Figure 3.7). A conventional sintering setting was selected which has a duration of 8 hours.

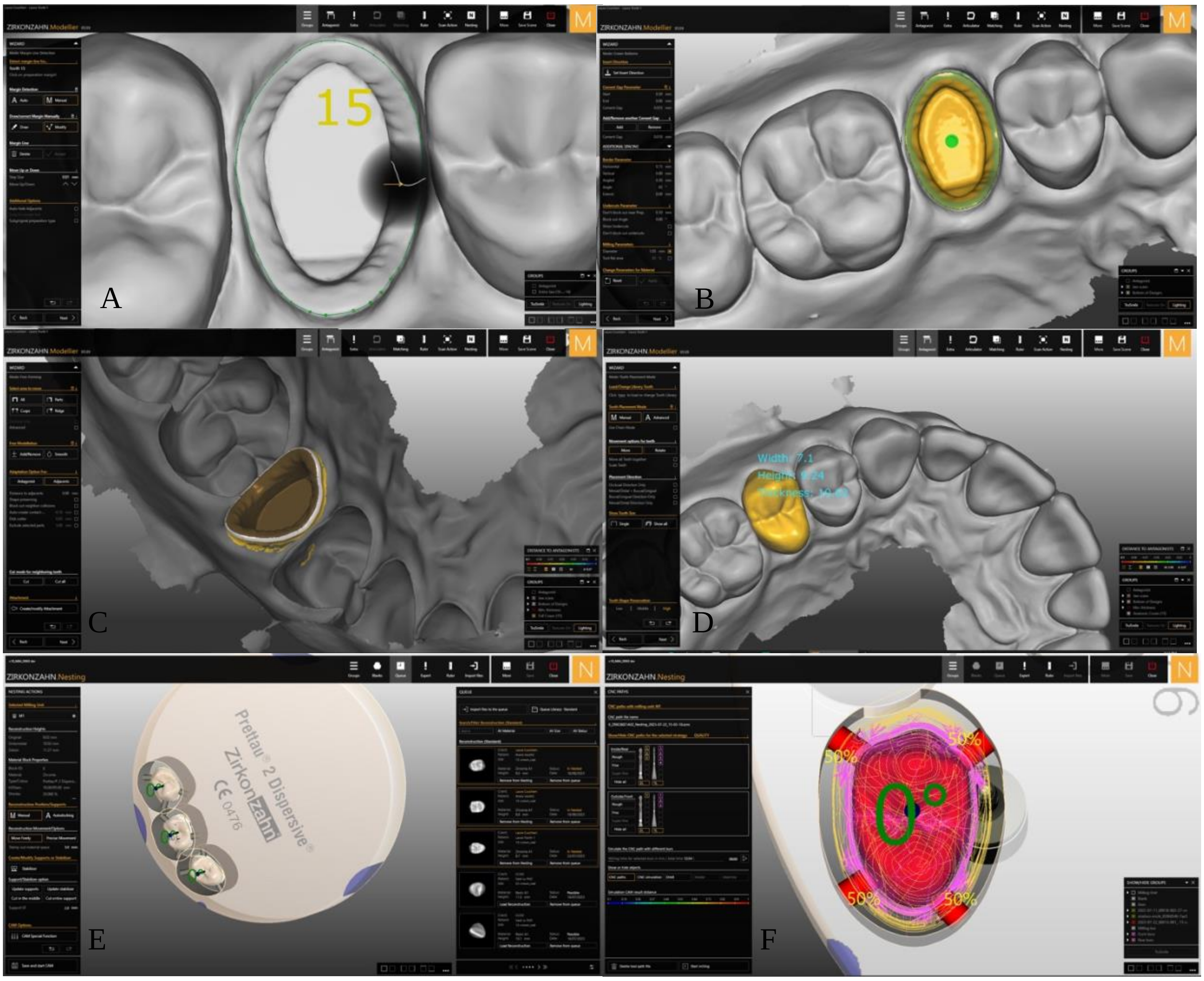

__Figure 3.6__ (A) Margin outlining using the manual function using the ZIRKONZAHN.Modellier software. (B) Insertion direction adjustment. (C) Contact adjustment. (D) Adjustments to tooth morphology and shape. (E) Three crowns in the ZIRKONZAHN Nesting software prior to milling with supports on the equatorial line demarcated as a green line. (F) CNC strategy with recommended burs.

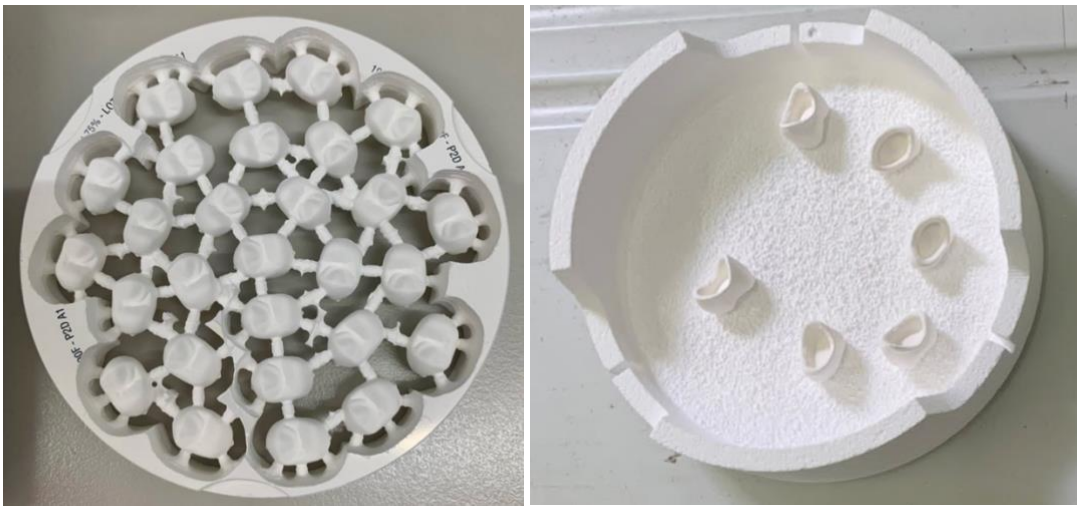

__Figure 3.7__ (Left) Zirconzahn Prettau 2 A3 blank with the milled crowns before removal of attachments. (Right) After attachment removal and polishing of the zirconia crown in the green stage using listed burs, the crowns were placed on a sintering tray with a base of fine-grain sintering granules as requested by the manufacturer before undergoing conventional sintering protocol. Granule size: 0.4mm-1.0mm

3.4 TRIPLE SCAN TECHNIQUE: PREPARATION

A provisional scanning aid was created with dental stone and straight-line markings that would eventually be used as a guide for the virtual cross-sectional planes. The initial prototype (Figure 3.8) had a large surface area which made it difficult for the scanner to patch the meshes and detect certain areas that appeared smooth. Therefore, having uneven and varying surface characteristics would allow the scanner to detect the scanned surface with more accuracy and speed. Scanning of the updated scanning plane (Figure 3.9) was faster with minimal difficulties in identifying the part of the block. The main disadvantages with the second block were: 1) the possibility of minor rotations of the stock resin tooth which gave slight inconsistencies and 2) the presence of grooves in one of the zones which were later found to be difficult to use in the point matching stages. The final guide (Figure 3.10) overcame the mentioned limitations along with a couple of other features namely: 1) perpendicular planes for easier cross-sectional planes and 2) the base of the acrylic stock tooth was adjusted and cut to enable a locking feature in the stone eliminating the possibility of rotation and improper placement.

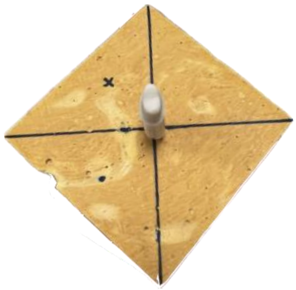

Figure 3.8 *Initial prototype made with casted stone in a square mould. Initial lines were made with permanent markers to determine where the final grooves needed to be made as virtual plane positioning guides.*

Figure 3.9 *Improved prototype with smaller surface area for easier scanning, deeper grooves, irregular areas for landmark identification for best-fit superimposition and reduced tooth exposure to reduce surface area for scanning of die.*

Figure 3.10 Final guide (left) with more distinct sections, buccolingual and mesiodistal lines at right-angles to the planes of the block with an anti-rotational indent at the base (middle) to prevent resin die (right) from rotations or inconsistent positioning.

Modifications were also made to the crowns. Due to the smooth surface and lack of multiple distinct landmarks on the milled crowns, the virtual superimposition of the scanned files using various CAD software (Exocad; Exocad GmbH, Darmstadt, Germany; ZEISS Inspect Optical 3D; Geomagic Control X, 3D systems) was found to be challenging. This was overcome by incorporating 2 reference points on the CAD file in the form of smooth spherical protrusions, one on the buccal aspect and another on the lingual.

3.5 Triple Scan Technique: Scanning Procedure

The triple-scan technique was implemented using multiple modifications in scanning techniques, superimposition of meshes, scanner brands and crown seating protocols.
The initial scanning protocol was carried out using the 3Shape Trios 5 Intra-oral scanner as follows:

1. Valustick sticky applicators (909 Premium Plus) were used to fix the dental crown in place during the scanning process.
2. The removable option was chosen followed by the full denture.
3. The scan denture option was selected.
4. The occlusal surface of the crown was scanned according to the manufacturer's suggestion.
5. The scanner wand was rotated to a 45–90-degree angle towards the approximal and buccal surface specifically focusing on the reference markers.

6. The scanner was stopped, and the stick was removed and placed in an approximal area.
7. If the stick was included in the scan, the mesh was trimmed using the cutting option accordingly.
8. The intaglio surface was then scanned starting from the occlusal as a reference starting point (CROWN SCAN-CS).
9. All the surfaces were then checked for voids and corrected accordingly. The colour setting was turned off to inspect the scanned surface further.
10. The crown was scanned when seated on the prepared tooth master model and both components were scanned with a single scan (SEATED SCAN-SS).
11. The master die and scanning aid assembly were scanned once (MASTER SCAN-MS) and used for all the digital analysis.

During the superimposition process and virtual seating assessment using the aforementioned CAD software, it was noted that there was a noticeable overlap of meshes (CS and MS). This is not clinically possible and is an error and limitation of the triple-scan technique associated with minor scanning discrepancies or the superimposition process. These errors were noted:

1) with the **Trios 5 scanner** with 3 scans (CS, SS and MS) after initial alignment and best-fit virtual alignment with **passive seating** of the crown on the preparation.

2) with the **Trios 5 scanner** with 3 scans (CS, MS and bite registration scan to align both scans in-situ) with manual alignment orientation* option with **passive seating** of the crown on the preparation.

3) with the **Trios 5 scanner** with 3 scans (CS, MS and bite registration scan to align both scans in-situ) with manual alignment orientation* option with **cementation** of the crown with **light-body silicone** on the preparation.

4) with the **Primescan** scanner with 3 scans (CS, MS and bite registration scan to align both scans in situ) with **passive seating** of the crown on the preparation.

*During the bite-registration scan of the seated crown, the Trios 5 was unable to orientate both scans in the correct position and needed the manual alignment option which required a total of two points per scan. Both cemented and passive seating attempts exhibited large discrepancies immediately after orientation on the 3Shape software in the margin line and crown position (Figure 3.11).

Figure 3.11 *Screenshots taken using 3Shape 3D viewer showing overlap of meshes (left and middle). Marginal discrepancy visible after bite registration stage using the Trios 5 scanner directly after the scans (right).*

When attempting to scan the seated crown on the preparation using the Primescan scanner, both scans aligned immediately without the need for additional adjustments/alignment.

The final methodology was adjusted as follows:

- All steps from section **3.5** (Steps 1-9) were carried out however the SS step was altered to a bite-registration scan instead.
- With every crown sample the MS (lower arch scan) and CS (upper arch scan) were scanned followed by the in-built bite-registration option on the Primescan software which superimposes the first two scans (upper and lower scans) during the SS scan.
- A small amount (1/3 of the crown full) of normal set light-body silicone material (Type 3 ISO4823 elite HD+ by Zhermack, Rovigo, Italy, LOT 408932) was inserted in the crown after partial exudation of the initial material.
- This was followed by the removal of excess material using a microbrush and sharp probe, cleaning the surface from residual silicone material.
- Constant finger pressure was applied evenly whilst a 5-minute timer was set to ensure complete setting of material (working time 2’00’ and 3’30 time in mouth).
- This was followed by a scan of the scanning aid and crown until full registration was noted by the software via a “tick” icon.
- The files were then exported via STL format.
- In contrast to the other four techniques, the latter workflow produced an alignment without overlapping meshes as shown in Figure 3.13.

Figure 3.12 *Scanning set up photo showing the two different crown groups in separate numbered boxes, the scanning aid and die, light body silicone material, micro-brushes and the adhesive tip for crown scanning.*

Figure 3.13 *Screenshot of 3Shape 3D viewer of the virtual alignment using the Primescan scanner and the scan of a cemented crown using light-body silicone.*

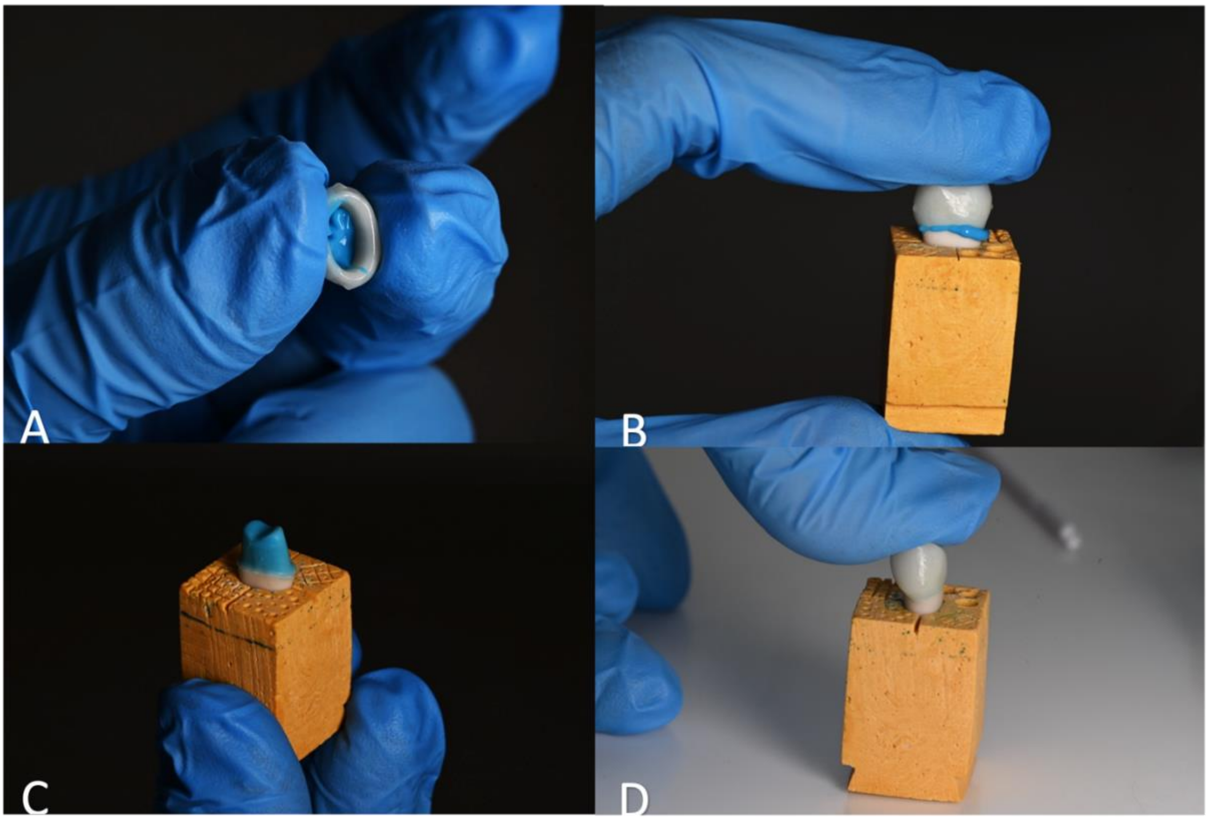

Figure 3.14 *Crown "cementation" for seated scan scanning. (A) Photograph of amount of light-body placement. (B) Excess light-body before removal. (C) Uniform distribution of light-body silicone after crown removal. (D) Constant fingerpressure positioning on hard surface after excess silicone removal.*

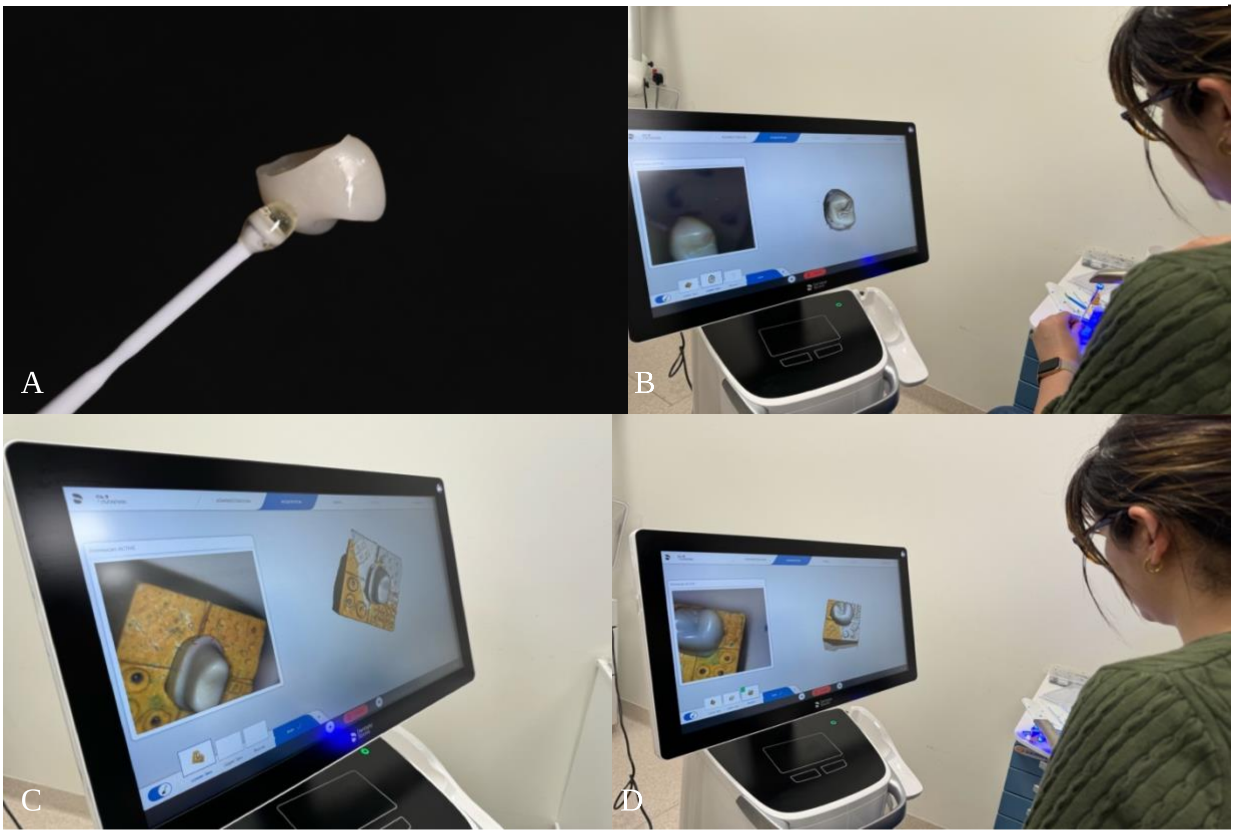

Figure 3.15 *(A) Close-up photograph of the adhesive tip placement during crown scanning (CS). (B) Scanning of the crown using the "upper arch" scan setting on Primescan, starting from the occlusal surface. (C) Scanning of the prepared tooth and scanning aid using the "lower arch" scan setting on Primescan. (D) Bite-registration scan of the seated and "cemented" crown until a tick is visible on the software which indicates alignment of both scans.*

3.6 SAMPLE ORGANISATION

To ensure that the crowns were not mixed, each crown was stored in a separate compartment in a separating box according to which group it belonged to. Each compartment was numbered, and that number corresponded to the saved STL. The files were named CS1, 2, 3 etc. if they were manufactured using the chairside workflow, and LB1, 2, 3 etc. if they belonged to the lab workflow group. The boxes were stored in the CAD-CAM & Digital Dentistry Laboratory (CCDD Lab) of the Faculty of Dental Surgery, University of Malta.

Figure 3.16 *Storage boxes showing each crown separate with dividers and numbered accordingly.*

3.7 MARGINAL AND INTERNAL GAP ANALYSIS

The MS and CS were imported to Zeiss Inspect 2023 (formally known as GOM Inspect) and the following steps were taken to assess the marginal and internal gaps through virtual buccolingual and mesiodistal cross-sections:

1. The MS file was imported first as the reference CAD file as a new part with the option "CAD body" selected.
2. CS was then imported and "Add to part" was selected.
3. Operations menu button followed by "alignment", "initial alignment" and the "define original alignment as initial alignment" option was selected enabling the scans to align according to the orientation of the bite registration scan.
4. Picture in picture (PIP) button selected followed by "clipping at plane". The plane to be assessed is drawn using the scanning aid as a guide. The plane is drawn 0.5mm to one side (right or left). This would lead to the cropping of the undesired area.
5. The mesh of the crown is hidden to visualise the preparation and the preparation is then selected.

6. The "Construct" button is selected followed by "Section" and "Single section". The positioning value is set at -0.5mm to enable the correct positioning of the virtual plane about the visible grooves on the scanning aid block.
7. Construct -> Section -> Single section (of crown) -> Position -0.5mm -> Evaluation section visible on the guidelines.
8. The crown button is turned on to visualise the mesh. The crown file is called the "Actual Element" whilst the prepared tooth on the scanning aid is considered to be a "Nominal Element".
9. The PIP button is selected again followed by "Clipping at element plane" in which the plane on the now visible crown is selected.
10. The internal case/gap between the actual and nominal elements which is the area that needs to be measured was selected (Figure 3.18).
11. The "Measuring Principle" option was selected followed by "Referenced Construction".
12. The "Check" option was then selected followed by the "dXYZ" option which measured the deviations in all axes.
13. The range on the colour map was set at 0.12mm (-120mm to +120mm).
14. The "Inspection" drop-down menu on the left-hand side menu was selected followed by the option "Curve" and then "Surface Curves (3D Deviations)" (Figure 3.17).
15. The "Labels" button was selected, and the "Equidistant Deviation Labels" option enables multiple points to appear.
16. The software enables the user to select a fixed distance between points, in this case, the interval distance was set at 0.5mm.
17. The first visible point in the marginal area where the crown and the prepared tooth surface start is selected at the starting point. This is the marginal gap measurement.
18. All the points are then exported as a Microsoft® Excel file.

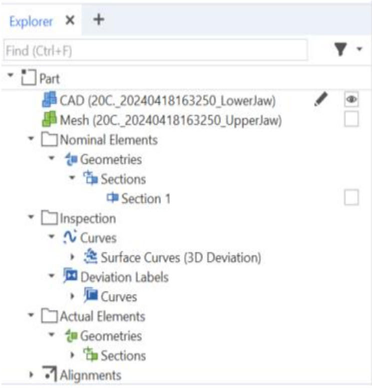

***Figure 3.17** Screenshot from ZEISS Inspect 3D of the side menu explorer column with the task history.*

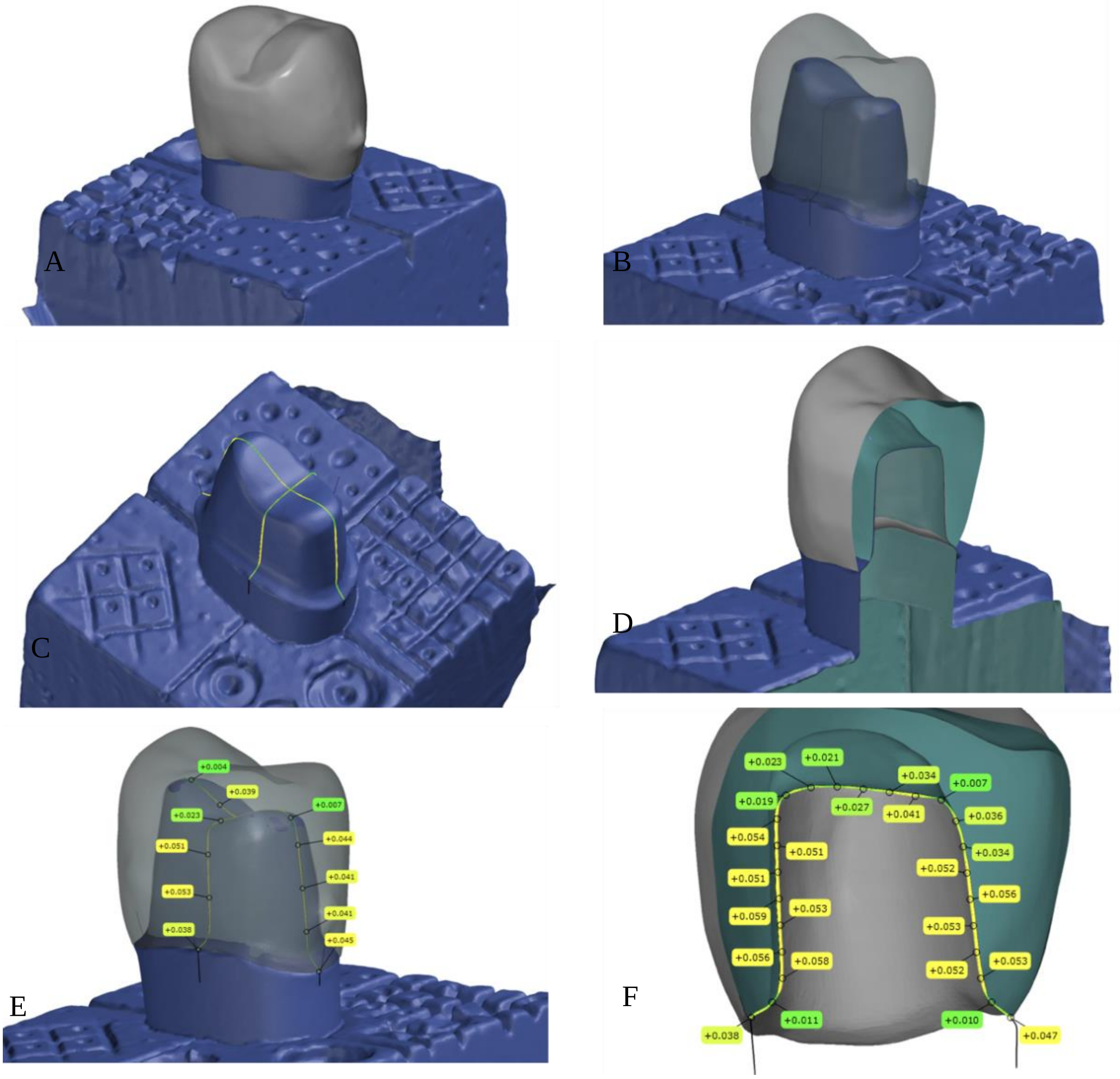

Figure 3.18 *ZEISS Inspect 3D screenshots showing the steps undertaken to obtain the final 2D cross-sectional images for marginal and internal gap analysis. (A and B) Virtual seating of the CS on the MS in the position registered by the bite registration scan using the Primescan scanner. (C) Virtual planes drawn using the grooved lines on the scanning aid block as a reference. (D) Cross-section view along the mesiodistal plane showing the internal gap and the tooth's prepared surface. (E) 3D view of the annotated marginal and internal gaps as positive measurements in mm. (F) 2D view of the annotated marginal and internal gaps as positive measurements in mm.*

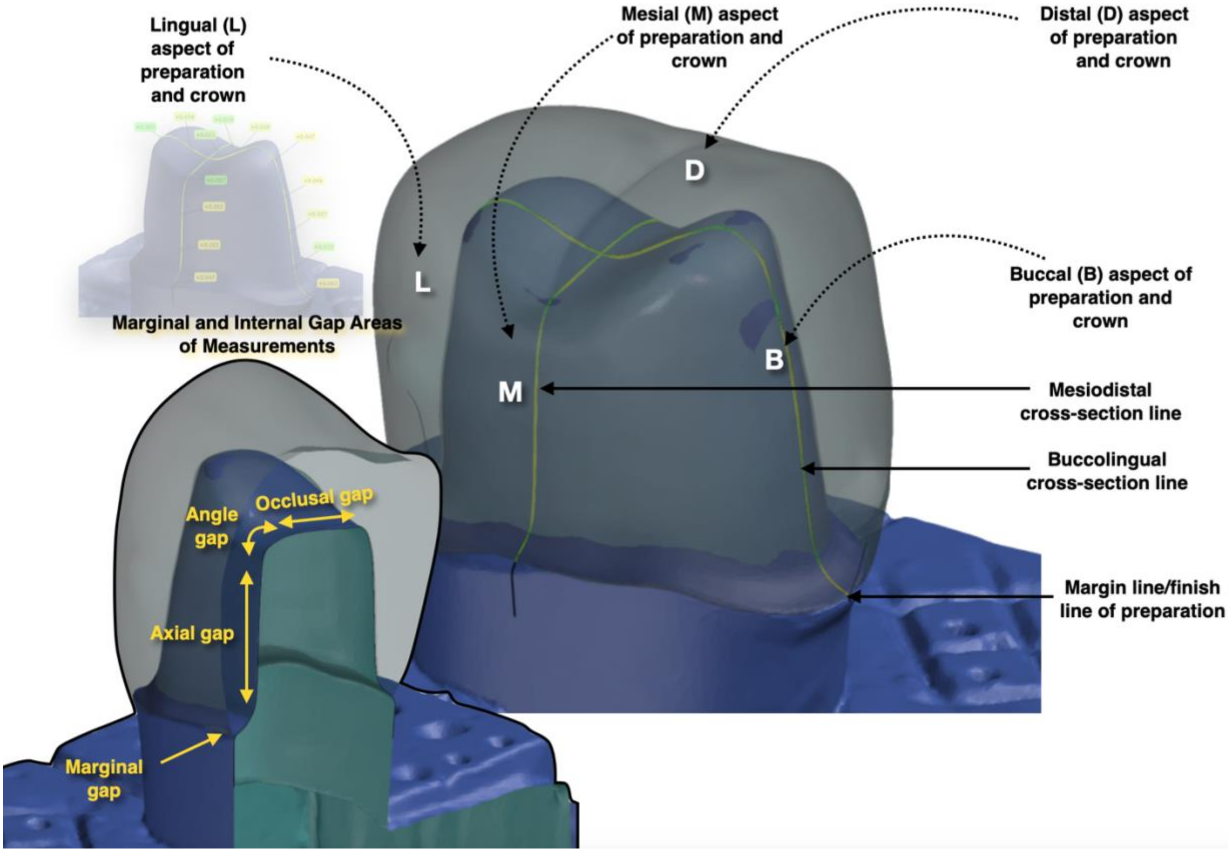

Figure 3.19 *Annotated screenshot of the internal view and seated crown on prepared tooth (using ZEISS Inspect 3D) demonstrating the important anatomical areas. On the bottom left corner mesiodistal cross-sectional view with the four areas of interest.*

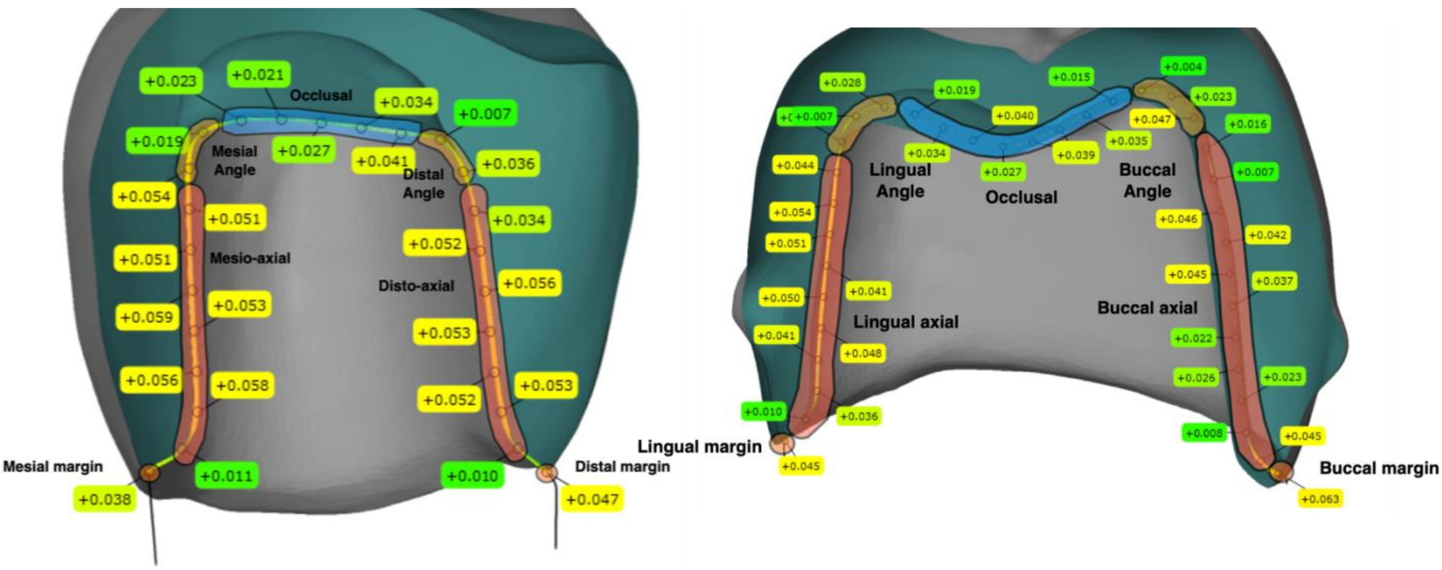

Figure 3.20 *Screenshots of mesiodistal (left) and buccolingual (right) sections from ZEISS Inspect 3D and colour coded sections based on the regions of interest. The mesiodistal section was divided into five subsections apart from the margins: distoaxial, distal angle, occlusal, mesial angle, and mesioaxial with 7, 2, 5, 2, 7 measuring points. The buccolingual section was also divided into five subsections apart from the margins: buccal axial, buccal angle, occlusal, lingual angle, and lingual axial with 11, 3, 8, 3, 9.*

3.8 TRUENESS ANALYSIS

The original CAD file was exported from both CAD software. The following steps describe how trueness analysis was carried out using Geomagic Control X:

1. The original CAD file was imported.
2. Make the file a “Reference file” by right-clicking on the imported file.
3. The scanned crown (mesh) file was then imported.
4. Initial alignment was carried out using the “Precise” option.
5. Best fit alignment was done after selecting the entire surface of the reference file.
6. The intaglio surface and marginal surface were merged into one using the “Region” and “Merge and Split” options, and collectively referred to as the internal surface.
7. 3D comparison was chosen followed by the selection of the area of interest.
8. Max. range 0.12mm and min. range -0.12mm
9. The “Colour Map” option was selected for better visualisation of the deviations.
10. For each crown the “Generate Report” option was selected and saved as an Excel file.
11. Each report consists of RMS values, ranges, standard deviation and variance.

Since normal distribution was rejected, the median and range of the 3D deviation values were obtained for the internal surface of both groups.

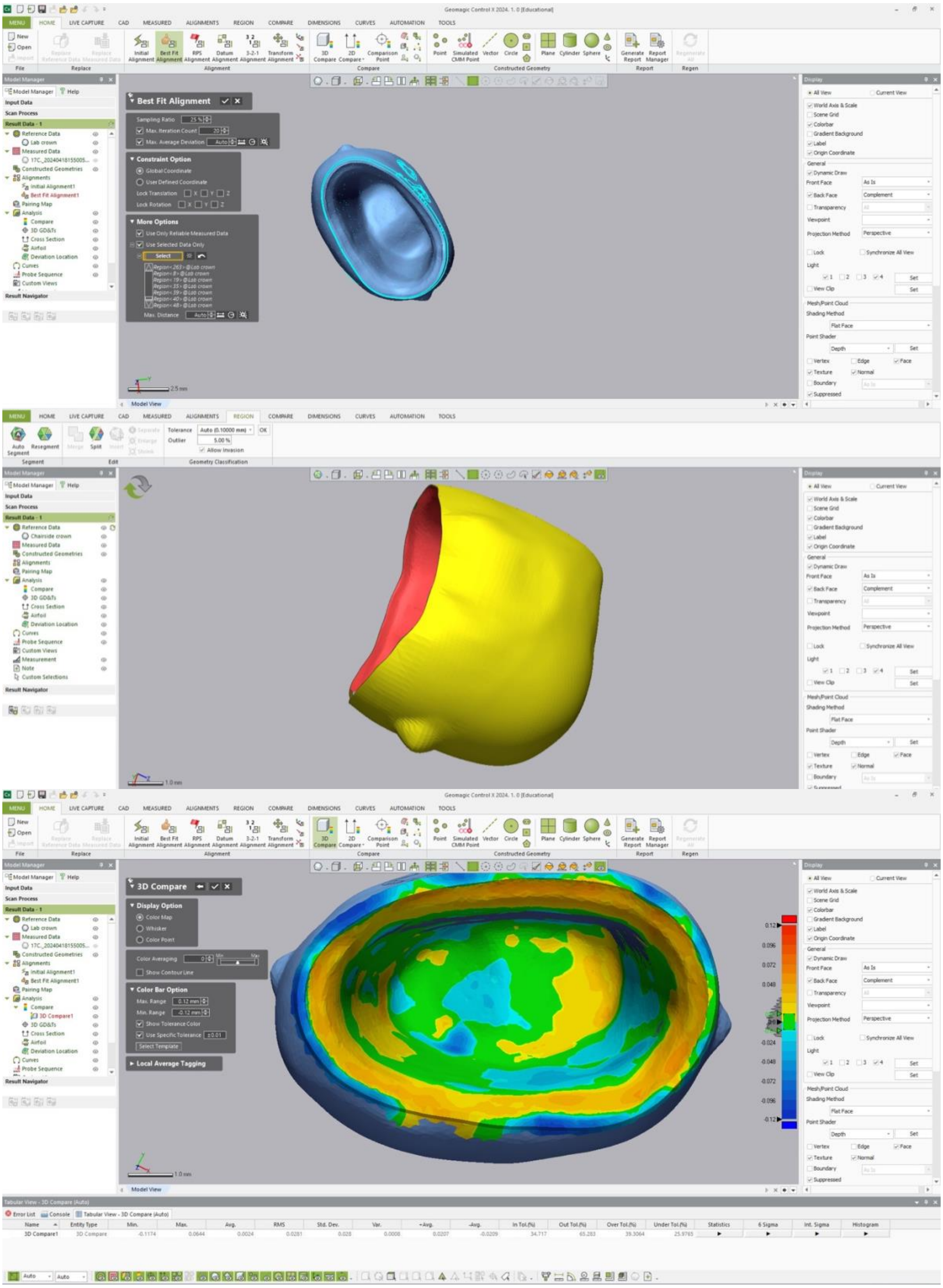

Figure 3.21 Geomagic Control X screenshots showing the model manager on the left-hand side with the several steps carried out to obtain the positive and negative deviations. The top screenshot shows the selection of the complete crown prior to the best fit alignment. The middle screenshot shows the internal surface selection which includes the intaglio surface and the marginal area using the "Region" and "Merge" options. The bottom screenshot shows the 3D compare parameters along with the colour map of the intaglio surface.

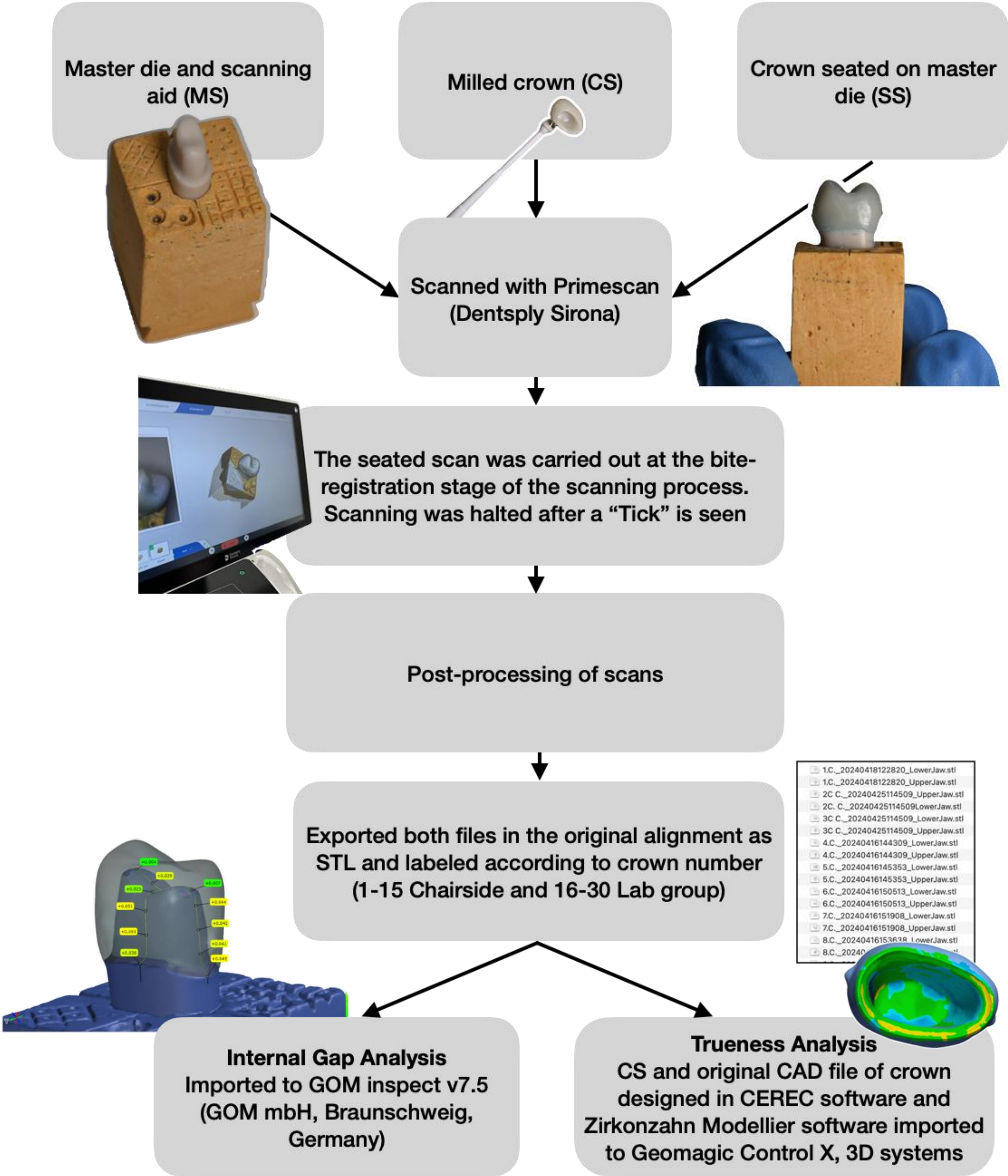

Figure 3.22 *Triple scan protocol for marginal discrepancy and trueness assessment.*

3.9 STATISTICAL ANALYSIS

As calculated by the Noether formula, the sample size was determined to have a statistical power of 80% at a significance level of 5% (Noether 1987). Since the sample size was less than 500, normality testing was carried out using the Shapiro-Wilk test for all variables. The data was inputted in Microsoft® Excel (Version 16.84; 2024 Microsoft). All statistical analyses were then performed using SPSS Statistics 28 software (SPSS, Inc. in Chicago, IL, USA), considering a 5% significance level.

Chapter 4: Results

All CAD-CAM zirconia crowns of both groups could be successfully designed, manufactured and seated onto the respective preparations on the master die. Statistical results were obtained from group comparisons for trueness, as well as variables related to marginal and internal fit.

4.1 TRUENESS ANALYSIS

The normality of measurement was rejected according to the Shapiro-Wilkin Test ($p<0.05$). Therefore, due to the absence of normal distribution non-parametric testing needs to be carried out. Since normal distribution was rejected, the median and range of the 3D deviation values were obtained for the internal surface of both groups.

Table 4.1 *Descriptive results (median and range) for comparison of root mean squared (RMS) of the internal surface of crowns manufactured by the chairside and lab workflows.*

Variable	Chairside (Dentsply, Sirona)	Laboratory (Zirkonzahn)	*P* value*
RMS of Internal Surface (µm)	30 ± 7.85 (25.3-52.2)	24.2 ± 6.08 (17.4-35.2)	0.041

*Mann-Whitney U-test. Bold font represents a statistically significant difference.

The Mann-Whitney U-Test was used as the crowns of both groups were considered to be independent samples with continuous dependent variables. Even though the same tooth preparation was used for crown design, every crown was individually designed and manufactured with one of the two different workflows assessed. For this reason, the samples were not paired. The Mann-Whitney U-test determines the presence or absence of statistically significant differences between the medians of the two groups. In this case, since the value of significance (*p*-value) is 0.041, which is below the threshold of 0.05, it suggests a difference between the two workflows. As show in Table 4.1, the internal trueness of crowns manufactured using the lab workflow was significantly higher than that of the chairside group with an RMS of 24.2 µm and 30 µm respectively (Figure 4.1). The colour deviation map used in this comparison is available in Figure 4.2.

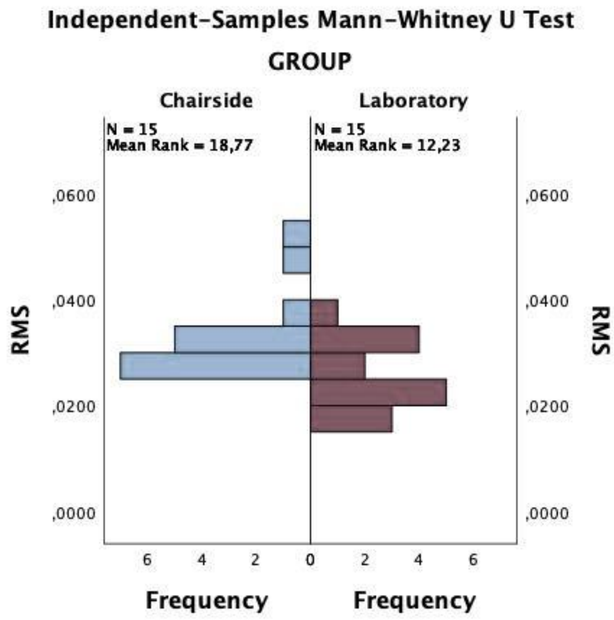

Figure 4.1 *Histogram comparing the RMS values of the zirconia crown produced by the two workflows.*

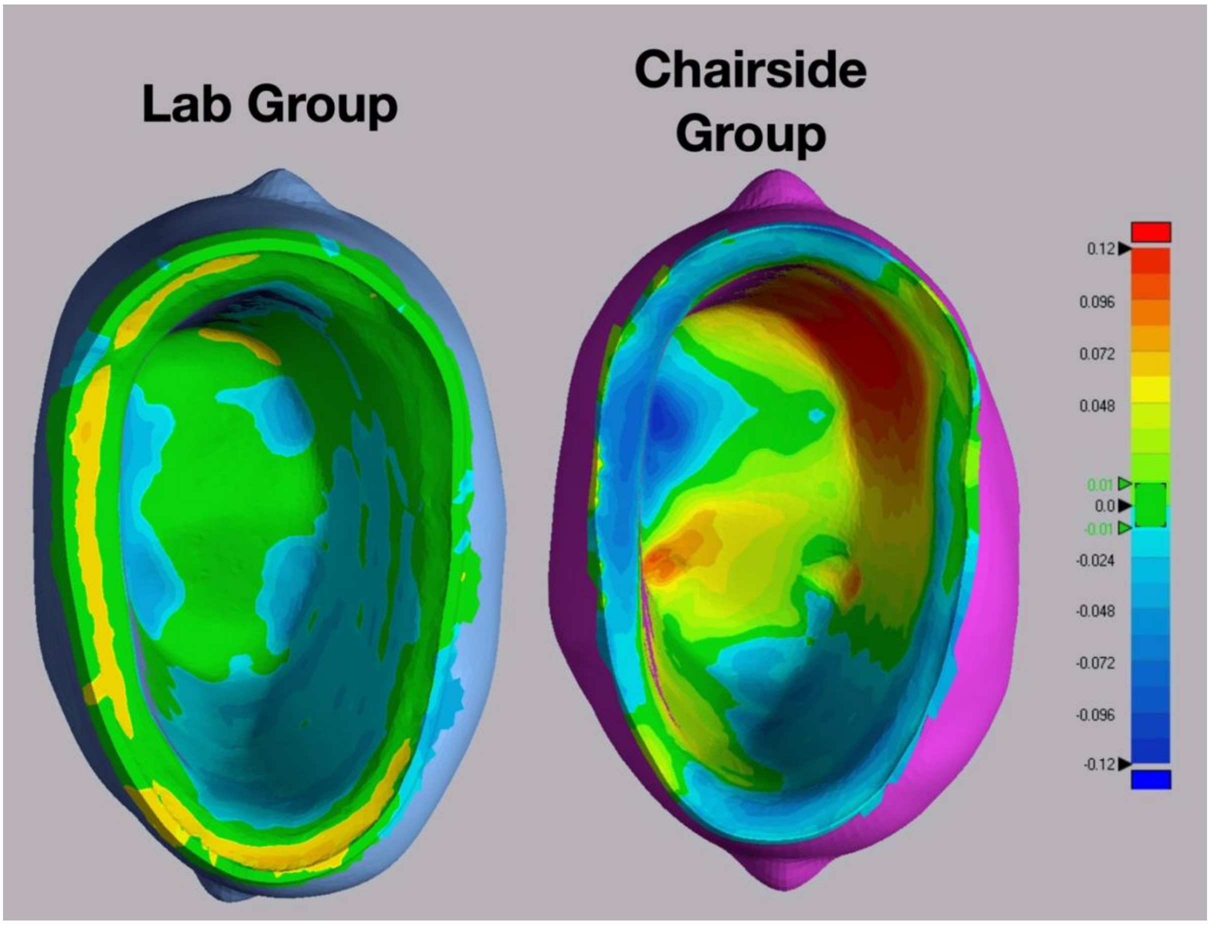

Figure 4.2 *3D colour deviation maps for lab and chairside group using Geomagic Control X. Positive deviations are displayed with yellow to red colours whilst negative deviations with cyan to blue.*

4.2 MARGINAL GAP

According to the Shapiro-Wilk test ($p>0.05$), the data was normally distributed. Since normality is assumed, and two independent groups are compared, the Independent Samples *t*-test was used to compare the internal gaps of the fabricated crowns using the two workflows. The rationale behind the use of the t-test is a means to compare the two groups' internal gap in micrometres. The smaller the gap the better the crown fit and the closer the measurements are to the system's parameters. The *p*-value, derived from the t-test is a measure of the probability of obtaining the tabulated value assuming the null hypothesis (no difference in marginal and internal fit of monolithic zirconia between the two workflows) is true. Results with *p* values below the predetermined threshold ($p = 0.05$) indicate the improbability of this result occurring by chance, thereby suggesting a statistically significant difference (Figure 4.2). A statistically significant difference was noted in three out of four areas: mesial ($p=0.03$), distal ($p=0.023$), and buccal ($p=0.011$). When compared to the lab group, the chairside group exhibited the highest marginal gap on the mesial aspect with a 74.8 ± 49.1μm gap and 74.8 ± 49.1 115.7 ± 46.9μm gap respectively ($p=0.030$). A statistically significant result was obtained for the overall marginal gap ($p<0.001$) with a mean gap of 100.7 ± 43.6 μm for the chairside group and 67.8 ± 59.0 μm for the lab group. All measured marginal areas were within the clinically acceptable limits of 120μm according to Mc Lean and von Franhoufer (1971).

One out of the 15 chairside crowns was excluded from the marginal and internal gap assessment due to large internal overlap of meshes even after several attempts to rescan.

Table 4.2 *Descriptive results of marginal gap measurements (mean and standard deviation).*

Location on Margin (μm)	Chairside Group Mean Gap ± SD	Lab Group Mean Gap ± SD	*p*-value*
Mesial gap	115.7 ± 46.9	74.8 ± 49.1	**0.030**
Distal gap	108.4 ± 47.6	65.5 ± 48.1	**0.023**
Lingual gap	87.9 ± 41.4	73.7 ± 93.8	0.609
Buccal gap	90.9 ± 35.5	57.3 ± 30.8	**0.011**
Overall Gap	100.7 ± 43.6	67.8 ± 59.0	**<0.001**

*Independent t-test. Bold font represents a statistically significant difference.

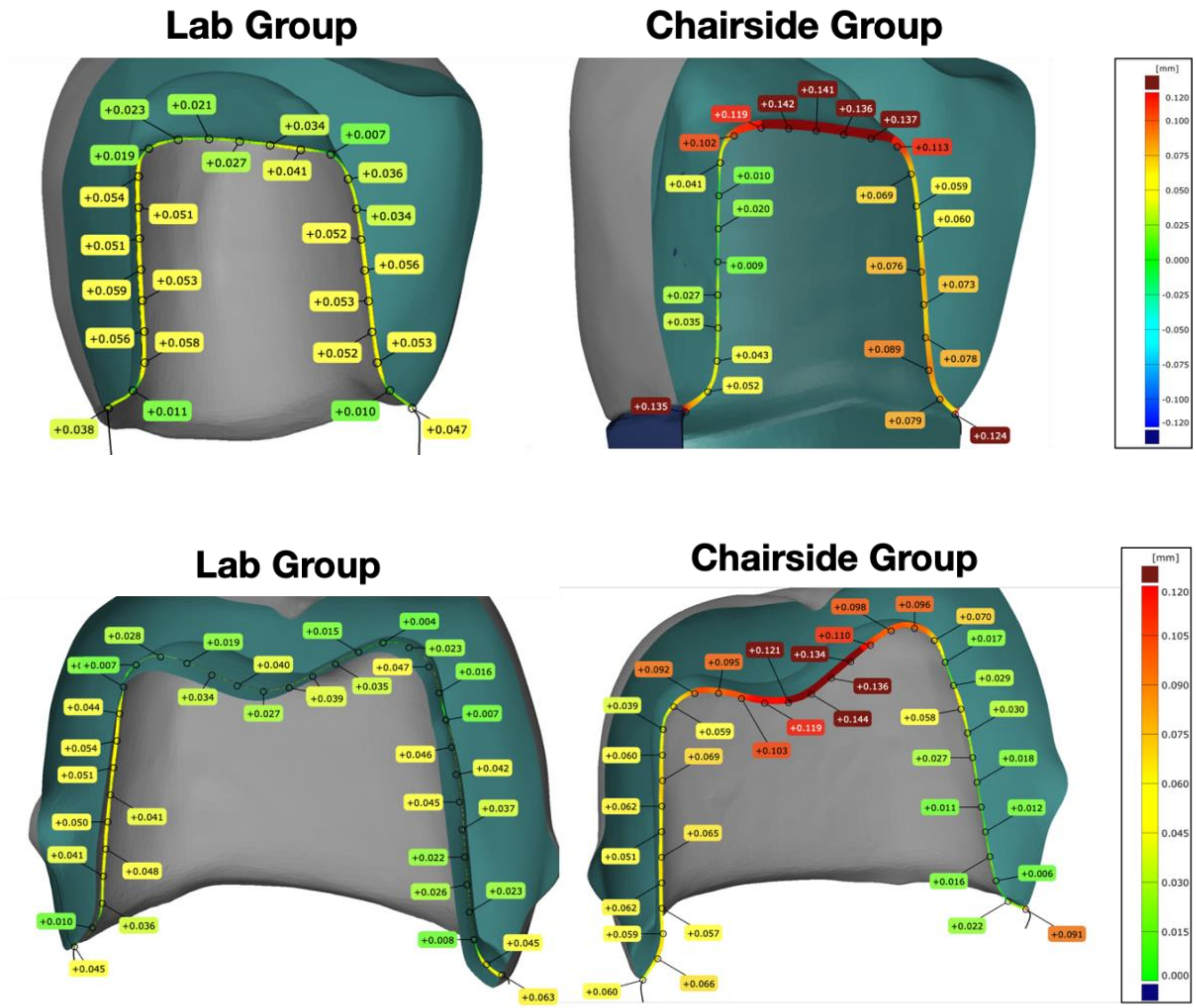

__Figure 4.3__ Screenshots of the (top) mesiodistal and (bottom) buccolingual cross-sectional view of a lab and chairside crown using ZEISS Inspect 3D.

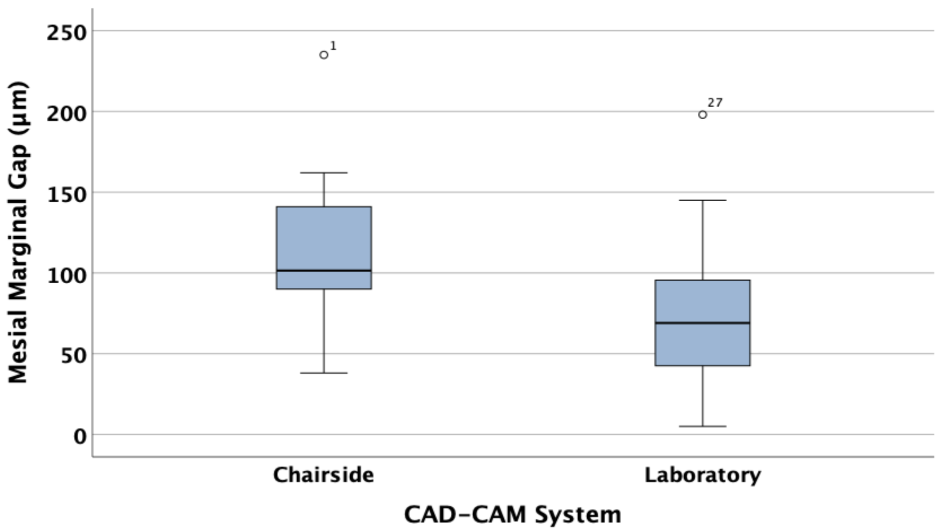

__Figure 4.4__ Box plot showing a statistically significant difference found between the mesial marginal gap of the chairside and lab group. The lab group showed lower gap values therefore outperforms the chairside workflow, according to the Independent Samples t-test (__p=0.030__).

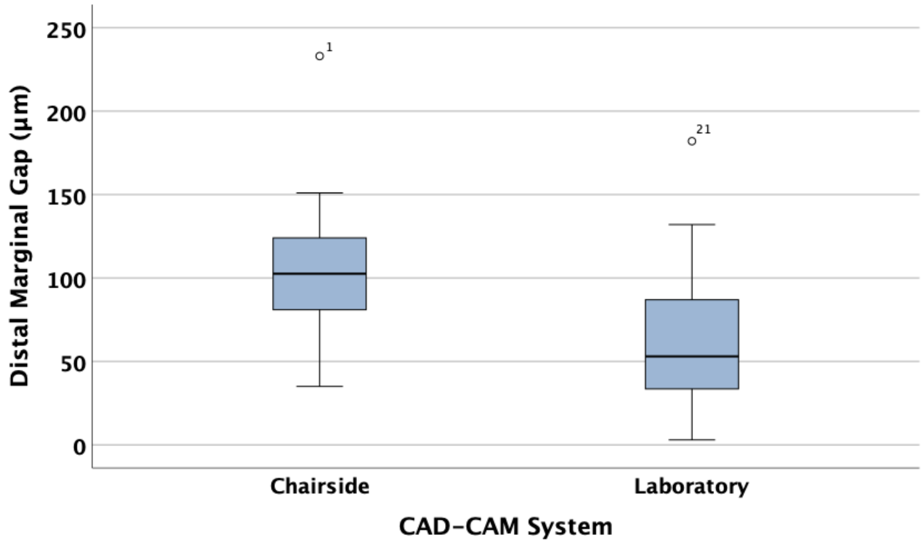

Figure 4.4 *Box plot showing a statistically significant difference found between the distal marginal gap of the chairside and lab group. The lab group showed lower gap values therefore outperforms the chairside workflow, according to the Independent Samples t-test (**p=0.023**).*

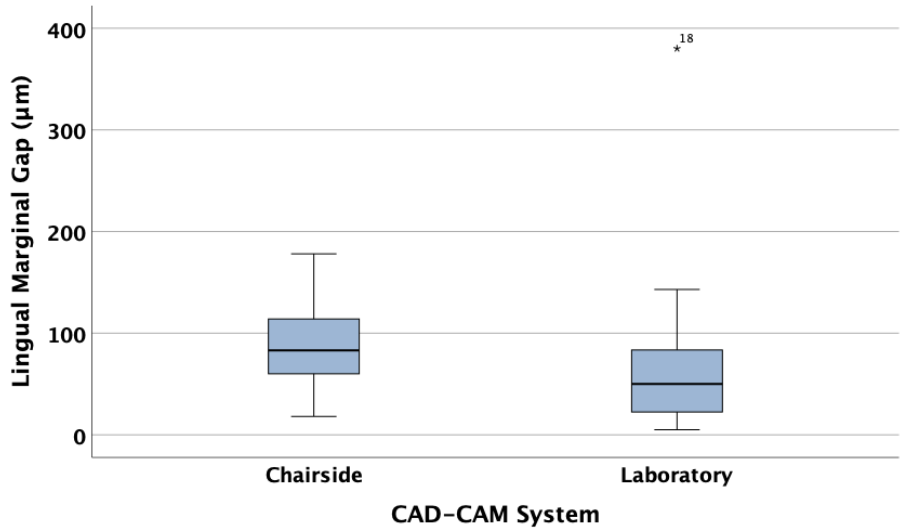

Figure 4.5 *Box plot showing no statistically significant difference found between the lingual marginal gap of the chairside and lab group. The lab group showed slightly lower gap values (**p=0.609**).*

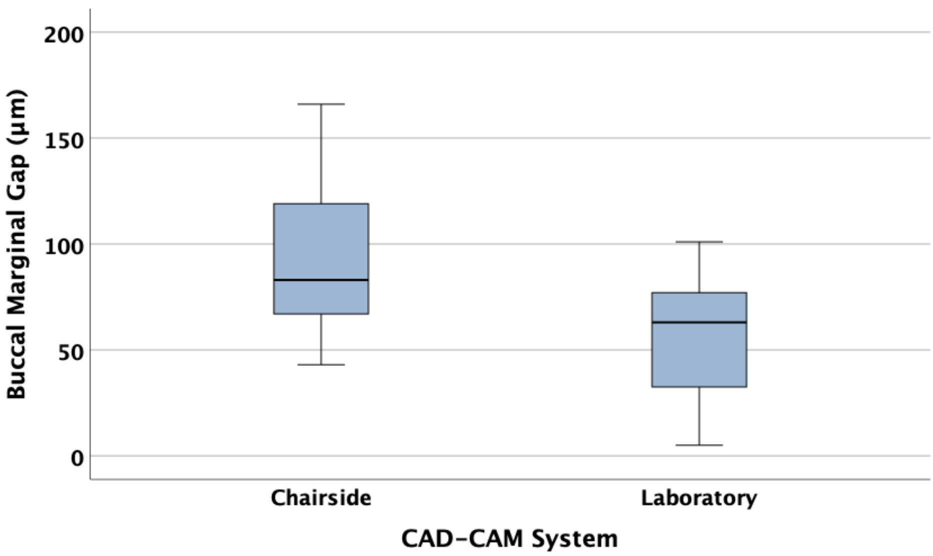

Figure 4.6 *Box plot showing a statistically significant difference found between the buccal marginal gap of the chairside and lab group. The lab group showed lower gap values therefore outperforms the chairside workflow, according to the Independent Samples t-test (**p=0.011**).*

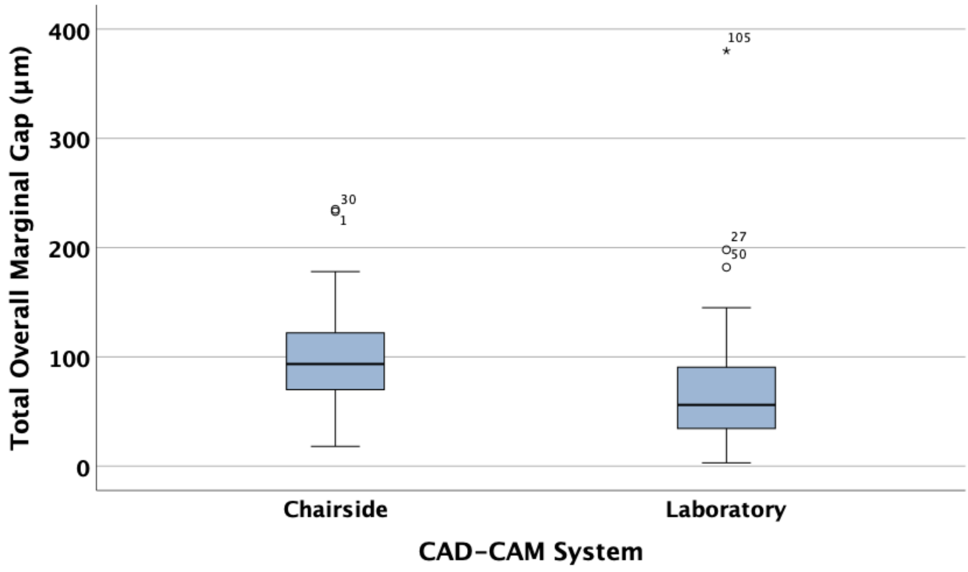

Figure 4.7 *Box plot showing a statistically significant difference found between the overall marginal gap of the chairside and lab group. The lab group showed lower gap values therefore outperforms the chairside workflow, according to the Independent Samples t-test (**p<0.001**).*

4.3 INTERNAL GAP

The Independent Samples *t*-tests revealed a statistically significant difference between the two groups. The mean gap values measurements of the chairside group were higher than the lab group, with significant differences in the MBO surface 123.1 ± 42.9 µm and 80.5 ± 45.9 µm (p=0.016), DA 88.2 ± 21.6 µm and 61.3 ± 27.0 µm (p=0.007), LA 78.7 ± 19.7 µm and 58.0 ± 27.2 µm (p=0.028), BLO 117 ± 34.7 µm and 74.4 ± 40.2 µm (p=0.005), and BA 91.5 ± 25.8 µm and 63.2 ± 32.7 µm (p=0.016) as shown in Tables 4.3 and 4.4.

A significant difference was found in the overall internal gap (p<0.001) except for the overall axial internal gap (p=0.443). The highest values were obtained on the occlusal internal gap with an overall of 120.1 ± 38.4 µm in the chairside group and 77.5 ± 42.5 µm in the lab group (p<0.001).

Table 4.3 *Descriptive results of internal gap measurements (mean and standard deviation).*

Variable	Chairside Group Mean Gap ± SD	Lab Group Mean Gap ± SD	*P* value*
MAX (µm)	71.6 ± 111.2	44.9 ± 23.0	0.373
MA (µm)	87.3. ± 23.8	69.2 ± 40.2	0.155
MBO (µm)	123.1 ± 42.9	80.5 ± 45.9	**0.016**
DA (µm)	88.2 ± 21.6	61.3 ± 27.0	**0.007**
DAX (µm)	63.04 ± 14.3	62.5 ± 18.1	0.943
LAX (µm)	53.2 ± 12.2	54.5 ± 19.1	0.816
LA (µm)	78.7 ± 19.7	58.0 ± 27.2	**0.028**
BLO (µm)	117 ± 34.7	74.4 ± 40.2	**0.005**
BA (µm)	91.5 ± 25.8	63.2 ± 32.7	**0.016**
BAX (µm)	39.5 ± 15.2	41.0 ± 19.0	0.817
Overall Angular Internal Gap (µm)	86.4 ± 22.7	62.9 ± 31.7	< **0.001**
Overall Axial Internal Gap (µm)	56.8 ± 56.6	50.8 ± 21.2	0.443
Overall Occlusal Internal Gap (µm)	120.1 ± 38.4	77.5 ± 42.5	< **0.001**
Overall Internal Gap (µm)	81 ± 48.1	60.9 ± 32.0	< **0.001**

*MAX mesial axial; MA mesial angle; MDO mesiodistal occlusal; DA; distal angle; DAX distoaxial; LAX linguoaxial; LA lingual axial; BLO buccolingual occlusal; BA buccal angle; BAX buccal axial. *Independent t-test. Bold font represents a statistically significant difference.*

*__Table 4.4__ Independent Samples t-test results for measurement location(s) with equal variances assumed of individual measurement data (p≤ 0.001); *indicates significance (p<0.05).*

Location	t	df	p-value	Mean Difference	Standard Deviation	95% CL Lower	95% CL Upper
Mesial Margin	2.290	27	0.03*	40.90	17.80	4.28	77.50
MAX	0.907	27	0.373	26.50	29.30	33.60	86.70
MA	1.460	27	0.155	18.10	12.40	7.30	43.50
MOD	2.580	27	0.016*	42.60	16.50	8.70	76.50
DA	2.940	27	0.007*	26.80	9.11	8.10	45.40
DAX	0.073	27	0.943	0.44	6.09	12.00	12.90
Distal Margin	2.413	27	0.023*	42.80	17.80	6.42	79.30
Lingual Margin	0.518	27	0.609	14.10	27.20	41.80	70.00
LAX	-0.023	27	0.818	1.39	6.00	13.70	10.90
LA	2.325	27	0.028*	20.60	8.87	2.40	38.80
BOL	3.050	27	0.005*	42.70	14.00	14.00	71.40
BA	2.572	27	0.016*	28.30	11.00	5.72	50.90
BAX	-0.235	27	0.817	1.50	6.42	14.70	11.60
Buccal Margin	2.731	27	0.011*	33.60	12.30	8.37	58.90

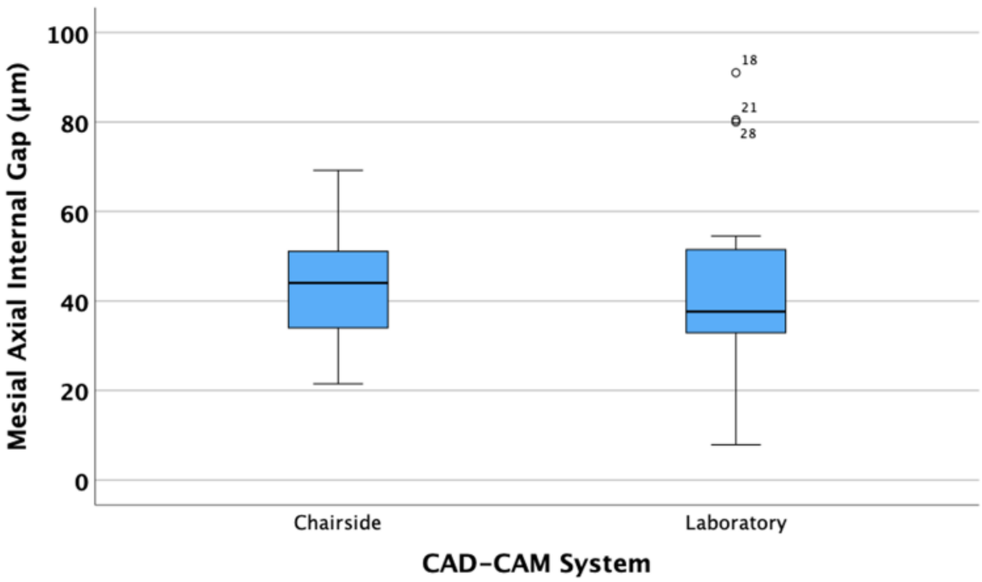

Figure 4.8 *Box plot showing no significant difference between the mesial axial internal gap of the chairside and lab group (p=0.373).*

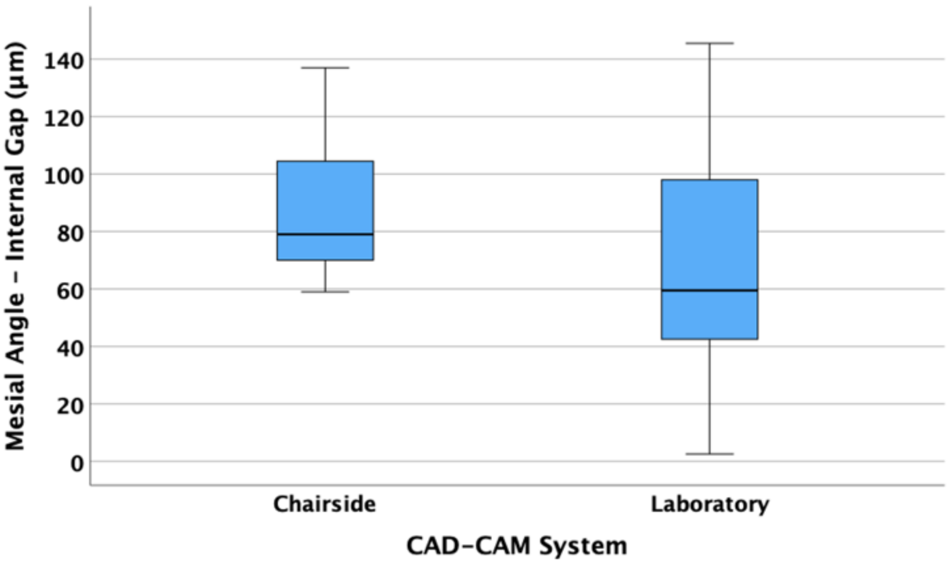

Figure 4.9 *Box plot showing no significant difference between the mesial angle internal gap of the chairside and lab group (p=0.155).*

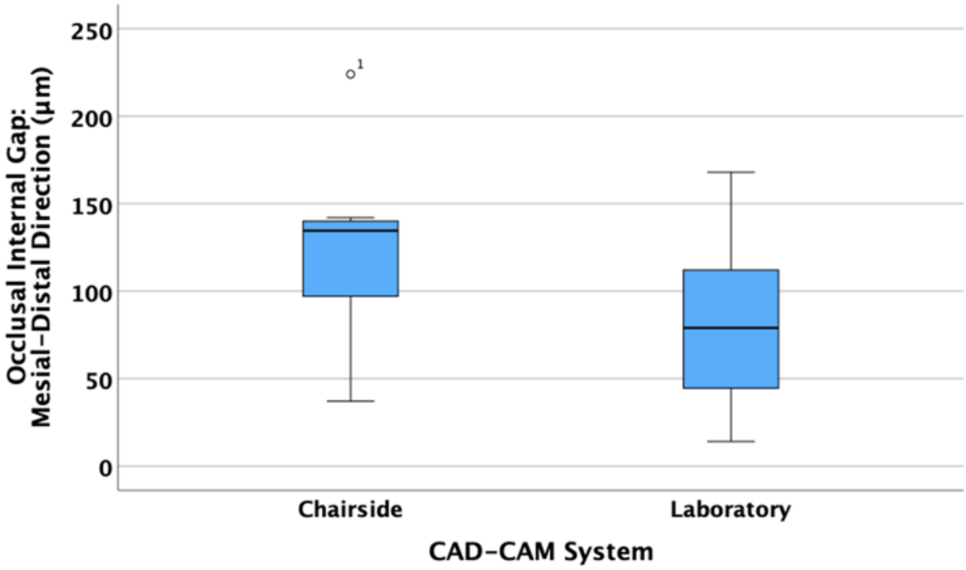

Figure 4.10 *Box plot showing a statistically significant difference found between the mesiodistal occlusal internal gap of the chairside and lab group (**p=0.016**).*

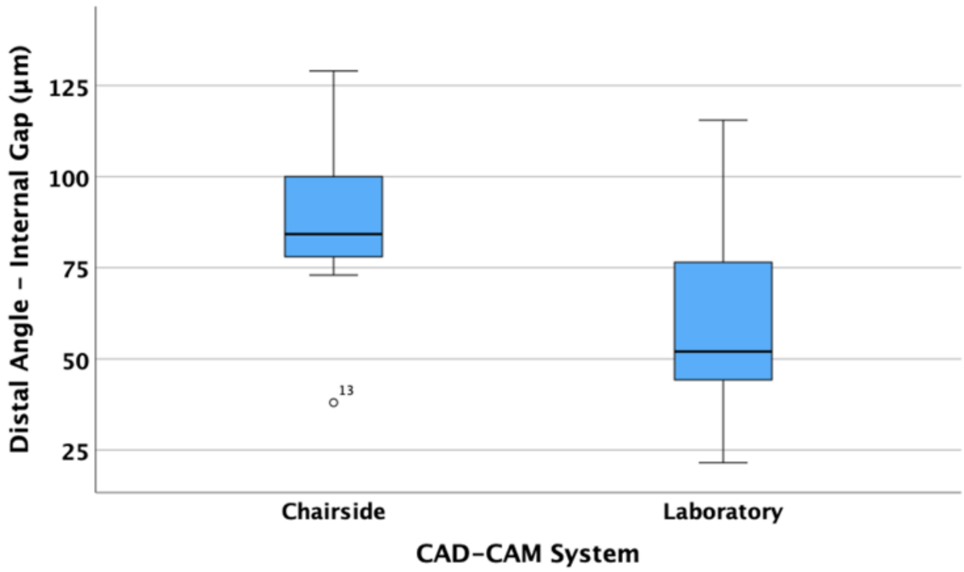

Figure 4.11 *Box plot showing a statistically significant difference found between the distal angle internal gap of the chairside and lab group. The lab group showed lower gap values therefore outperforms the chairside workflow, according to the Independent Samples t-test (p=0.007).*

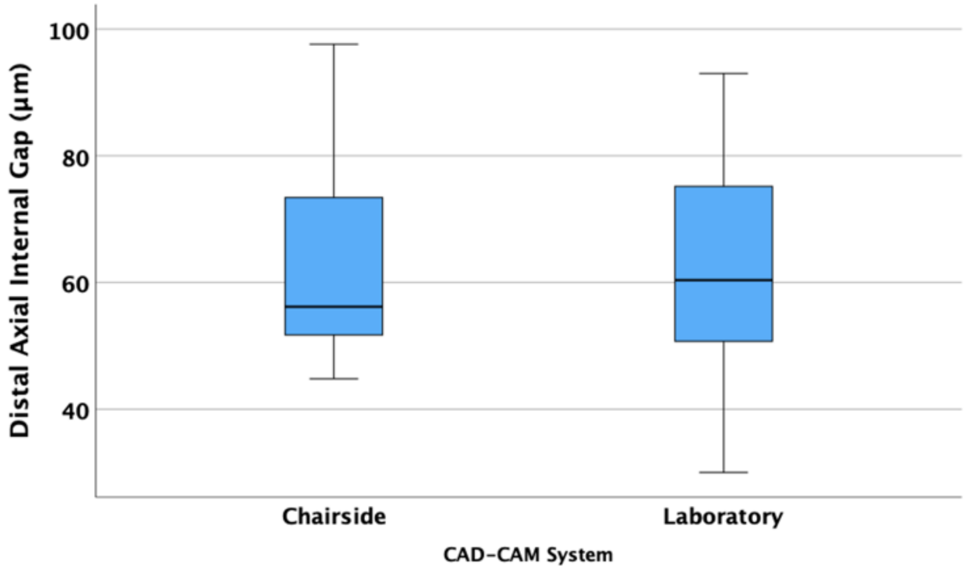

Figure 4.12 *Box plot showing no significant difference between the distal axial internal gap of the chairside and lab group (p=0.155).*

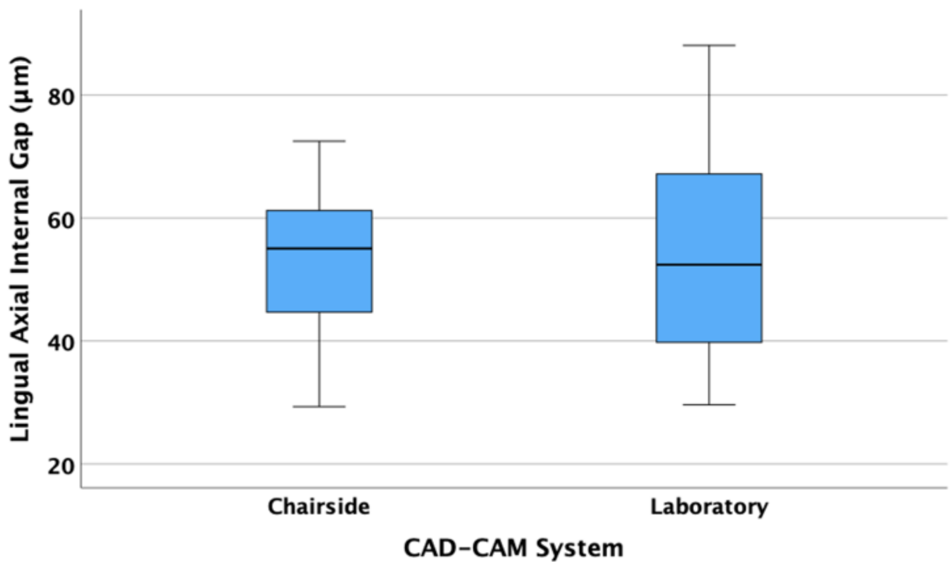

Figure 4.13 *Box plot showing no significant difference between the lingual axial internal gap of the chairside and lab group (p=0.816).*

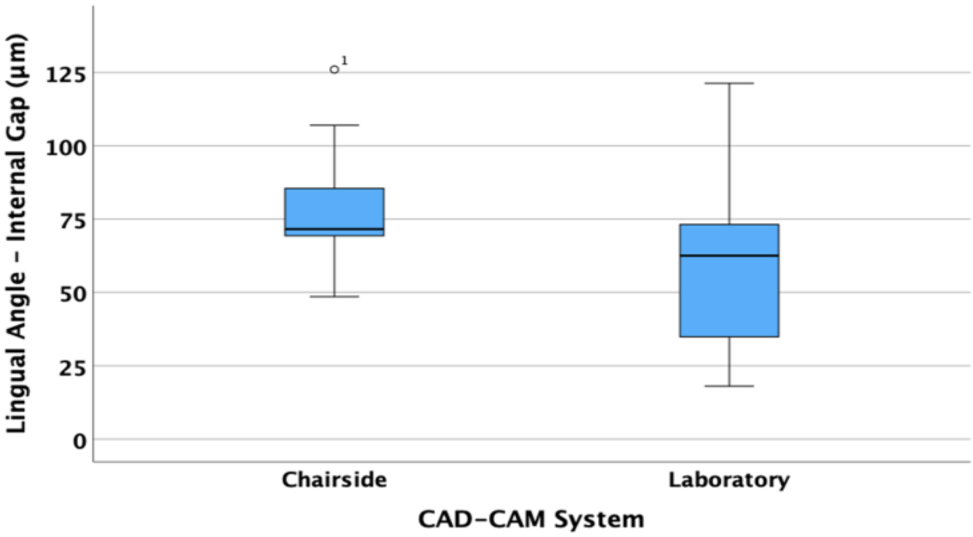

Figure 4.14 *Box plot showing a statistically significant difference found between the lingual angle internal gap of the chairside and lab group. The lab group showed lower gap values therefore outperforms the chairside workflow, according to the Independent Samples t-test (**p=0.028**).*

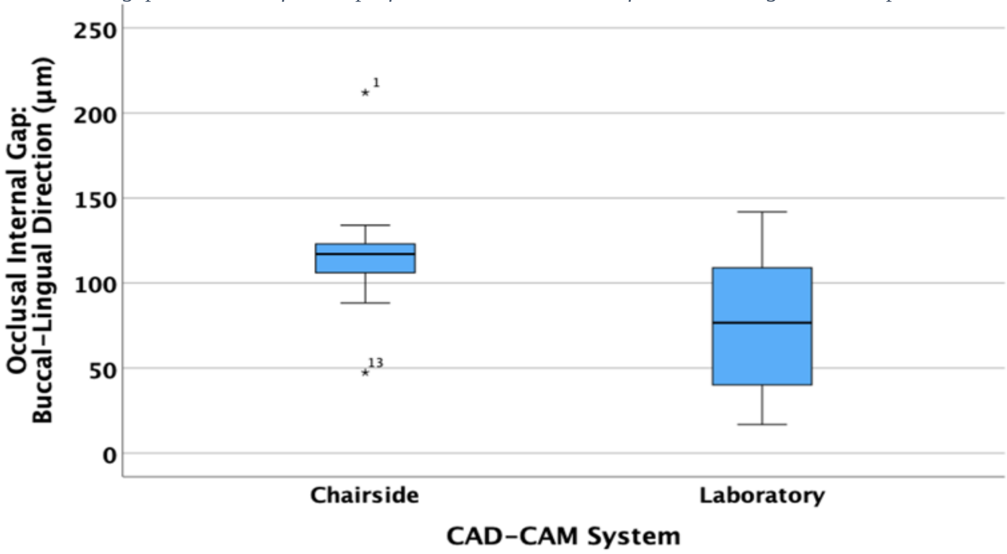

Figure 4.15 *Box plot showing a statistically significant difference found between the buccolingual occlusal internal gap of the chairside and lab group. The lab group showed lower gap values therefore outperforms the chairside workflow, according to the Independent Samples t-test (**p=0.005**).*

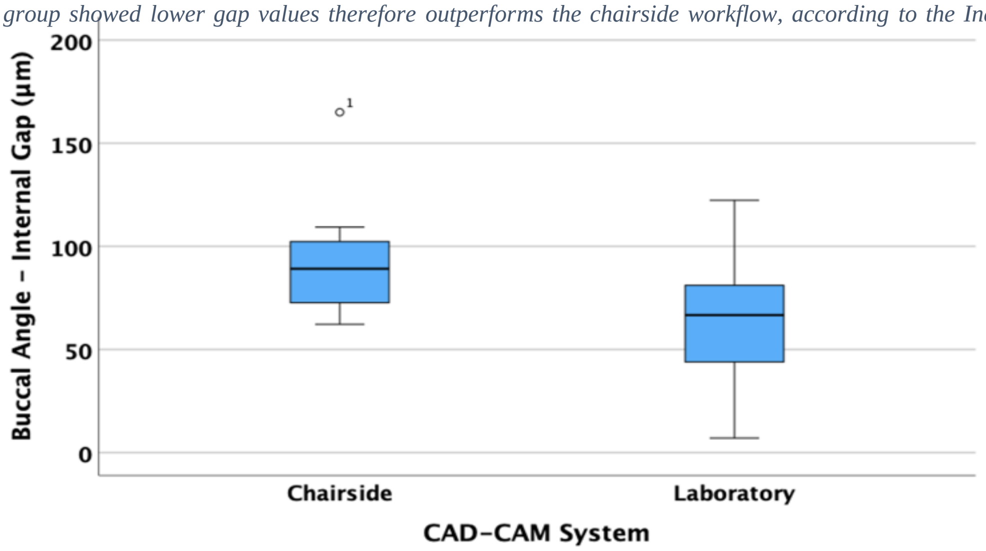

Figure 4.16 *Box plot showing a statistically significant difference found between the buccal angle internal gap of the chairside and lab group. The lab group showed lower gap values therefore outperforms the chairside workflow, according to the Independent Samples t-test (**p=0.016**).*

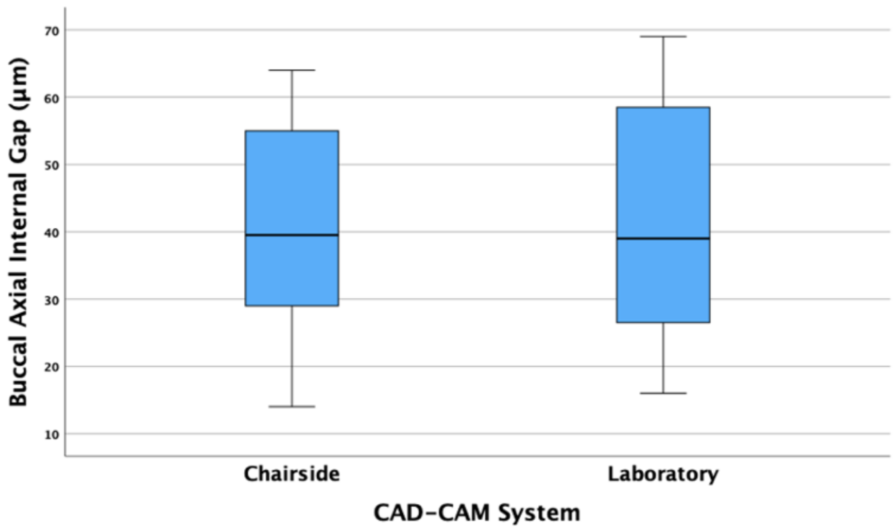

Figure 4.17 *Box plot showing no significant difference between the buccal axial internal gap of the chairside and lab group (p=0.817).*

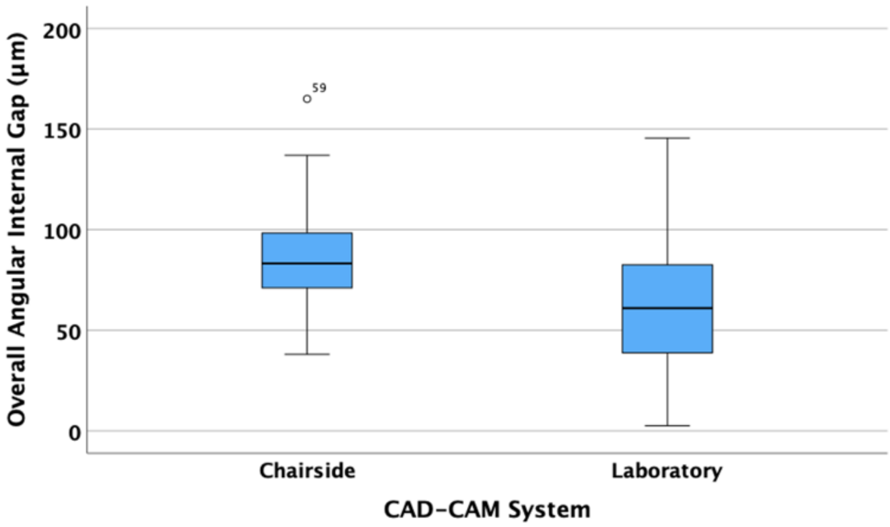

Figure 4.18 *Box plot showing a statistically significant difference found between the overall angular gap of the chairside and lab group. The lab group showed lower gap values therefore outperforms the chairside workflow, according to the Independent Samples t-test (**p<0.001**).*

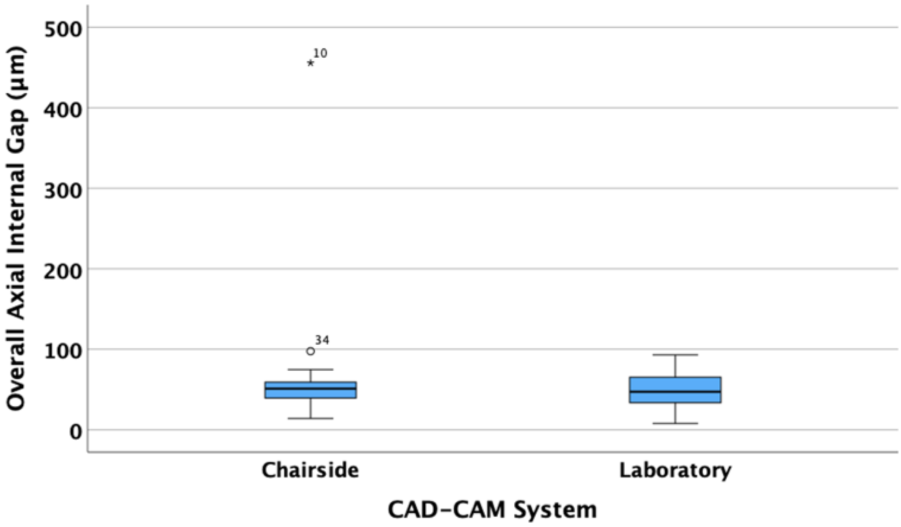

Figure 4.19 *Box plot showing no significant difference between the buccal axial internal gap of the chairside and lab group (p=0.443).*

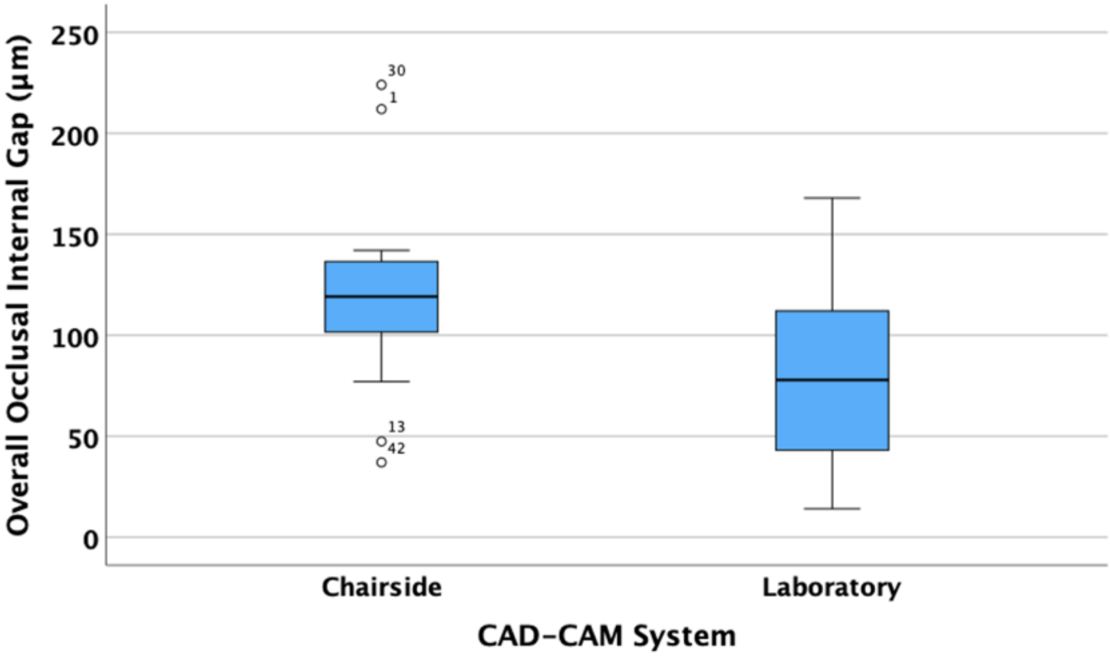

Figure 4.20 *Box plot showing a statistically significant difference found between the overall occlusal gap of the chairside and lab group. The lab group showed lower gap values therefore outperforms the chairside workflow, according to the Independent Samples t-test (**p<0.001**).*

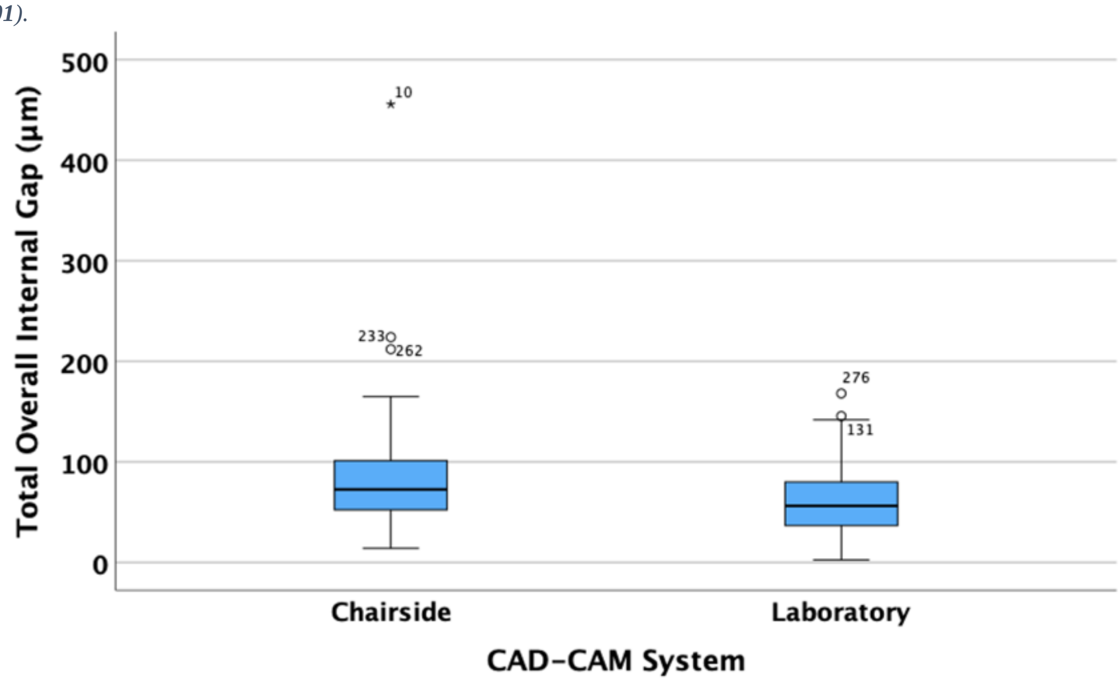

Figure 4.21 *Box plot showing a statistically significant difference found between the overall internal gap of the chairside and lab group. The lab group showed lower gap values therefore outperforms the chairside workflow, according to the Independent Samples t-test (**p<0.001**).*

Chapter 5: Discussion

This study aimed at clarifying differences in clinical outcomes of treatments performed with two different strategies working with a digital workflow. Clinicians are faced with two options when it comes to zirconia crown fabrication: chairside or lab workflow. Chairside workflows have the advantage of efficiently producing a single or small FDP in a short period of time enabling single-visit treatments. On the other hand, laboratory workflows allow the fabrication of complex prostheses with a more robust software and hardware set-up with a relatively higher investment (Turkyilmaz & Yun, 2022). Loss of retention and caries are the most common reasons for FDP failure, both influenced by the adaptation of the restoration also referred to as internal fit and marginal adaptation. Large marginal discrepancy leads to plaque accumulation, increasing the possibility of caries, periodontal disease, and exposure of luting cements giving rise to restoration failure (Felton et al., 1991; Paul et al., 2020; Pedroche et al., 2016; Refaie et al., 2023; Wettstein et al., 2008). From a clinician's point of view, one of the most important question is whether there is a significant difference between the types of workflows regarding to important clinical outcomes such as internal fit and marginal adaptation. Although there is some evidence that is in agreement with the present study, this study used the latest technological devices for each type of workflow to measure and analyse the trueness and internal fit of the fabricated prosthesis.

5.0 Internal Gap Assessment

The most important consideration when comparing chairside and lab zirconia crown manufacturing is the milling axes. With a rotating workpiece at the x-axis and the spindle operating in X-, Y-, and Z- axis, chairside milling machines are capable of producing accurate and precise restorations especially for single unit crowns. Having an additional axis, the laboratory 5-axis milling machines can fabricate complex designs with a higher degree of accuracy (Kirsch et al., 2017). The CEREC MCXL (Dentsply Sirona) milling device has been used in several studies most of which comparing it to other CAD-CAM milling devices (Camargo et al., 2022; Hamza & Sherif, 2016). This justifies the use of the successor of this popular chairside system (Primemill; Dentsply Sirona) in the present study. According to Camrago and collaborators (2022) and Hamza & Sherif (2016) the CEREC MCXL underperformed in regard to crown adaptation and had the highest marginal discrepancy when compared to 5-axis milling machines. Micro-CT was also used to assess the crown adaptation by measuring the cement-space thickness according to guidelines published in 2020 (Santos et al., 2020). They found the chairside group to have the highest cement-space thickness of 100 μm compared to the 5-axis LX-O (Matsuura Machinery) and the inkjet Carmel 1400 (Xjet) 3D printer with 81μm and 94μm respectively. However, cement-space thickness does not provide sufficient information on the actual crown adaptation during the preparation.

It would be inaccurate to directly compare the marginal and internal gap of the lab crowns which were designed with a spacer of 35μm with the chairside crowns at a spacer setting of 60μm (Hasanzade et al., 2020b). When describing the final gap measurements, the initial setting and predicted specifications of the CAD software need to be taken into consideration, with the measurements directly compared with what was planned. It would also not be reasonable to mill the respective crowns with the same settings on both devices by ignoring the manufacturer's instructions. This justifies the different parameters for each workflow used in this study in an attempt to represent and respect the recommended settings for each group as it would occur for any clinical case. Some studies have opted for the same spacer thickness of 50μm (Sanchez-Lara et al., 2023) for each system, others have designed the crown with one CAD system with a specific spacer thickness (e.g. 40μm [Abualsaud & Alalawi, 2022]; 50μm [Hamza & Sherif, 2016]; 80μm [Camargo et al., 2022]) and exported for fabrication with different CAM systems. In doing so, one is mainly comparing the milling device rather than the whole CAD-CAM system. The scope of this study was to compare the fabricated prostheses manufactured by the two very different workflows. This includes crown design and software parameters (CAD) followed by the manufacturing stages (CAM) with their respective milling and sintering machines. The lab and chairside workflows not only differ in hardware but have several software differences such as margin detection which influence the adaptation and final prosthesis design, otherwise overlooked if the same CAD .stl file was used for all systems.

5.1 Accuracy of Scanner

Since this study is assessing micrometre differences between meshes, it is crucial that the scanner of choice has high accuracy, also referred to as trueness and precision. In a study carried out by Róth et al. (2022), the CEREC Primescan (2019) was ranked the highest in terms of accuracy with a total score of 7.4 out of 10 (4.2 points trueness + 3.2 points precision). The Trios 4 Pod had the highest accuracy for full-arch scans however, regarding single abutment, inlay cavity, and bridge calipers, Primescan was found to be superior (Róth et al., 2022). This justifies the choice of an intraoral scanner for the current study.

5.2 Triple Scan Techniques

The *in vitro* cross-sectioning method was and is still widely used in the literature as it measures the cement gap directly from the specimen. This gives rise to an accurate measurement especially with the use of high-quality imaging in combination with high magnification. This method's main limitation is its destructive nature and its 2D assessment (Camargo et al., 2022). These limitations in conjunction with uniform and precise cross-sectioning angles raised concerns and the need to find alternative methods which over-come these challenges. The SRT was used as a non-destructive alternative to marginal gap assessment which can be used *in vivo.* It allows the assessment of internal gaps on multiple planes by replicating the cement space thickness using light-body silicone material which occupies the space (Laurent et al., 2008). The major drawback of such a well-studied method is the dimensional changes and potential tearing of the silicone material of choice. It is described to be technique sensitive and requires appropriate silicone materials and a sectioning guide to produce reproducible results. Segerström et al. (2019) found that there was a 2%-11% over estimation of gaps. The use of silicone material paved the way for the dual scan method which is a digital alternative to SRT (Lee, H. et al., 2017). This method allows 3D or 2D analysis of dental restoration margins by scanning the light-body silicone surface after crown seating. However, this is still limited to the properties of the silicone material and the experience of the operator. The scanning of silicone surfaces was also found to have reflective surfaces potentially introducing errors in the scanning process and the final marginal gap evaluation (Kuhn et al., 2014). Given the methodologies employed by previous authors, it became evident that the current study's approach needed to address certain limitations. Consequently, a more contemporary method was selected that not only surmounts these challenges but also aligns with our research objectives. The rationale behind the method of choice for this study emphasises on reproducibility, cost-effectiveness, and independence from material and technique-sensitive procedures like the SRT and micro-CT.

To overcome this, the triple-scan method allows virtual seating of the crown on the abutment tooth and enables 2D and 3D analysis of the virtual marginal gaps/cement space. The accuracy of this method is influenced by the precision of overlaying data during the alignment process (Hasanzade et al., 2020a; Son et al., 2019). Several authors have proceeded with this methodology in different ways. One study found that the triple scan technique exhibited lower values of internal gap when compared the silicone replica technique (El-Ashkar et al., 2023) whilst another study found no statistically significant differences between the two methods (Loetzerich et al., 2023). El-Ashkar and collaborators (2023) suspected that the light body elevated the crown, increasing the internal gap. It was not specified the type and duration of the pressure excreted on the crown during the "cementation" process. In the mentioned study, three *in-vitro* measurement techniques were used and compared. Light body material was used only for the silicone replica technique whereas for the other two methodologies (TST and DV) the cement space was unoccupied.

Hamza and collaborators (2016) seated the crowns on a metal die and measured the vertical marginal discrepancy distance using a binocular microscope x100 magnification to assess the marginal fit without cementation. They argued that this primary adaptation is usually lost with cementation. Variables are introduced with cementation which include cement type, viscosity and cementation techniques (Hamza, T. A. et al., 2013). However, other studies have included a cementation step using either Fit Checker Advanced (GC corp) (Zhu et al., 2023) or light body silicone (Hasanzade et al., 2020b) after constant pressure to allow setting of the material. This is more clinically relevant as the final prosthesis would need to be well adapted during and after cementation. Both Zhu and collaborators (2023) and Hasanzade and collaborators (2020) performed the TSM after "cementation". Geomagic studio was used (Geomagic Control X, 2018.0.1; 3D Systems, Rock Hill, SC, USA) and used four reference markers and the best-fit alignment to superimpose the scanned data. The potential presence of scanning deviations is the main source of error with this method, although this study identified deviations below 10μm after best-fit alignment with a high-quality scanner.

In the present study, Primescan (Dentsply, Sirona) was used and superimposed both scans (CS and MS) with a bite-registration scan after cementation of the crown with light-body silicone material. In order to standardise the cementation process as much as possible, timed (5 minutes) constant finger pressure along the long axis of the tooth was carried out before scanning similar to other studies (Çin et al., 2023; Habib et al., 2014; Hamad et al., 2019). This is similar to clinical situations in which finger pressure is used during the cementation process of the prosthesis. Hasanzade and collaborators (2020) used CEREC Omnicam MCXL (CEREC; Omnicam Sirona Dental System, Bensheim, Germany) for crown fabrication and ATOS Core Scanner (ATOS Core 5Mp 80 mm; Rev.02; GOM, Braunschweig; Germany) for the TSM with a total of 4 scans. During the light-body silicone "cementation" process, a 50N fixed load was placed on the restoration. Fasih and collaborators (2023) exerted a 50N force using a stabiliser device (Stabilizer; SANTAM). The files were then analysed using GOM software (GOM inspect v7.5, GOM mbH, Braunschweig, Germany). Both studies influenced the methodology of the present study.

The scanning aid made of dental stone with irregular landmarks was adapted from previous studies, incorporating irregular engravings and grooves and four pointed corners (Hasanzade et al., 2020b; Loetzerich et al., 2023). The straight lines were used to assist in the virtual buccolingual and mesiodistal plane creation, for reproducibility, similar to Hasanzade's concept of an aluminium base. The initial prototype exhibited a larger plane with minimal irregular markings and indentations posing problems with both scanning and superimposition. The second prototype had diagonal lines which were hard to replicate the virtual planes at the same angle. Therefore, the final design overcame the mentioned challenges.

Since multiple 3D analysing software were used to get to the final methodology it was imperative that the incorporation of many landmarks and reference markers were included from the start. The smooth prominent markers included in the crown CAD design were used herein as reference points (Figure 5.1), one on the lingual and another on the buccal aspect. These areas were necessary for any future analysis, whether to allow best-fit alignment, point-by-point matching, or alignment registration during scanning for the triple-scan technique (Holst et al., 2011; Sanchez-Lara et al., 2023; Zhu et al., 2023).

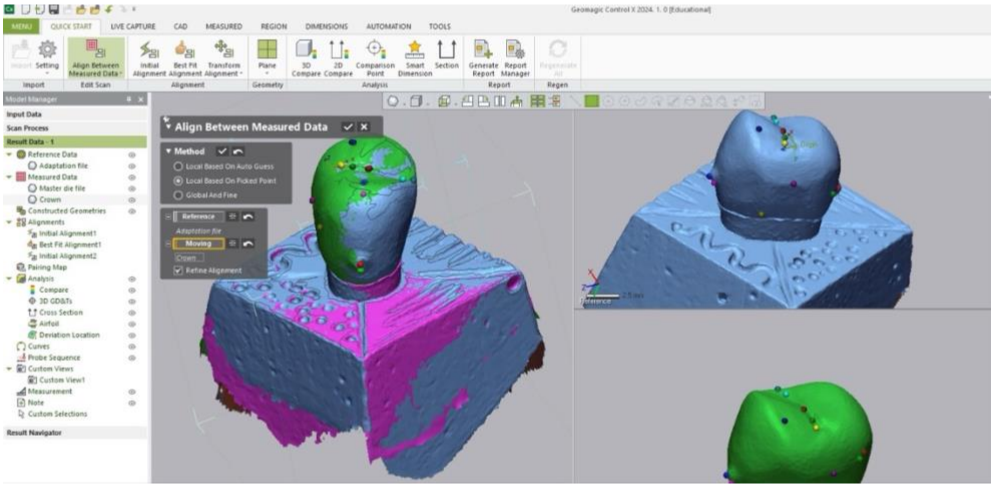

Figure 5.1 *Screenshot of manual alignment using reference markers on Geomagic Control X.*

In a study published in 2023, a software that incorporated an algorithm which calculates the smallest possible positive distance between the crown and preparation surface was used, this enabled a representative virtual fit without overlapping meshes (Loetzerich et al., 2023). Unlike this study, the present study encountered these challenges with multiple scans and needed to be overcome. For several crowns a virtual overlap of the STL files was noted which would not be possible clinically. A modified best-fit algorithm overcomes this as the virtual penetration of the crown and die would not be permitted by the aforementioned software. The use of AIXFit by Loetzerich and collaborators (2023) was proven to be a straightforward method for 3D analysis. Unfortunately, this was not possible with the software (Geomagic Control X or GOM Inspect/ ZEISS Inspect 3D) used in this study (Figure 5.2). After several attempts, as discussed in Section 3.5, it was found that the use of cement, in this case light-body silicone, and the use of the in-build CEREC bite-registration scan, the two scan (CS and MS) can be superimposed with minimal to no virtual overlap in the majority of cases.

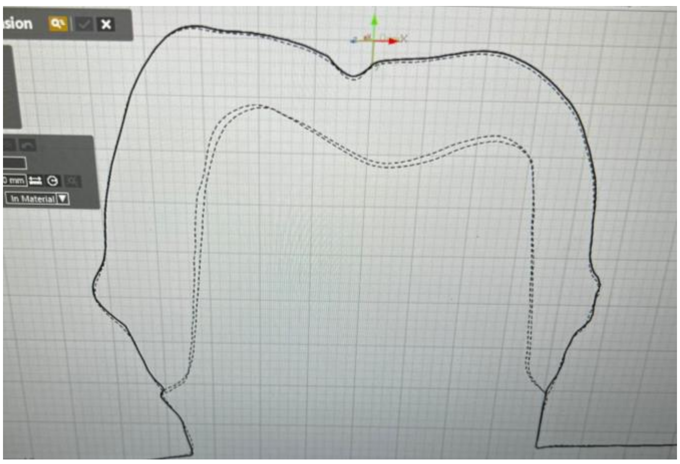

Figure 5.2 *Two-dimensional cross-section analysis using Geomagic Control X along the virtual bucco-lingual plane. Visible overlap of meshes along the intaglio surface of the crown.*

5.3 Gap Measurements and Zoning

The major advantage of using the triple scan technique for marginal gap assessment is the ability to assess the internal fit from different planes using virtual sectional planes. Points of measurement vary between studies, however the majority of authors divided the internal gap into four: marginal, axial, angle/cusp and occlusal (Son et al., 2019). Marginal discrepancy is considered to be the space between the restoration and the preparation. Points of measurement vary amongst studies e.g. in one study it was measured 0.5 mm in the occlusal direct from the preparation margin (Dahl, Bjørn Einar et al., 2017b). Son et al. (2019) measured 10 points on each side with a total of 40 points using TSM and SRT. When using the SRT one can still obtain multiple points however limited to the cross-section, for example, one study used 32 measurements in total for each replica: 12 marginal, 12 axial and 8 occlusal (Hamad et al., 2019). The number of points of marginal gap measurement vary amongst studies using the TSM: 4 (Park, Jin-Young et al., 2017), 10 (Son et al., 2019; Svanborg et al., 2019), and 40 (Boitelle et al., 2018; Fasih et al., 2023). In this study, to allow standardisation between the samples, the gap measurements were carried out by the same researcher. Data was collected after practice and guidance by another researcher in the field to improve accuracy and practice before to the final measurement sampling (Mai et al., 2018).

In a systematic review published in 2020, based on studies published between 2013 and 2018, the combined marginal gap of single and multiunit zirconia FDPs was found to be 83 µm with an accuracy of 59 µm (Svanborg, 2020). This value is within the range of the current study with an overall marginal gap was found to be 100.7 ± 43.6 µm for the chairside and 67.8 ± 59.0 µm for the lab group ($p<0.001$). According to Svanborg (2020) the internal gap was found to be 111 µm with an accuracy of 61 µm which is higher than the present study's results of 81 ± 48.1 µm for the chairside group and 60.9 ± 32.0 µm for the lab group ($p<0.001$). Many of the studies mentioned in this review (n=19) used digital impression techniques with the majority using SRT (n=9) and the cement and sectioning technique (n=3) for fit assessment. The current study's results comply with Hamza & Sherif (2016), in which the MCXL milling machine, a chairside 4-axis machine (Dentsply Sirona), showed a higher marginal discrepancy than the Zirkonzahn milling unit M1 (Zirkonzahn GmbH) with a 19.9µm mean difference ($p<0.001$). In the present study the mean difference in overall marginal discrepancy was found to be 32.9 µm ($p<0.001$). CEREC MC X5 with the inLab CAD-CAM system was found to have a marginal gap of 85μm ±2, a gap lower than the milling of monolithic zirconia in a milling centre with a 133μm ± gap (Meirowitz et al., 2019).

Based on the results obtained in the present study the largest gap in the intaglio region was found in the occlusal surface. A statistically significant difference was noted between the groups with the lab group exhibiting lower measurements of 80.5 ± 45.95 μm (MDO) (p=0.016) and 74.4 ± 40.2 μm (BLO) (p=0.005) compared to the chairside counterparts 123 ±42.9 μm (MDO) and 117 ± 34.7 μm (BLO) with a large overall occlusal internal gap of 77.5 ± 42.5 μm (lab group) and 120.1 ± 38.4 μm (chairside group) ($p<0.001$). This complies with Camargo and collaborators (2022) in which crown adaptation was found to be the least desirable in the occlusal third. In the literature there was a tendency for a gradual increase in gap values from the axial walls to the occlusal surface (Çin et al., 2023). This may be due to some inconsistencies in the actual shrinkage occurring during sintering in which the CAD software fails to sufficiently compensate for this shrinkage (Schriwer et al., 2017). Hamad and collaborators (2019) obtained high occlusal and marginal gaps of 224.47 ± 51.93 μm and 137.05 ± 32.46 μm respectively. In this study, lower values were obtained for both workflows. Similar results to this 2019 study for the axial internal surface were also obtained in the present study, with lower values from the entire intaglio surface with 56.8 ± 56.6 μm (chairside) and 50.8 ± 21.2 μm (p=0.443). The chairside group from the current study performed similar to the 5-axis milling machine (Whitepeaks Dental Solutions, Wesel, Germany) used by a study in 2019, which found a 76.19 ± 23.94 μm internal gap compared to the current results of 71.6 ± 111.2 μm (MAX), 63.0 ±14.3 μm (DAX), 53.2 ±12.2 μm (LAX) and 39.5 ±15.2 μm (BAX) (Hamad et al., 2019). The higher values in their study could be attributed to the fact that SRT was used, and this is accompanied by the limitations of silicone mentioned in section 5.3. A total of 32 measurements were taken as opposed to this study in which 25 measurements in the mesiodistal aspect and 36 in the buccolingual aspect were taken amounting to 61 measurements.

The present study's lab group obtained results similar to those of Son et al. (2019) with a marginal gap of 74.8 ± 49.1 μm (MM), 65.5 ± 48.1 μm (DM), 73.7 ± 93.8 μm (LM), 57.3 ± 30.8 μm (BM), and an overall of 67.8 ± 59.0 μm, compared to their result of 74.1 ± 26.1 μm in the TSM group. The mean occlusal gap for the mentioned study was similar to this study's chairside group with a gap of 120.3 ± 20.9 µm compared to the current findings of 120.1 ± 38.4 µm.

When comparing gaps, it would be inaccurate to assume that both groups were expected to have the same measurements, especially on the internal surface, as the initial parameters suggested by the manufacturer were different for both workflows to obtain the ideal fit in addition the difference in hardware. Following the manufacturer's recommendation, the chairside Zirconia+ crowns were fabricated with a 60µm cement space as opposed to a 35µm space in the lab's Prettau 2 crowns this is the study's main limitation. Similar to previous studies comparing the Zirkonzahn M1 milling device with relatively older devices, Dentsply Sirona's latest chairside milling device (Primemill) performed with clinically acceptable cement space and marginal gaps (Kirsch et al., 2017; McLean, 1971b). There were statistically significant differences in both marginal and intaglio regions between the two workflows. Nevertheless, the differences are not enough to disregard the chairside workflow as a worthy contender for single unit monolithic zirconia crowns due to its acceptable measurements which did not exceed the threshold indicated by the literature.

5.4 Trueness Analysis

3D mesh trueness can be evaluated by superimposing the measured data (the milled crown) and the reference data (original CAD file) using 3D inspection software. This enables numerical analysis along with a colour map representing the positive and negative deviations. The root mean square (RMS) value has been used in studies to describe trueness, with a low value representing small deviations hence high fabrication trueness (Cho et al., 2019). There are no guidelines in the interpretation of RMS values for what is considered to be a good or bad fit. However, it was proposed that an RMS of 10µm is considered to have a high trueness, whereas 50µm represents a poor fit (Peters et al., 1999). The RMS is calculated based on all cloud points in the selected region (e.g. intaglio surface) using the following formula as described by Casucci et al. (2023):

$$\mathrm{RMS} = \frac{\sqrt{\sum_{i=1}^{n} (X_{1,i} - X_{2,i})^2}}{\sqrt{n}}$$

n= total number of measuring points

$X_{1,i}$ measuring points *i* on the reference data

$X_{2,I}$ measuring points *i* on the crown scan data

It was concluded that 3- and 4-axis milling machines have lower trueness than 5-axis machines 61±22μm for the intaglio surface and 55±18μm occlusal, and 55±18μm and 41±15μm respectively (Bosch et al., 2014; Kirsch et al., 2017). Trueness is influenced by the accuracy of the machine and also the sintering shrinkage as monolithic crowns are usually milled in the partially sintered state (Moldovan et al., 2011a).

Geomagic Control X (Geomagic Inc, Morrisville, NC, USA) was the software of choice to analyse trueness for this study, similar to previous studies (Casucci et al., 2023; Cho et al., 2019). This software calculates the RMS automatically upon area selection. During the crown scan, the highly accurate intraoral scanner (Primescan; Dentsply-Sirona) with a mean trueness of 7.44 ± 0.17 μm and precision of 3.74 ± 0.60 μm (Kim et al., 2022) was used to scan the entire crown. Previous studies did not use an intraoral scanner but used other devices for 3D analysis such as non-contact scanners (ATOS Core 5Mp 80 mm; Rev.02; GOM, Braunschweig; Germany) (Hasanzade et al., 2020a), tabletop scanners (Straumann; Dental Wings Inc, Montreal, Canada) (Sanchez-Lara et al., 2023) and lab/desktop scanners such as the E1 by 3Shape (Son et al., 2019) and inEos X5 by Sirona Dental Systems (Kirsch et al., 2017).

In this study, the scanned data (reference CAD file and SC file) was imported to Geomagic Control X and superimposed onto the reference CAD file. Each crown was divided into the external and internal surface, with the marginal areas included in the intaglio surface, collectively referred to as the internal surface. After selecting the entire crown surface, the initial alignment followed by the best-fit alignment enabled the virtual superimposition of both meshes. The best-fit alignment utilises point-to-point distance or linear distance measurement algorithm. This was followed by determining the tolerance level which in this case was changed to ±0.12mm in accordance with Abualsaud & Alalawi (2022). Other studies have used ±0.10mm (Casucci et al., 2023; Wang et al., 2019b; Yeager et al., 2023) and ±0.05mm (Cho et al., 2019). In addition to an RMS value, the software also creates a colour-difference map depending on the deviation values provided. The colour map represents the negative (blue) and positive (red) deviations.

Cho and collaborators (2019) obtained RMS values of 50 μm or less for both chairside and lab groups. In this study, the chairside group used a 4-axis wet milling machine (DWX-4W; Roland

DG, Shizuoka, Japan) whilst a 5-axis milling machine (Arum 5x-300; DoowonID, Daejeon, Korea) was used for the lab group. Although having the same number of axes would have been ideal for direct comparison, there are no 5-axis chairside milling machines for zirconia crown fabrication. Most of the inner surfaces obtained the acceptable limit of ± 50μm except for of the occlusoaxial line angle. The lab group in the mentioned study exhibited higher trueness than the chairside group with 37.4 ±2.41 and 43.0 ±3.67 respectively (P= <0.001). This is comparable with the current study. However, the RMS values obtained were lower than the aforementioned 2019 study, with an RMS of 24.2 ± 6.08 and 30 ± 7.88 (p=0.041). Despite this statistically significant difference, both are clinically acceptable results as suggested by Mc Lean and von Franhoufer (1971) (Boitelle et al., 2018; Camargo et al., 2022; Contrepois, Mathieu et al., 2013; Hasanzade et al., 2020b).

Another study found that monolithic zirconia crowns milled with a 5-axis milling machine (PrograMill PM7, Ivoclar Vivadent, Schaan, Liechtenstein) exhibited an overall trueness of 18.53 ±3.03 (Abualsaud & Alalawi, 2022). A significant difference was noted between the milling and 3D printing (CERAMAKER C900 Flex, 3DCeram Sinto, Bonnac-la-Côte, France) of zirconia crowns with a trueness of 20.29 ± 3.82 and 23.90 ± 1.60 (p=0.0130). The use of Copran® Zri zirconia discs (Whitepeaks Dental Solutions GmbH, Wesel, Germany) in the mentioned 5-axis milling device gave rise to a superior trueness than the current study.

In a previous study comparing the trueness and precision of glass ceramic and zirconia crown milling, Geomagic Control X was also used (Al Hamad et al., 2021b). VITABLOCS mark II (Vita Zahnfabrik) glass ceramic material exhibited higher trueness (41.4 ± 3.49 internal surface) than the inCoris TZI by Dentsply, Sirona (83.89 ± 1.74 internal surface). Both were milled with a high-precision 5-axis milling machine (inLab MC X5; Dentsply Sirona). This demonstrates the difference between zirconia blocks/disc brands. This contrasts with the present study, as Prettau 2 zirconia discs of the Zirkonzahn workflow outperformed the inCoris TZI used in the aforementioned study in terms of trueness.

One of the limitations of the present study, is that the RMS values of the external surfaces were not assessed and compared. This was due to the inability to standardise the removal of supports and the pre-sintering polishing protocol. This may lead to under or over-contoured areas which would in turn influence the trueness of the crown. Even though the external surface was not assessed in this study the attachments were placed away from the contact area similar to clinical situations. In doing so this reduces deviations in that area preventing open interproximal contacts and reducing the need for chairside adjustments. However, this is beyond the scope of this study as the area of interest is the intaglio and marginal area. Another limitation is that deviations are present between crowns even within the same group which may be attributed to changes to the milling burs (wear). Additionally, the position of each crown on the disc, in the case of the lab group, concerning the milling burs and the spindle is different, giving rise to small deviations (Al Hamad et al., 2021b).

5.5 Clinical Relevance

As noted in the methodology, chairside milling and sintering for monolithic zirconia crown fabrication requires less than an hour, with pre-sintering steps and cooling times included. The fabrication of a partially sintered zirconia crown in a lab-based setting has a minimum duration of 8 hours under conventional sintering conditions alone. Even though some devices, including the one used in this study (Zirkonzahn Turbo; Zirkonzahn GmbH, Gais, Italy), have speed and ultra-speed sintering processes, the process is still longer than the chairside workflow. In addition to this, not many studies have compared the implications of shortened sintering times. Some studies have found smaller marginal gaps with high-speed sintering compared to conventional sintering (Kauling et al., 2020b; Lee, S. et al., 2023). No significant differences in internal gaps were noted when comparing both sintering speeds (Lee, S. et al., 2023). The fast (3.5h) and ultra-fast (75 min) sintering settings of laboratory-grade sintering machines are still not short enough to opt for a single visit crown. Using devices that fabricate prostheses with high trueness would give rise to fewer chairside adjustments before cementation. The lab group exhibited a significantly higher trueness compared to the chairside group with a superior internal and marginal fit. When selecting the workflow of choice, the final crown fit and its relation to adjacent and antagonist teeth determines not only the prognosis of the prosthesis but also the time required to obtain the ideal occlusion and contact point. Therefore, opting for a chairside workflow that is faster on paper may not always be the case as further adjustments may be required during the delivery stage along with other limitations especially in more complex cases.

5.6 Sources of Error and Limitations

Although the TSM can be used *in-vivo*, the main limitation of this study is the fact that all tests were made *in-vitro*, without the inability to perform such tests in a clinical setting with patient-dependent factors such as saliva, gingiva, and limited mouth-opening (Sanchez-Lara et al., 2023).

The use of any device especially CAD-CAM software requires a certain level of proficiency which is only achieved after long-term use and application. Throughout the entire CAD-CAM workflow for both groups there was attention to detail and several attempts were made to ensure that the correct steps were taken however this will always be a limitation. Since the intra-oral scanner was not designed for the scanning of a single crown, it is difficult to determine whether the scan was sufficient and representative. Although there is not scanning protocol for single crown scanning, the scanning sequence was based on published literature.

Another limitation was the narrow time frame, as it would have been ideal to use other software for marginal adaptation assessment, compare a passively seated crown to a cemented crown, and also construct a device that would seat exactly on the designed crown and exert an equally distribute amount of pressure during the cementation process as opposed to contrast finger pressure. Although resin/acrylic teeth have been used in previous studies as master dies for fit assessment the use of extracted human teeth is more representative.

The quality and lifespan of the milling tools influence the milling accuracy of the prosthesis in addition to the damage incurred to the milling equipment (Roperto et al., 2018). Tool wear has been investigated in the literature, with tough materials exhibiting greater tool wear. Since this study used partially sintered zirconia, which is softer than the fully sintered type, there is substantially less wear. That being said, tool wear is still present and influences milling parameters such as depth of cut, rate of feed and cutting speed, and the path of milling (Lebon et al., 2015). Both CAD-CAM software used in this study identified the percentage usage and indicated the instance in which the burs required replacement. An attempt to overcome this is the use of a brand-new set of burs. The milling process was completed without any errors or substitution warnings however there will always be an element of wear and variations between crowns.

Although several attempts were made to determine which scanner, scanning guide, software, and scanning technique would best represent the crown-preparation interface, the main limitation of this study is the inevitable superimposition of data during surface matching and any inaccuracies that arise during the best-fit alignment process. Further studies are recommended to incorporate other methods of virtual superimposition and the comparison between each method to determine the best protocol for a non-destructive fully digital marginal gap assessment.

Future *in-vitro* and clinical studies would be recommended to compare these devices along with other new devices in the market. This study could not carry out cost-analysis which would influence the clinician's decision about which workflow is favourable. This study did not measure the duration of design and fabrication steps for each crown within the different workflows investigated. Future research could delve into a more detailed time analysis of these specific steps to provide a comprehensive understanding of the time requirements involved in the production of monolithic zirconia crowns.

Chapter 6: Conclusion

Within the limitations of this *in-vitro* study, the findings observed herein suggest that both CAD-CAM systems fabricate monolithic zirconia crowns with clinically acceptable cement-space and marginal fit. However, the laboratory workflow using a high-end CAD-CAM system (Zirkonzahn), and its respective milling and sintering devices, exhibited statistically significant higher trueness and better marginal and internal fit than the chairside workflow using the CEREC system by Dentsply Sirona.

Therefore, the conclusions to our null hypotheses are:

- The null hypothesis that marginal and internal fit of monolithic zirconia restorations would not be affected by the type of digital workflow **was rejected**.
- The null hypothesis that trueness of monolithic zirconia restorations would not be affected by the type of digital workflow **was rejected**.

References

Abualsaud, R., & Alalawi, H. (2022). Fit, precision, and trueness of 3D-printed zirconia crowns compared to milled counterparts. *Dentistry Journal, 10*(11), 215.

Ahmed, W. M., Abdallah, M., McCullagh, A. P., Wyatt, C. C., Troczynski, T., & Carvalho, R. M. (2019). Marginal discrepancies of monolithic zirconia crowns: The influence of preparation designs and sintering techniques. *Journal of Prosthodontics, 28*(3), 288-298.

Ahmed, W. M., Shariati, B., Gazzaz, A. Z., Sayed, M. E., & Carvalho, R. M. (2020). Fit of tooth-supported zirconia single crowns—A systematic review of the literature. *Clinical and Experimental Dental Research; Clin Exp Dent Res, 6*(6), 700-716. 10.1002/cre2.323

Aktas, G., Sahin, E., Vallittu, P., Özcan, M., & Lassila, L. (2013). Effect of colouring green stage zirconia on the adhesion of veneering ceramics with different thermal expansion coefficients. *International Journal of Oral Science, 5*(4), 236-241.

Al Hamad, K. Q., Al-Rashdan, R. B., Al-Rashdan, B. A., & Baba, N. Z. (2021a). Effect of milling protocols on trueness and precision of ceramic crowns. *Journal of Prosthodontics, 30*(2), 171-176.

Al Hamad, K. Q., Al-Rashdan, R. B., Al-Rashdan, B. A., & Baba, N. Z. (2021b). Effect of milling protocols on trueness and precision of ceramic crowns. *Journal of Prosthodontics, 30*(2), 171-176.

Al-Haj Husain, N., Özcan, M., Dydyk, N., & Joda, T. (2022). Conventional, speed sintering and high-speed sintering of Zirconia: A systematic review of the current status of applications in dentistry with a focus on precision, mechanical and optical parameters. *Journal of Clinical Medicine, 11*(16), 4892.

Alqutaibi, A. Y., Ghulam, O., Krsoum, M., Binmahmoud, S., Taher, H., Elmalky, W., & Zafar, M. S. (2022). Revolution of current dental zirconia: A comprehensive review. *Molecules, 27*(5), 1699.

Al-Rafee, M. A. (2020). The epidemiology of edentulism and the associated factors: A literature Review. *Journal of Family Medicine and Primary Care, 9*(4), 1841.

Ashraf, Y., Sabet, A., Hamdy, A., & Ebeid, K. (2020). Influence of preparation type and tooth geometry on the accuracy of different intraoral scanners. *Journal of Prosthodontics, 29*(9), 800-804.

Azouzi, I., Kalghoum, I., Hadyaoui, D., Harzallah, B., & Cherif, M. (2018). Principles and guidelines for managing tooth wear: A review. *Int Med Care, 2*(01), 1-9.

Beuer, F., Naumann, M., Gernet, W., & Sorensen, J. A. (2009). Precision of fit: zirconia three-unit fixed dental prostheses. *Clinical Oral Investigations, 13*, 343-349.

Boening, K. W., Wolf, B. H., Schmidt, A. E., Kästner, K., & Walter, M. H. (2000). Clinical fit of Procera AllCeram crowns. *The Journal of Prosthetic Dentistry, 84*(4), 419-424. 10.1067/mpr.2000.109125

Boitelle, P., Tapie, L., Mawussi, B., & Fromentin, O. (2018). Evaluation of the marginal fit of CAD-CAM zirconia copings: comparison of 2D and 3D measurement methods. *The Journal of Prosthetic Dentistry, 119*(1), 75-81.

Boitellea, P., Tapieb, L., Mawussic, B., & Fromentind, O. (2016). 3D fitting accuracy evaluation of CAD/CAM copings–comparison with spacer design settings Evaluation 3D de l 'exactitude de l 'adaptation de chapes fabriquées par CFAO–Comparaison avec les valeurs de paramétrage du joint. *International Journal of Computerized Dentistry, 19*(1), 27-43.

Bosch, G., Ender, A., & Mehl, A. (2014). A 3-dimensional accuracy analysis of chairside CAD/CAM milling processes. *The Journal of Prosthetic Dentistry, 112*(6), 1425-1431.

Camargo, B., Willems, E., Jacobs, W., Van Landuyt, K., Peumans, M., Zhang, F., Vleugels, J., & Van Meerbeek, B. (2022). 3D printing and milling accuracy influence full-contour zirconia crown adaptation. *Dental Materials; Dent Mater, 38*(12), 1963-1976. 10.1016/j.dental.2022.11.002

Casucci, A., Verniani, G., Habib, R., Ricci, N. M., Carboncini, C., & Ferrari, M. (2023). Accuracy of Four Intra-Oral Scanners in Subgingival Vertical Preparation: An In Vitro 3-Dimensional Comparative Analysis. *Materials, 16*(19), 6553.

Cho, J., Yoon, H., Han, J., & Kim, D. (2019). Trueness of the inner surface of monolithic crowns fabricated by milling of a fully sintered (Y, Nb)-TZP block in chairside CAD–CAM system for single-visit dentistry. *Materials, 12*(19), 3253.

Christensen, G. J. (1966). Marginal fit of gold inlay castings. *The Journal of Prosthetic Dentistry, 16*(2), 297-305.

Çin, V., İzgi, A. D., Kale, E., & Yilmaz, B. (2023). Marginal and internal fit of monolithic zirconia crowns fabricated by using two different cad-cam workflows: An in vitro study. *Prosthesis, 5*(1), 35-47.

Contrepois, M., Soenen, A., Bartala, M., & Laviole, O. (2013). Marginal adaptation of ceramic crowns: A systematic review. *The Journal of Prosthetic Dentistry, 110*(6), 447-454.e10. 10.1016/j.prosdent.2013.08.003

Contrepois, M., D.D.S., Soenen, A., D.D.S., Bartala, Michel,D.D.S., PhD., & Laviole, Odile,D.D.S., PhD. (2013). Marginal adaptation of ceramic crowns: A systematic review. *The Journal of Prosthetic Dentistry; J Prosthet Dent, 110*(6), 447-454.e10. 10.1016/j.prosdent.2013.08.003

Cortes, A. R. (2022). Digital dentistry: a step-by-step guide and case atlas. John Wiley & Sons.

Cortes, A. R., Agius, A., & No-Cortes, J. (2022). Factors Affecting Trueness of Intraoral Scans: An Update. *Applied Sciences, 12*(13), 6675.

Dahl, B. E., Dahl, J. E., & Rønold, H. J. (2018). Digital evaluation of marginal and internal fit of single-crown fixed dental prostheses. *European Journal of Oral Sciences, 126*(6), 512-517. 10.1111/eos.12576

Dahl, B. E., Rønold, H. J., & Dahl, J. E. (2017a). Internal fit of single crowns produced by CAD-CAM and lost-wax metal casting technique assessed by the triple-scan protocol. *The Journal of Prosthetic Dentistry, 117*(3), 400-404.

Dahl, B. E., Rønold, H. J., & Dahl, J. E. (2017b). Internal fit of single crowns produced by CAD-CAM and lost-wax metal casting technique assessed by the triple-scan protocol. *The Journal of Prosthetic Dentistry, 117*(3), 400-404.

Davidowitz, G., & Kotick, P. G. (2011). The use of CAD/CAM in dentistry. *Dental Clinics, 55*(3), 559-570.

Dawson, P. E. (2006). *Functional occlusion: from TMJ to smile design*. Elsevier Health Sciences.

Dolan, T. A., Gilbert, G. H., Duncan, R. P., & Foerster, U. (2001). Risk indicators of edentulism, partial tooth loss and prosthetic status among black and white middle-aged and older adults. *Community Dentistry and Oral Epidemiology, 29*(5), 329-340.

Edwards Rezende, C. E., Sanches Borges, A. F., Macedo, R. M., Rubo, J. H., & Griggs, J. A. (2017). Dimensional changes from the sintering process and fit of Y-TZP copings: Micro-CT analysis. *Dental Materials; Dent Mater, 33*(11), e405-e413. 10.1016/j.dental.2017.08.191

El-Ashkar, A., Taymour, M., & El-Tannir, A. (2023). Evaluation of the marginal and internal gaps of partially crystallized versus fully crystallized zirconia-reinforced lithium silicate CAD-CAM crowns: An in vitro comparison of the silicone replica technique, direct view, and 3-dimensional superimposition analysis. *The Journal of Prosthetic Dentistry, 129*(5), 769-776.

Fasih, P., Tavakolizadeh, S., Monfared, M. S., Sofi-Mahmudi, A., & Yari, A. (2023). Marginal fit of monolithic versus layered zirconia crowns assessed with 2 marginal gap methods. *The Journal of Prosthetic Dentistry, 130*(2), 250. e1-250. e7.

Felton, D. A., Kanoy, B. E., Bayne, S. a., & Wirthman, G. P. (1991). Effect of in vivo crown margin discrepancies on periodontal health. *The Journal of Prosthetic Dentistry, 65*(3), 357-364.

Fransson, B., Øilo, G., & Gjeitanger, R. (1985). The fit of metal-ceramic crowns, a clinical study. *Dental Materials, 1*(5), 197-199.

Habib, S. R., Asiri, W., & Hefne, M. J. (2014). Effect of anatomic, semi-anatomic and non-anatomic occlusal surface tooth preparations on the adaptation of zirconia copings. *The Journal of Advanced Prosthodontics, 6*(6), 444-450.

Hamad, K. Q., Quran, F. A., Jalam, S. A., & Baba, N. Z. (2019). Comparison of the accuracy of fit of metal, zirconia, and lithium disilicate crowns made from different manufacturing techniques. *J Prosthodont, 28*(5), 497-503.

Hamza, T. A., Ezzat, H. A., El-Hossary, M. M. K., Katamish, H. A. E. M., Shokry, T. E., & Rosenstiel, S. F. (2013). Accuracy of ceramic restorations made with two CAD/CAM systems. *The Journal of Prosthetic Dentistry, 109*(2), 83-87.

Hamza, & Sherif. (2016). In vitro evaluation of marginal discrepancy of monolithic zirconia restorations fabricated with different CAD-CAM systems. *The Journal of Prosthetic Dentistry; J Prosthet Dent, 117*(6), 762-766. 10.1016/j.prosdent.2016.09.011

Hamza, & Sherif. (2017). In vitro evaluation of marginal discrepancy of monolithic zirconia restorations fabricated with different CAD-CAM systems. *The Journal of Prosthetic Dentistry, 117*(6), 762-766. 10.1016/j.prosdent.2016.09.011

Hasanzade, M., Koulivand, S., Moslemian, N., & Alikhasi, M. (2020a). Comparison of three-dimensional digital technique with two-dimensional replica method for measuring marginal and internal fit of full coverage restorations. *The Journal of Advanced Prosthodontics, 12*(3), 173.

Hasanzade, M., Moharrami, M., & Alikhasi, M. (2020b). How adjustment could affect internal and marginal adaptation of CAD/CAM crowns made with different materials. *The Journal of Advanced Prosthodontics, 12*(6), 344.

Holmes, J. R., Bayne, S. C., Holland, G. A., & Sulik, W. D. (1989). Considerations in measurement of marginal fit. *The Journal of Prosthetic Dentistry, 62*(4), 405-408.

Holst, S., Karl, M., Wichmann, M., & Matta, R. T. (2011). A new triple-scan protocol for 3D fit assessment of dental restorations. *Quintessence International; Quintessence Int, 42*(8), 651-657.

Ilie, N., & Stawarczyk, B. (2015). Quantification of the amount of blue light passing through monolithic zirconia with respect to thickness and polymerization conditions. *The Journal of Prosthetic Dentistry, 113*(2), 114-121.

Jansen, J. U., Lümkemann, N., Letz, I., Pfefferle, R., Sener, B., & Stawarczyk, B. (2019). Impact of high-speed sintering on translucency, phase content, grain sizes, and flexural strength of 3Y-TZP and 4Y-TZP zirconia materials. *The Journal of Prosthetic Dentistry, 122*(4), 396-403.

Ji, M., Park, J., Park, S., Yun, K., Oh, G., & Lim, H. (2015). Evaluation of marginal fit of 2 CAD-CAM anatomic contour zirconia crown systems and lithium disilicate glass-ceramic crown. *The Journal of Advanced Prosthodontics, 7*(4), 271-277.

Kaizer, M. R., Gierthmuehlen, P. C., Dos Santos, M. B., Cava, S. S., & Zhang, Y. (2017). Speed sintering translucent zirconia for chairside one-visit dental restorations: Optical, mechanical, and wear characteristics. *Ceramics International, 43*(14), 10999-11005.

Kauling, A. E., Güth, J., Erdelt, K., Edelhoff, D., & Keul, C. (2020a). Influence of speed sintering on the fit and fracture strength of 3-unit monolithic zirconia fixed partial dentures. *The Journal of Prosthetic Dentistry, 124*(3), 380-386.

Kauling, A. E., Güth, J., Erdelt, K., Edelhoff, D., & Keul, C. (2020b). Influence of speed sintering on the fit and fracture strength of 3-unit monolithic zirconia fixed partial dentures. *The Journal of Prosthetic Dentistry, 124*(3), 380-386.

Kernen, F., Schlager, S., Alvarez, V. S., Mehrhof, J., Vach, K., Kohal, R., Nelson, K., & Flügge, T. (2022). Accuracy of intraoral scans: An in vivo study of different scanning devices. *The Journal of Prosthetic Dentistry, 128*(6), 1303-1309.

Kim, J., Son, S., Lee, H., Yoo, Y., Hong, S., & Park, J. (2022). Influence of adjacent teeth on the accuracy of intraoral scanning systems for class II inlay preparation. *Journal of Esthetic and Restorative Dentistry, 34*(5), 826-832.

Kirsch, C., Ender, A., Attin, T., & Mehl, A. (2017). Trueness of four different milling procedures used in dental CAD/CAM systems. *Clinical Oral Investigations; Clin Oral Investig, 21*(2), 551-558. 10.1007/s00784-016-1916-y

Komine, F., Honda, J., Kusaba, K., Kubochi, K., Takata, H., & Fujisawa, M. (2020). Clinical outcomes of single crown restorations fabricated with resin-based CAD/CAM materials. *Journal of Oral Science, 62*(4), 353-355.

Kontis, P., Güth, J., & Keul, C. (2022). Correction to: Accuracy of full-arch digitalization for partially edentulous jaws—a laboratory study on basis of coordinate-based data analysis. *Clinical Oral Investigations, 26*(4), 3663.

Kontis, P., Güth, J., Schubert, O., & Keul, C. (2021). Accuracy of intraoral scans of edentulous jaws with different generations of intraoral scanners compared to laboratory scans. *The Journal of Advanced Prosthodontics, 13*(5), 316.

Kuhn, K., Ostertag, S., Ostertag, M., Walter, M. H., Luthardt, R. G., & Rudolph, H. (2014). Comparison of an analog and digital quantitative and qualitative analysis for the fit of dental copings. *Computers in Biology and Medicine; Comput Biol Med, 57*, 32-41. 10.1016/j.compbiomed.2014.11.017

Laurent, M., Scheer, P., Dejou, J., & Laborde, G. (2008). Clinical evaluation of the marginal fit of cast crowns–validation of the silicone replica method. *Journal of Oral Rehabilitation, 35*(2), 116-122.

Lebon, N., Tapie, L., Vennat, E., & Mawussi, B. (2015). Influence of CAD/CAM tool and material on tool wear and roughness of dental prostheses after milling. *The Journal of Prosthetic Dentistry, 114*(2), 236-247.

Lee, H., Kim, H., Noh, K., Paek, J., & Pae, A. (2017). A simplified method for evaluating the 3-dimensional cement space of dental prostheses by using a digital scanner. *The Journal of Prosthetic Dentistry, 118*(5), 584-586.

Lee, S., Choi, G., Choi, J., Kim, Y., & Kim, H. (2023). Effect of high-speed sintering on the marginal and internal fit of CAD/CAM-fabricated monolithic zirconia crowns. *Scientific Reports, 13*(1), 17215.

Li, R., Chen, H., Wang, Y., & Sun, Y. (2021). Suitability of the triple-scan method with a dental laboratory scanner to assess the 3D adaptation of zirconia crowns. *The Journal of Prosthetic Dentistry, 125*(4), 651-656.

Li, R., Xu, T., Wang, Y., & Sun, Y. (2023). Accuracy of zirconia crowns manufactured by stereolithography with an occlusal full-supporting structure: An in vitro study. *The Journal of Prosthetic Dentistry, 130*(6), 902-907.

Liang, S., Yuan, F., Luo, X., Yu, Z., & Tang, Z. (2018). Digital evaluation of absolute marginal discrepancy: a comparison of ceramic crowns fabricated with conventional and digital techniques. *The Journal of Prosthetic Dentistry, 120*(4), 525-529.

Liu, L., Guo, J., YX, D. U., Wang, Q., & Qiu, L. (2019). Comparison of mechanical properties of three machinable resin ceramic composite materials. *Shanghai Kou Qiang Yi Xue= Shanghai Journal of Stomatology, 28*(1), 25-29.

Loetzerich, J. M., Raith, S., & Reich, S. (2023). Verification of a digital approach for three-dimensional evaluation of marginal and internal fit. *The Journal of Prosthetic Dentistry,*

Mahmood, D. J. H., Braian, M., Larsson, C., & Wennerberg, A. (2019). Production tolerance of conventional and digital workflow in the manufacturing of glass ceramic crowns. *Dental Materials; Dent Mater, 35*(3), 486-494. 10.1016/j.dental.2019.01.015

Mai, H., Lee, K. E., Ha, J., & Lee, D. (2018). Effects of image and education on the precision of the measurement method for evaluating prosthesis misfit. *The Journal of Prosthetic Dentistry, 119*(4), 600-605.

Manisha, J., Srivastava, G., Das, S. S., Tabarak, N., & Choudhury, G. K. (2023). Accuracy of single-unit ceramic crown fabrication after digital versus conventional impressions: A systematic review and meta-analysis. *The Journal of Indian Prosthodontic Society, 23*(2), 105-111.

Martins, L. M., Lorenzoni, F. C., Melo, A. O. d., Silva, L. M. d., Oliveira, J. L. G. d., Oliveira, P. C. G. d., & Bonfante, G. (2012). Internal fit of two all-ceramic systems and metal-ceramic crowns. *Journal of Applied Oral Science, 20*, 235-240.

McLean, J. W. (1971a). The estimation of cement film thickness by an in vivo technique. *British Dental Journal, 131*(3), 107-111.

McLean, J. W. (1971b). The estimation of cement film thickness by an in vivo technique. *Br Dent J, 131*, 107-111.

Mejía, J. B. C., Wakabayashi, K., Nakamura, T., & Yatani, H. (2017). Influence of abutment tooth geometry on the accuracy of conventional and digital methods of obtaining dental impressions. *The Journal of Prosthetic Dentistry, 118*(3), 392-399.

Memari, Y., Mohajerfar, M., Armin, A., Kamalian, F., Rezayani, V., & Beyabanaki, E. (2019). Marginal adaptation of CAD/CAM all-ceramic crowns made by different impression methods: A literature review. *Journal of Prosthodontics, 28*(2), e536-e544.

Mitchell, C. A., Pintado, M. R., & Douglas, W. H. (2001). Nondestructive, in vitro quantification of crown margins. *The Journal of Prosthetic Dentistry, 85*(6), 575-584.

Miura, S., Fujita, T., Tsukada, S., Teshigawra, D., Saito-Murakami, K., & Fujisawa, M. (2022). Comparative evaluation of the reproductive trueness of zirconia crowns fabricated using additive manufacturing and conventional milling. *Int J Prosthodont, 35*, 410-413.

Miyazaki, T. (2007). Dental CAD/CAM: Current Status and Future Perspective. Paper presented at the Abstracts of the General Sessions of the Japanese Society for Dental Materials and Devices 50th General Session of the Japanese Society for Dental Materials and Devices in Conjunction with International Dental Materials Congress 2007, 7.

Moldovan, O., Luthardt, R. G., Corcodel, N., & Rudolph, H. (2011a). Three-dimensional fit of CAD/CAM-made zirconia copings. *Dental Materials; Dent Mater, 27*(12), 1273-1278. 10.1016/j.dental.2011.09.006

Moldovan, O., Luthardt, R. G., Corcodel, N., & Rudolph, H. (2011b). Three-dimensional fit of CAD/CAM-made zirconia copings. *Dental Materials, 27*(12), 1273-1278.

Monaco, C., Arena, A., Štelemėkaitė, J., Evangelisti, E., & Baldissara, P. (2019). In vitro 3D and gravimetric analysis of removed tooth structure for complete and partial preparations. *Journal of Prosthodontic Research, 63*(2), 173-178.

Morsy, N., El Kateb, M., Azer, A., & Fathalla, S. (2021). Fit of zirconia fixed partial dentures fabricated from conventional impressions and digital scans: A systematic review and meta-analysis. *The Journal of Prosthetic Dentistry,* Mously, H. A., Finkelman, M., Zandparsa, R., & Hirayama, H. (2014). Marginal and internal adaptation of ceramic crown restorations fabricated with CAD/CAM technology and the heat-press technique. *The Journal of Prosthetic Dentistry, 112*(2), 249-256.

Nakamura, T., Nakano, Y., Usami, H., Okamura, S., Wakabayashi, K., & Yatani, H. (2020). In vitro investigation of fracture load and aging resistance of high-speed sintered monolithic tooth-borne zirconia crowns. *Journal of Prosthodontic Research, 64*(2), 182-187.

Nawafleh, N. A., Mack, F., Evans, J., Mackay, J., & Hatamleh, M. M. (2013). Accuracy and reliability of methods to measure marginal adaptation of crowns and FDPs: a literature review. *Journal of Prosthodontics*, *22*(5), 419-428.

Noether, G. E. (1987). Sample size determination for some common nonparametric tests. *Journal of the American Statistical Association*, *82*(398), 645-647.

Øilo, G., & Evje, D. M. (1986). Film thickness of dental luting cements. *Dental Materials, 2*(2), 85-89. 10.1016/S0109-5641(86)80058-6

Park, J., Hämmerle, C. H., & Benic, G. I. (2017). Digital technique for in vivo assessment of internal and marginal fit of fixed dental prostheses. *The Journal of Prosthetic Dentistry, 118*(4), 452-454.

Park, J., Bae, S., Lee, J., Kim, J., Kim, H., & Kim, W. (2017). Evaluation of the marginal and internal gaps of three different dental prostheses: comparison of the silicone replica technique and three-dimensional superimposition analysis. *The Journal of Advanced Prosthodontics, 9*(3), 159.

Paul, N., Swamy, K. R., Dhakshaini, M. R., Sowmya, S., & Ravi, M. B. (2020). Marginal and internal fit evaluation of conventional metal-ceramic versus zirconia CAD/CAM crowns. *Journal of Clinical and Experimental Dentistry, 12*(1), e31.

Pedroche, L. O., Bernardes, S. R., Leão, M. P., Kintopp, C. C. d. A., Correr, G. M., Ornaghi, B. P., & Gonzaga, C. C. (2016). Marginal and internal fit of zirconia copings obtained using different digital scanning methods. *Brazilian Oral Research, 30*

Peters, M., Delong, R., Pintado, M. R., Pallesen, U., Qvist, V., & Douglas, W. H. (1999). Comparison of two measurement techniques for clinical wear. *Journal of Dentistry, 27*(7), 479-485.

Pilo, R., Folkman, M., Arieli, A., & Levartovsky, S. (2018). Marginal fit and retention strength of zirconia crowns cemented by self-adhesive resin cements. *Operative Dentistry, 43*(2), 151-161.

Pimenta, M. A., Frasca, L. C., Lopes, R., & Rivaldo, E. (2015). Evaluation of marginal and internal fit of ceramic and metallic crown copings using x-ray microtomography (micro-CT) technology. *The Journal of Prosthetic Dentistry*, *114*(2), 223-228.

Pjetursson, B. E., Sailer, I., Makarov, N. A., Zwahlen, M., & Thoma, D. S. (2015). All-ceramic or metal-ceramic tooth-supported fixed dental prostheses (FDPs)? A systematic review of the survival and complication rates. Part II: Multiple-unit FDPs. *Dental Materials*, *31*(6), 624-639.

Pontevedra, P., Lopez-Suarez, C., Rodriguez, V., Pelaez, J., & Suarez, M. J. (2022). Randomized clinical trial comparing monolithic and veneered zirconia three-unit posterior fixed partial dentures in a complete digital flow: three-year follow-up. *Clinical Oral Investigations*, *26*(6), 4327-4335.

Refaie, A., Fouda, A., Bourauel, C., & Singer, L. (2023). Marginal gap and internal fit of 3D printed versus milled monolithic zirconia crowns. *BMC Oral Health, 23*(1), 448.

Reich, S., Wichmann, M., Nkenke, E., & Proeschel, P. (2005). Clinical fit of all-ceramic three-unit fixed partial dentures, generated with three different CAD/CAM systems. *European Journal of Oral Sciences, 113*(2), 174-179.

Resende, C. C. D., Barbosa, T. A. Q., Moura, G. F., do Nascimento Tavares, L., Rizzante, F. A. P., George, F. M., das Neves, F. D., & Mendonça, G. (2021). Influence of operator experience, scanner type, and scan size on 3D scans. *The Journal of Prosthetic Dentistry, 125*(2), 294-299.

Revilla-León, M., Methani, M. M., Morton, D., & Zandinejad, A. (2020). Internal and marginal discrepancies associated with stereolithography (SLA) additively manufactured zirconia crowns. *The Journal of Prosthetic Dentistry, 124*(6), 730-737.

Rezende, C. E. E., Borges, A. F. S., Macedo, R. M., Rubo, J. H., & Griggs, J. A. (2017). Dimensional changes from the sintering process and fit of Y-TZP copings: Micro-CT analysis. *Dental Materials, 33*(11), e405-e413.

Roperto, R. C., Lopes, F. C., Porto, T. S., Teich, S., Rizzante, F. A. P., Gutmacher, Z., & de Sousa-Neto, M. D. (2018). CAD/CAM diamond tool wear. *Quintessence International, 49*(10)

Róth, I., Czigola, A., Fehér, D., Vitai, V., Joós-Kovács, G. L., Hermann, P., Borbély, J., & Vecsei, B. (2022). Digital intraoral scanner devices: a validation study based on common evaluation criteria. *BMC Oral Health, 22*(1), 140.

Rues, S., Zehender, N., Zenthöfer, A., Bömicke, W., Herpel, C., Ilani, A., Erber, R., Roser, C., Lux, C. J., & Rammelsberg, P. (2023). Fit of anterior restorations made of 3D-printed and milled zirconia: An in-vitro study. *Journal of Dentistry, 130*, 104415.

Rungruanganunt, P., Kelly, J. R., & Adams, D. J. (2010). Two imaging techniques for 3D quantification of pre-cementation space for CAD/CAM crowns. *Journal of Dentistry; J Dent, 38*(12), 995-1000. 10.1016/j.jdent.2010.08.015

Ryu, J., Kim, Y., Kong, H., Chang, H., & Jung, J. (2020). Marginal and internal fit of 3D printed provisional crowns according to build directions. *The Journal of Advanced Prosthodontics, 12*(4), 225.

Sachs, C., Groesser, J., Stadelmann, M., Schweiger, J., Erdelt, K., & Beuer, F. (2014). Full-arch prostheses from translucent zirconia: accuracy of fit. *Dental Materials, 30*(8), 817-823.

Sailer, I., Makarov, N. A., Thoma, D. S., Zwahlen, M., & Pjetursson, B. E. (2015). All-ceramic or metal-ceramic tooth-supported fixed dental prostheses (FDPs)? A systematic review of the survival and complication rates. Part I: Single crowns (SCs). *Dental Materials, 31*(6), 603-623.

Sanchez-Lara, A., Hosney, S., Lampraki, E., Conejo, J., Blatz, M. B., Barmak, A. B., Ercoli, C., & Chochlidakis, K. (2023). Evaluation of marginal and internal fit of single crowns manufactured with an analog workflow and three CAD-CAM systems: A prospective clinical study. *Journal of Prosthodontics,* Sannino, G., Germano, F., Arcuri, L., Bigelli, E., Arcuri, C., & Barlattani, A. (2014). Cerec CAD/CAM chairside system. *ORAL & Implantology, 7*(3), 57.

Santos, T., Ferreira, C. G., Araújo, O., Machado, A. S., Silva, A., & Lopes, R. T. (2020). Methodology to analyze the marginal fit of odontological crowns through tridimensional parameters using X-ray microCT technique. *Radiation Physics and Chemistry, 167*, 108290.

Sasany, R., & Yilmaz, B. (2023). Marginal discrepancy and fracture load of thermomechanically fatigued crowns fabricated with different CAD-CAM techniques. *Journal of Prosthodontics, 32*(7), 602-607.

Segerström, S., Wiking-Lima de Faria, J., Braian, M., Ameri, A., & Ahlgren, C. (2019). A validation study of the impression replica technique. *Journal of Prosthodontics, 28*(2), e609-e616.

Solá-Ruiz, M. F., Leon-Martine, R., Labaig-Rueda, C., Selva-Otalaorrouchi, E., & Agustín-Panadero, R. (2022). Clinical outcomes of veneered zirconia anterior partial fixed dental prostheses: A 12-year prospective clinical trial. *The Journal of Prosthetic Dentistry, 127*(6), 846-851.

Son, K., Lee, S., Kang, S. H., Park, J., Lee, K., Jeon, M., & Yun, B. (2019). A comparison study of marginal and internal fit assessment methods for fixed dental prostheses. *Journal of Clinical Medicine, 8*(6), 785.

Stawarczyk, B., Keul, C., Eichberger, M., Figge, D., Edelhoff, D., & Lümkemann, N. (2017a). Three generations of zirconia: From veneered to monolithic. Part I. *Quintessence International (Berlin, Germany : 1985), 48*(5), 369-380. 10.3290/j.qi.a38057

Stawarczyk, B., Keul, C., Eichberger, M., Figge, D., Edelhoff, D., & Lümkemann, N. (2017b). Three generations of zirconia: From veneered to monolithic. Part II. *Quintessence International (Berlin, Germany : 1985), 48*(6), 441-450. 10.3290/j.qi.a38157

Sulaiman, F., Chai, J., & Wozniak, W. T. (1997). A comparison of the marginal fit of In-Ceram, IPS Empress, and Procera crowns. *International Journal of Prosthodontics, 10*(5)

Sulaiman, T. A., Abdulmajeed, A. A., Donovan, T. E., Vallittu, P. K., Närhi, T. O., & Lassila, L. V. (2015). The effect of staining and vacuum sintering on optical and mechanical properties of partially and fully stabilized monolithic zirconia. *Dental Materials Journal, 34*(5), 605-610.

Suttor, D., Bunke, K., Hoescheler, S., Hauptmann, H., & Hertlein, G. (2001). LAVA--the system for all-ceramic ZrO2 crown and bridge frameworks. *International Journal of Computerized Dentistry, 4*(3), 195-206.

Svanborg, P. (2020). A systematic review on the accuracy of zirconia crowns and fixed dental prostheses. *Biomaterial Investigations in Dentistry, 7*(1), 9-15.

Svanborg, P., Andersson, M., Reinedahl, T., & Alstad, T. (2019). Comparison of the 3D triple-scan protocol and the impression replica technique for 3-unit tooth-supported fixed dental prostheses. *Biomaterial Investigations in Dentistry, 6*(1), 32-34.

Tabesh, M., Nejatidanesh, F., Savabi, G., Davoudi, A., & Savabi, O. (2022). Marginal Accuracy of Lithium Disilicate Full-Coverage Single Crowns Made by Direct and Indirect Digital or Conventional Workflows: A Systematic Review and Meta-Analysis. *Journal of Prosthodontics, 31*(9), 744-753.

Tabesh, M., Nejatidanesh, F., Savabi, G., Davoudi, A., Savabi, O., & Mirmohammadi, H. (2021). Marginal adaptation of zirconia complete-coverage fixed dental restorations made from digital scans or conventional impressions: A systematic review and meta-analysis. *The Journal of Prosthetic Dentistry, 125*(4), 603-610.

Thoma, D. S., Sailer, I., Ioannidis, A., Zwahlen, M., Makarov, N., & Pjetursson, B. E. (2017). A systematic review of the survival and complication rates of resin-bonded fixed dental prostheses after a mean observation period of at least 5 years. *Clinical Oral Implants Research, 28*(11), 1421-1432.

Turkyilmaz, I., & Yun, S. (2022). Chairside versus external laboratory milling in fabricating CAD/CAM surgical and restorative products in dental practice. *Primary Dental Journal, 11*(4), 53-55.

Wang, W., Yu, H., Liu, Y., Jiang, X., & Gao, B. (2019a). Trueness analysis of zirconia crowns fabricated with 3-dimensional printing. *The Journal of Prosthetic Dentistry, 121*(2), 285-291.

Wang, W., Yu, H., Liu, Y., Jiang, X., & Gao, B. (2019b). Trueness analysis of zirconia crowns fabricated with 3-dimensional printing. *The Journal of Prosthetic Dentistry, 121*(2), 285-291.

Wettstein, F., Sailer, I., Roos, M., & Hämmerle, C. H. (2008). Clinical study of the internal gaps of zirconia and metal frameworks for fixed partial dentures. *European Journal of Oral Sciences, 116*(3), 272-279.

Yeager, B., Çakmak, G., Zheng, F., Johnston, W. M., & Yilmaz, B. (2023). Error analysis of stages involved in CBCT-guided implant placement with surgical guides when different printing technologies are used. *The Journal of Prosthetic Dentistry,*

Zeltner, M., Sailer, I., Mühlemann, S., Özcan, M., Hämmerle, C. H., & Benic, G. I. (2017). Randomized controlled within-subject evaluation of digital and conventional workflows for the fabrication of lithium disilicate single crowns. Part III: marginal and internal fit. *The Journal of Prosthetic Dentistry, 117*(3), 354-362.

Zhang, Y., & Lawn, B. R. (2018a). Novel zirconia materials in dentistry. *Journal of Dental Research, 97*(2), 140-147.

Zhang, Y., & Lawn, B. R. (2018b). Novel zirconia materials in dentistry. *Journal of Dental Research, 97*(2), 140-147.

Zhu, H., Zhou, Y., Jiang, J., Wang, Y., & He, F. (2023). Accuracy and margin quality of advanced 3D-printed monolithic zirconia crowns. *The Journal of Prosthetic Dentistry,*

Zucuni, C. P., Dapieve, K. S., Rippe, M. P., Pereira, G. K. R., Bottino, M. C., & Valandro, L. F. (2019). Influence of finishing/polishing on the fatigue strength, surface topography, and roughness of an yttrium-stabilized tetragonal zirconia polycrystals subjected to grinding. *Journal of the Mechanical Behavior of Biomedical Materials, 93*, 222-229.

Zucuni, C. P., Guilardi, L. F., Rippe, M. P., Pereira, G. K. R., & Valandro, L. F. (2018). Polishing of ground Y-TZP ceramic is mandatory for improving the mechanical behavior. *Brazilian Dental Journal, 29*, 483-491.

Appendices

Appendix A *Ethics Approval Letter*

L-Università ta' Malta

Faculty of Dental Surgery

University of Malta
Msida MSD 2080, Malta

Tel: +356 2340 1675

www.um.edu.mt/ds

Date: 05.03.2024

Dear Ms Laura Althea Cuschieri,

I refer to your Research Ethics and Data Protection application (application ID: DSG-2023-00025).

The Faculty Research Ethics Committee (FREC) has reviewed your application and has determined that your research is in conformity with the University of Malta's Research Code of Practice.

Yours Sincerely,

Ms Sharlene Cachia
FREC - Secretary